5-12-2023

An investigation into transcription fidelity and its effects on C. elegans and S. cerevisiae health and longevity

Olivia S. Dinep-Schneider
Mississippi State University, od44@msstate.edu

An investigation into transcription fidelity and its effects on C. elegans and S. cerevisiae health and longevity

By

Olivia S. Dinep-Schneider

Approved by:

Jean-Francois Gout (Major Professor)
Florencia Meyer
Ying Wang
Justin A. Thornton (Graduate Coordinator)
Rick Travis (Dean, College of Arts & Sciences)

A Thesis
Submitted to the Faculty of
Mississippi State University
in Partial Fulfillment of the Requirements
for the Degree of Master of Science
in Biology
in the Department of Biological Sciences

Mississippi State, Mississippi

May 2023

Name: Olivia S. Dinep-Schneider

Date of Degree: May 12, 2023

Institution: Mississippi State University

Major Field: Biology

Major Professor: Jean-Francois Gout

Title of Study: An investigation into transcription fidelity and its effects on C. elegans and S. cerevisiae health and longevity

Pages in Study: 94

Candidate for Degree of Master of Science

mRNA molecules form an intermediate in the transfer of sequences from DNA to ribosomes in order to guide protein production. Errors can be introduced into mRNA, producing aberrant proteins which place a strain on cellular regulatory machinery, causing increased risks of apoptosis, cancer, and decreased fitness. These errors may be introduced due to decreased transcriptional proofreading capabilities, exposure to chemicals, or mistakes in RNA editing machinery. It is important to investigate these causes of transcription errors to better understand the long-neglected area of mRNA fidelity which has such significant impacts on our cellular functions. In this paper, it was determined that addition of adenine opposite from abasic sites, not genomic uracil pairing with adenine, are a probable cause of G-to-A transcription errors. That exposure to Roundup causes increased levels of transcription errors, potentially due to oxidative stress. And finally, that off-target ADAR gene editing of transcripts occurs at high levels.

DEDICATION

To my family

ACKNOWLEDGEMENTS

I would like to acknowledge the help and support given to me by my P.I., Dr. Jean-Francois Gout, and the rest of my lab.

I would also like to acknowledge the following:

DST1-Δ, WT, and UNG1-Δ C. elegans strains were provided by the CGC, which is funded by NIH Office of Research Infrastructure Programs (P40 OD010440).

S. cerevisiae WT strain and rearing training were kindly provided by Dr. Donna Gordon of the MSU Biology Department.

Rolling Circle protocol troubleshooting assistance by Dr. Marc Vermulst of the USC Leonard Davis School of Gerontology.

Survival curve statistical analysis assistance by Dr. John C. Schneider, retired professor of the MSU Biochemistry, Molecular Biology, Entomology, and Plant Pathology Department.

YEpTOP2PGAL1 plasmid kindly provided by the lab of Dr. Brenda L. Bass of the University of Utah Biochemistry Department.

TABLE OF CONTENTS

LIST OF TABLES

LIST OF FIGURES

CHAPTER I

INTRODUCTION TO TRANSCRIPTION ERRORS

1.1 Introduction

Since its appearance in 1957, the Central Dogma of Biology has been used to describe the informational pathway in cells, wherein biological sequences prescribed by DNA are transcribed to RNA, following which the RNA sequences are translated into proteins, with these proteins bringing about cellular functions (Crick, 1958). As an integral part of this pathway, messenger RNA (mRNA) molecules are an important precursor in protein production since they convey sequence information from DNA in the nucleus to ribosomes in the cytoplasm in order to guide protein production.

mRNA consists of a single-stranded sequence of ribonucleotides linked by phosphodiester bonds. The bases which form these mRNA sequences are the purines adenine (A) and guanine (G), and the pyrimidines cytosine (C) and uracil (U). Uracil replaces thymine (T), which is one of the two possible pyrimidines present in DNA. Adenine preferentially binds opposite to uracil (opposite to thymine in DNA), and guanine opposite to cytosine (Brenner et al., 1961).

mRNAs are formed by the transcription of genes by the RNA Polymerase II (RNA Pol II) complex, creating a sequence complementary to the copied DNA template strand. In the case of protein coding genes, this process produces a strand known as pre-mRNA, which in eukaryotes requires post-transcriptional processing to become functional. This may include

splicing to remove introns, addition of a RNA 7-methylguanosine cap to the 5´ end, addition of a Poly(A) tail to the 3´ end, post-transcriptional editing, and polyadenylation. While transcription and post-transcriptional processing occurs primarily in the nucleus, where the DNA is located, mature mRNA must be transported to the cytoplasm where ribosomes and transfer RNAs (tRNAs) are located for protein translation to be possible (Cooper, 2000).

Following transport to the cytoplasm, mRNA molecules interact with the translational complex formed from ribosomal proteins and ribosomal RNAs (rRNAs) in order to be used as a template for protein translation. A single mRNA transcript can be translated multiple times before it is degraded (Cooper, 2000).

Due to this transport of information from the genome in order to produce the proteome, mRNA is a completely integral part of cellular function.

1.2 mRNA Fidelity- an Underexplored but Vital System

Despite the importance of mRNA for cellular life as we know it, little research has been done on the fidelity of this vital system until relatively recently. This is primarily due to the historical lack of reliable technologies for studying mRNA transcription fidelity, but also in part due to the assumption that mRNA, given its transient characteristics, is less important and affects cellular health less than DNA or proteins do.

This latter assumption is due to the extremely short half-life of mRNAs compared to that of proteins and DNA, and was applied to low-level or single mRNA errors, not those which occurred at an extremely high frequency. While a DNA mutation can be passed on to daughter cells or offspring, and proteins can survive in cells for long periods of time, mRNAs exist for only seconds to minutes on average, leading to the erroneous supposition that low-level or single errors do not persist in the cell for long enough to cause real damage to cellular health

(Baudrimont et al., 2017). This assumption has been proven to be incorrect. To the contrary, mRNA errors can cause increased risks of apoptosis, cancer, and overall decreases in health levels (Anagnostou et al., 2021; Baysal et al., 2017; Brégeon & Doetsch, 2011; Kapur & Ackerman, 2018; Vermulst et al., 2015). The effects of mRNA errors on cellular health outcomes has been thought to be due to a few different interrelated issues. First, a mRNA with an error in it may produce aberrant proteins. In addition to the cellular costs of producing these transcripts as well as the resulting proteins, which may have reduced, absent, or harmful functions, the detection and removal of increased levels of error-filled transcripts and faulty proteins places a strain on the cellular regulatory machinery which are tasked with their detection and removal. This reduces the ability of cells to respond to other internal or external stressors and properly regulate internal processes, making it difficult to maintain homeostasis.

For these reasons, it is important to understand more regarding transcription errors and how they affect cellular and organismal health.

While the existence of mRNA as an intermediary between DNA and proteins was posited by Brenner, Crick, and Jacob in 1960, and evidence proving it a reality was published in 1961 (Brenner et al., 1961), mRNA was only first successfully sequenced in 1977 (Hong et al., 2020). In the years following, mRNA and cDNA sequencing was primarily used to determine intron and exon locations, then progressed to gene expression assays. Despite this, mRNA fidelity remained difficult to analyze. Only extremely high-level mRNA errors were reliably detectable, making it impossible to determine the actual state of mRNA errors during any given experimental condition. While advancements in technology such as Next-Generation sequencing and single-cell sequencing improved the toolbox available for mRNA researchers, drawbacks in these techniques still made it impossible to distinguish low-level “background” RNA errors from

reverse transcription errors due to base misincorporation by reverse transcriptases, or from erroneous base calls due to the sequencing methods themselves (Hong et al., 2020). It was not until the late 2010s that ultra-high-fidelity sequencing methods were developed based on the replication methods of small circular genomes, such as those in some bacteriophages, viroids, and plasmids. This sequencing method is referred to as Circle-Seq, or Rolling Circle Amplification.

In normal circular replication, the double-stranded DNA or genomic RNA is nicked to open a single-stranded section. Replication proceeds around the circular genome, displacing the original second strand and forming a new one. When replication reaches the origin point, three complete strands of the genetic material are present—one single strand displaced from the original, and one double strand composed of one original and one new strand. The single strand is then replicated again, forming a new double-stranded copy of the genome (Kusumoto-Matsuo et al., 2011). This process was appropriated for use in RNA sequencing. The mRNA produced by the cells under experimental conditions is fragmented, and the 5′ and 3′ ends of these linear fragments are ligated together, which transforms each linear fragment into a circular fragment. These circular sequences are then reverse-transcribed by a reverse transcriptase, which does not halt the reverse-transcription process when reaching the origin point, due to its ability to displace the newly-synthesized second strand. This allows the reverse transcriptase to proceed around the circularized mRNA fragment several times, producing a long cDNA strand in which the original sequence from the circularized mRNA is repeated several times. This allows the sequence from each mRNA to be compared back against itself. If an error is present in each of the repeated sequences, then it is most likely a legitimate mRNA error produced in the cell. If it is present in only one of the repeats, then it is a reverse transcription or sequencing error, and can be removed

from the data pool during bioinformatic processing (Figure 1.1). This allows for ultra-high-fidelity quantification of transcription errors, as well as detection of singly-occurring errors, which is something that is not possible with currently available conventional sequencing methods (Fritsch et al., 2018; Gout et al., 2013, 2017; Tsai et al., 2017). Discovery of Rolling Circle Amplification has therefore revolutionized transcription fidelity research, allowing great advancements in this field.

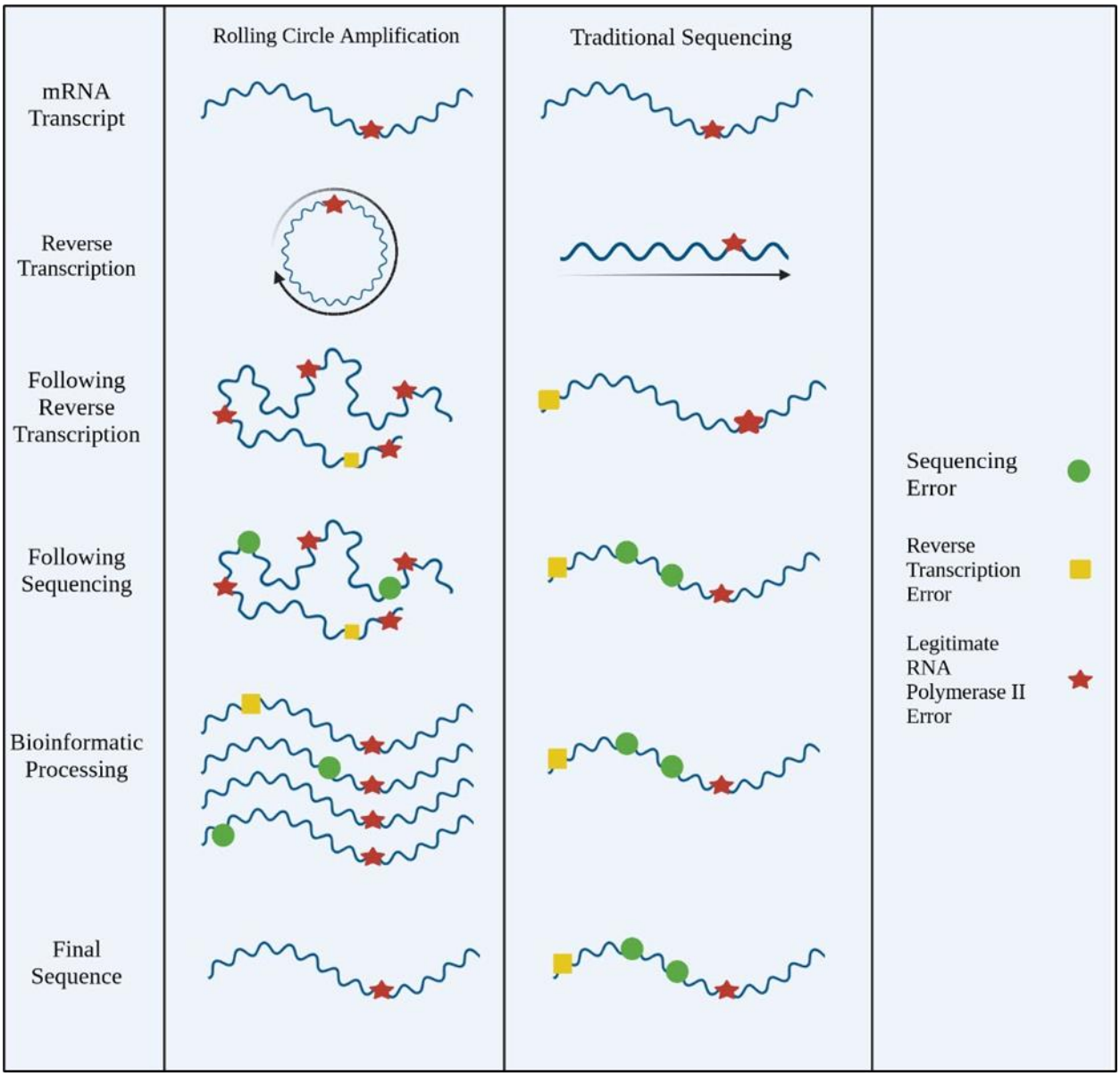

Figure 1.1 Comparison of Traditional and Rolling Circle Sequencing

Comparison of Traditional and Rolling Circle sequencing amplification methods. The wavy line represents an mRNA sequence. The red star represents a legitimate error, the yellow square represents a reverse transcription error, and the green circle represents a sequencing error. Rolling Circle amplification allows self-comparison of the original mRNA sequence, meaning that any errors of non-cellular origin can be cleared from the final sequence, giving much higher accuracy in determining the true number and type of RNA errors than is produced by traditional sequencing methods.

1.3 mRNA Errors

During an mRNA transcripts lifetime, errors may occur which may lead to sequence differences in the amino acid composition of the resulting proteins, and in turn cause alterations in their function. mRNA errors occur when a difference arises between the “normal” sequence prescribed by the template DNA, and the sequence delivered by an mRNA molecule to the ribosome for protein production. During transcription, these errors may arise due to various reasons such as damage to DNA nucleotides altering preferential base pairing or interfering with the normal function of RNA Pol II, simple base misincorporation mistakes made by wild-type RNA Pol II, or RNA Pol II mutations which decrease fidelity. In addition, RNA damage due to chemical or physical means, as well as off-target RNA editing by ADAR or APOBEC-driven editing mechanisms, may occur post-transcriptionally, leading to mRNA sequence errors which could be detrimental to cellular health and functions (Anagnostou et al., 2021).

When DNA damage occurs, a nucleotide may be damaged and altered to form a non-standard nucleotide which is not one of the normal bases A, T, C, or G. Non-standard bases may interact differently with DNA replication or RNA transcription machinery compared to their non-damaged precursors, pairing preferentially with a different nucleotide or ribonucleotide than the original nucleotide at that location would have. If these mutations are not immediately removed and replaced, then transcription of the mutated nucleotide may occur, leading to an mRNA with a non-standard sequence (Brégeon & Doetsch, 2011).

When mRNA is transcribed by an RNA Pol II complex, mismatches may occur. The frequency of RNA Pol II mismatches, as well as reduced proofreading capabilities to identify and repair these errors, may increase when RNA Pol II mutations are present. While certain RNA Pol subunits and transcription factors are not integral for the function of the transcriptional

complex as a whole, their loss greatly reduces fidelity, either by increasing the incidence of mismatches or by reducing the ability of the affected RNA Pol complexes to recognize and repair mismatches when they occur. Some of these include the knockout of RNA Pol II subunit RPB9, the point mutation of RNA Pol II subunit RPB1-E1103G, and as is discussed below in Chapter II, the knockout of RNA Pol II transcription factor TFIIS (also known as DST1). It is interesting to note that loss or alteration of function in these different transcriptional factors and subunits all lead to an increase in the G-to-A error rate compared to the control (Gout et al., 2017).

Finally, damage or off-target editing of pre-existing mRNA may occur. While normal mRNA editing may be necessary for some normal transcript function or proteome plasticity in some cases, such as during neurological development, these editing systems may go awry. When this occurs, mRNAs which are not usually targets of RNA editing may be modified by editing systems if they have enough sequence or structural similarity with the ordinary editing target. These editing events will act similarly to transcriptional errors or direct damage to mRNAs, given that they alter the normal mRNA sequence and thus the resulting proteins (Tonkin et al., 2002).

CHAPTER II

INVESTIGATING CONSEQUENCES OF GENOMIC URACIL ON TRANSCRIPTION FIDELITY IN *C. ELEGANS*

2.1 Introduction

Transcription errors generally occur due to three main causes; aberrant base insertions by RNA polymerase during transcription due to DNA damage sites, simple error on the part of RNA polymerase machinery, or mutations in the DNA itself leading to "nonstandard" mRNA sequence production. There exist certain knockout or point mutations in RNA Pol II which have been shown to greatly increase the rate at which these errors occur, or decrease the efficacy of error recognition and repair machinery.

It might be expected that these errors are equally distributed, with each different type of point mutation occurring at roughly the same rate, but this was not found to be the case. (Gout et al., 2013, 2017). In all eukaryotic wild-type (WT) organisms studied so far, C-to-U errors were by far the greatest base-substitution RNA error discovered. This trend is almost exclusively driven by an increase in errors where guanine was replaced with adenine (G-to-A errors), leading to a paired increase in C-to-U errors (Gout et al., 2013, 2017). In DNA, G-to-A mutations have been hypothesized to be due primarily to the presence of genomic uracil. In mutant model organism strains where RNA Pol II mutations lead to decreases in proofreading, functionality, and fidelity, (G-to-A errors) were much more commonly found than all other types of errors, as

well as being greatly increased in comparison to the G-to-A error levels found in WT individuals (Gout et al., 2013, 2017).

The actual cause of these G-to-A errors in mRNA, and their impact on cellular health, is currently unknown.

2.2 G-to-A Errors and Genomic Uracil

During normal mRNA transcription, a cytosine (C) in the template strand of DNA would be paired with guanine (G) by RNA Pol II.

If RNA Pol II mismatched the bases, a G-to-A error could occur if an adenine was added opposite of a cytosine instead of a guanine, transcribing the normal DNA sequence improperly. In order for this to explain the high levels of G-to-A errors, C-A pairings would need to be preferentially formed and maintained in comparison to all other types of mismatched base pairs. This could happen if C-A mismatch pairings were more stable than all other types of mismatches, however there is no evidence to suggest this. Additionally, there is no corresponding elevation in the A-to-G error rate, which might be expected were base pairing strength the force behind this phenomenon. Therefore, it is unlikely that RNA Pol II is simply mismatching cytosine with adenine at such a high frequency due to an affinity of these nucleotides for each other.

In the case of DNA damage-caused G-to-A errors, a cytosine would deaminate to form genomic uracil. Cytosine is known to deaminate frequently to form genomic uracil spontaneously or when induced by chemical or physical means (Duncan & Miller, 1980; Kreutzer & Essigmann, 1998; Lewis et al., 2016; Sassa et al., 2016). Uracil (U) is a base which normally only is found in RNA, and which is generally paired preferentially with genomic adenine. It has been hypothesized that genomic uracil, in addition to other additional factors such

as abasic sites, may be responsible for G-to-A errors during DNA replication (Auerbach et al., 2005; Hagen et al., 2006; Olinski et al., 2021; Sire et al., 2008). While this hypothesis has been explored in the context of DNA replication, it is still unclear how RNA polymerases process genomic uracil and abasic sites, so their relative contribution to transcription infidelity remains unknown. (Fadda & Pomès, 2011; Krokan et al., 2001, 2002).

In WT organisms this change of cytosine to genomic uracil may be recognized by proofreading mechanisms during transcription, preventing G-to-A errors. The frequency of G-to-A errors was shown to increase drastically in cells with impaired proofreading capabilities (Gout et al., 2013, 2017).

Despite the logic behind the hypothesis that genomic uracil binding with adenine during RNA transcription is the primary cause of G-to-A errors, this may not actually be the case. An alternative hypothesis is that the presence of genomic uracil itself is not responsible for G-to-A errors, but rather specifically the presence of abasic sites formed during the removal of genomic uracil and DNA repair process (Figure 2.1).

Adenines being inserted opposite from abasic sites during RNA transcription could potentially be due to a phenomenon similar to the A-Rule found in some species. The A-Rule states that in some species, adenine is preferentially inserted opposite from abasic sites during DNA replication (Laverty et al., 2017; Liu et al., 2018; Strauss, 1991).

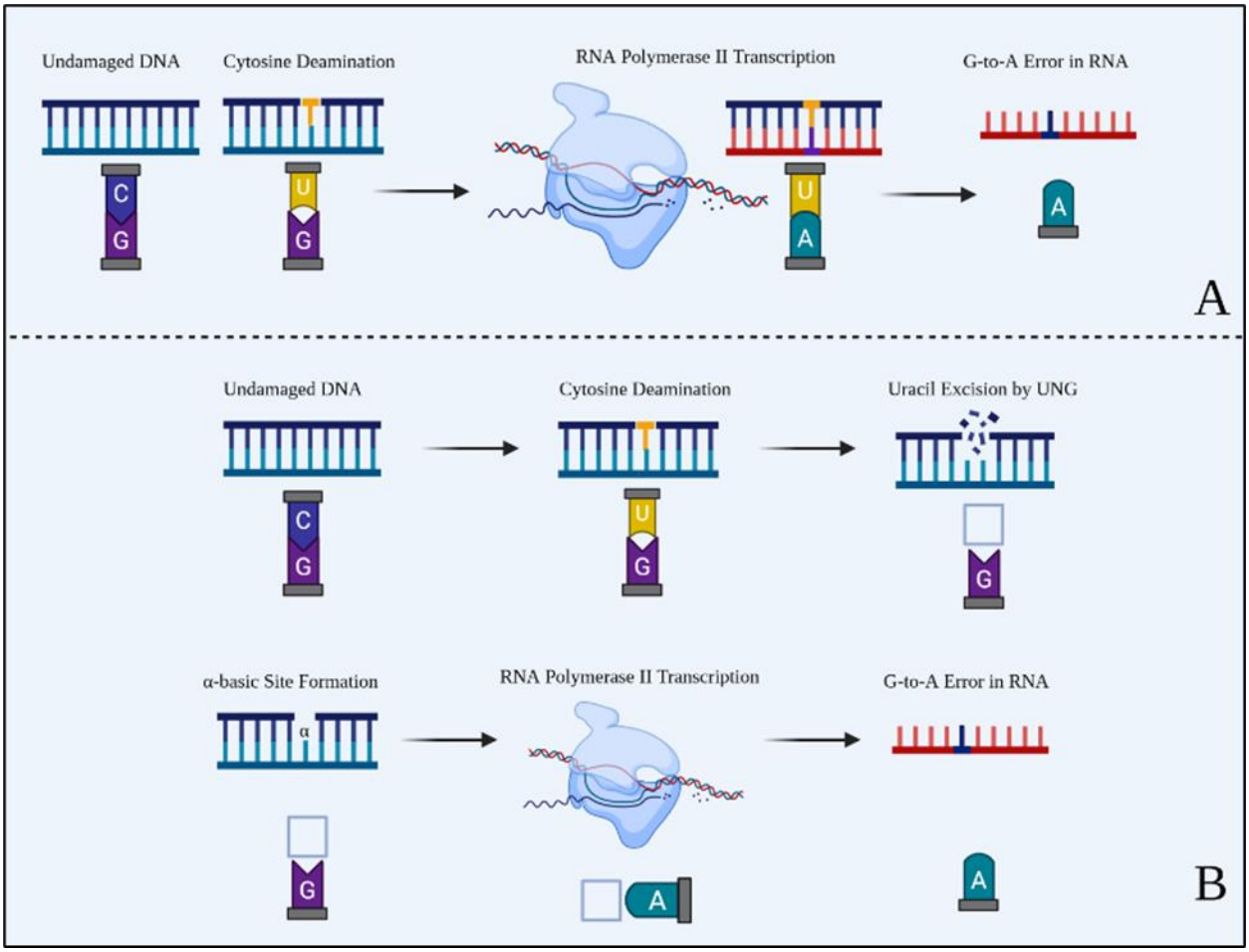

Figure 2.1 Two Possibilities for G-to-A Error Formation

Two hypotheses regarding the formation of transcription errors due to the presence of genomic uracil. (A). G-to-A transcription errors occurring as the result of base pairing between genomic uracil and adenine during transcription, and (B). G-to-A errors occurring as the result of aberrant adenine insertions at abasic sites. DNA=blue, RNA=red, genomic uracil=yellow, erroneous adenine=purple.

2.3 *C. elegans* Strains

In order to investigate the cause of this transcriptional phenomenon, a strain of homozygous double knockout (dHz-Δ) *Caenorhabditis elegans* worms was developed using two single-knockout strains obtained from the University of Minnesota Caenorhabditis Genetics Center. The chosen strains to create the dHz-Δ strain were UNG1-Δ and DST1-Δ.

The DST1 gene in *Saccharomyces cerevisiae* encodes Transcription Factor IIS (TFIIS), one of the transcription factors binding to RNA Pol II. It is associated with transcription initiation and fidelity (Awrey et al., 1997; Koyama et al., 2003; Malagon et al., 2004). Knockout of this gene had previously been shown to increase levels of transcription errors in *C. elegans*, likely by reducing stability of the RNA Pol II complex (Gout et al., 2017). While the exact mechanism for the associated reduction in transcription fidelity is unknown, there are two main possibilities. When DST1 is knocked out, RNA Pol II will lose the ability to backtrack and repair detected DNA damage or mismatches. This will cause the RNA Pol II complex to stall at the site of the impairment, however eventually the complex may bypass the site and proceed forward, thus incorporating an error which would, in the presence of the DST1 subunit, have been repaired. Alternatively, DST1 knockout may reduce stability of the RNA Pol II complex sufficiently to make it either more difficult for RNA Pol II to recognize damage or misincorporation, or easier for stalled transcription to immediately bypass these sites without waiting for repair. This would prevent recognition and repair of these areas, thus increasing the transcription error rate (Gout et al., 2017; Owiti et al., 2017).

The UNG1 gene in Homo Sapiens encodes the gene Uracil-DNA Glycosylase (UDG), which excises uracil bases in the genome caused by cytosine deamination, forming abasic sites which are then recognized by repair mechanisms for template strand-based repair. It does this by scanning DNA for the presence of uracil. When a genomic uracil base is detected by UDG, it cleaves the glycosidic bond between the uracil and the phosphodiester backbone of DNA, removing it from the DNA strand. This creates an abasic site, which is a site on a DNA or RNA strand which contains neither a purine or pyrimidine base (Impellizzeri et al., 1991; Krokan et al., 2001; Sarno et al., 2019). In *C. elegans*, only two DNA glycosylases exist, UNG1, and

NTH1. While NTH1 can somewhat rescue the UNG1-Δ condition, the enzymatic activity is limited when applied to uracil excision, since it primarily acts to remove damaged thymine bases from the genome (Elsakrmy et al., 2020; Rao et al., 2014; Y. Yang et al., 2019). This means that many genomic uracil sites will not be excised by these DNA glycosylases, leading to a buildup of genomic uracil in the genomes of UNG1-Δ individuals, even under normal levels of cytosine deamination.

2.3.1 Two Hypotheses

If genomic uracil pairing with adenine during transcription is the cause of increased G-to-A error rates, increased levels of genomic uracil should combine with proofreading-deficient RNA Pol II to increase the overall number of errors that are integrated into mRNAs. This would be expected to show a G-to-A error rate in the dHz-Δ condition higher than that found in either parent strain.

If genomic uracil is not the direct cause of the observed high levels of G-to-A errors, but rather the presence of abasic sites, then knockout of UNG1 would prevent the formation of abasic sites, leading to fewer locations where the more error-prone RNA Pol II can make a mistake in transcription. This would be expected to show a G-to-A error rate in the dHz-Δ condition which is intermediate to either parent strain.

2.4 Materials and Methods

2.4.1 Transcription Error Analysis

WT, UNG1-Δ, and DST1-Δ *C. elegans* worms obtained from the Caenorhabditis Genetics Center were grown in a 20 ºC incubator on agar plates with an E. coli lawn, in accordance with the protocols set out in the online nematode protocol repository WormBook

(Stiernagle, 2006). UNG1-Δ and DST-Δ strains of *C. elegans* were heat shocked in an incubator at 31.5 ºC for 5 hours in order to induce the development of male worms. 8-10 juvenile male UNG1-Δ worms were transferred to plates containing single juvenile hermaphrodite DST1-Δ worms. The worms were allowed to cohabitate until eggs were observed on the plates, following which the adult worms were removed, and the eggs reared until hatching to form the F1 generation. Single F1 hermaphrodite worms were transferred to fresh agar plates and allowed to self-fertilize, forming the F2 generation. Single F2 hermaphrodite worms were transferred to fresh agar plates and allowed to self-fertilize, forming the F3 generation. By the F2 generation, individuals carrying a double homozygous knockout for both the UNG1-Δ and DST1-Δ genes would have these knockouts fixed in the population, however a sufficient quantity of these double homozygous knockout individuals would be required for DNA extraction and PCR amplification, necessitating the production of the F3 generation. PCR confirmation of double homozygous knockout strain dHz-Δ was performed using an Extract-N-Amp kit (Sigma-Aldrich) followed by gel electrophoresis (Figure A.7).

All four worm strains were reared for four days, to ensure a sufficient quantity of adult worms for RNA extraction. Eight agar plates of worms were used per replicate. Worms were gently washed from the plates using 2mL deionized water and collected in 15mL tubes. The collected worms were gently centrifuged to pellet, before removing the supernatant. This process was repeated two more times in order to remove contaminants and produce clean worm samples. A final centrifugation formed 100µL worm pellets. Replicate 100µL worm pellets were lysed using a RiboPure kit (Thermo-Fisher) and Phenol:Chloroform:Isoamyl alcohol (Ambion), and placed in 1.5 mL screw cap tubes containing ice-cold zirconia beads (Thermo-Fisher). These tubes were vortexed at maximum speed for 10 minutes in order to lyse cell walls. Following

extraction of the resulting supernatant, DNA and RNA contamination was removed using DNase I (Thermo-Fisher) and oligo(dT) beads (Thermo-Fisher), respectively. Fragmentation of the mRNA prior to circularization was performed using RNase III (Thermo-Fisher), followed by cleanup using an Oligo Clean & Concentrator kit (Zymo). mRNA fragment circularization was achieved using a 2-hour ligase protocol, followed by a reverse transcription protocol employing a reverse transcriptase with strand displacement capabilities (Thermo-Fisher). Second strand synthesis and end repair were performed on the resulting cDNA. Successful completion of the Rolling Circle protocol was determined using TapeStation (Aligent) electrophoresis to quantify the resulting cDNA fragment size, and Qubit Fluorometer (Invitrogen) fluorescent quantification of RNA, mRNA, and cDNA abundance. The entire Rolling Circle protocol was performed in accordance with the protocol set out in (Fritsch et al., 2018).

Following completion of the Rolling Circle protocol, cDNA samples were sent for sequencing at the University of New Hampshire Hubbard Center for Genome Studies. Bioinformatics analysis was performed by Dr. J-F Gout as recommended in (Fritsch et al., 2018; Gout et al., 2017).

2.4.2 Longevity and Motility Assay

WT, UNG1-Δ, DST1-Δ, and dHz-Δ strain *C. elegans* worms were reared in accordance with the protocols set out in the WormBook (Stiernagle, 2006) until gravid hermaphrodites were observed in the population. A bleach synchronization was performed (Porta-de-la-Riva et al., 2012). This exposed plates of worms which contained a number of gravid hermaphrodites to a solution containing 0.8% bleach for 3 minutes, before pelleting the worms, removing the supernatant containing bleach, and washing the worms three times using M9 buffer in order to remove any traces of bleach remaining on the pellets, which were then re-plated on fresh agar

plates. The bleach solution kills the adult worms, but does not kill the unhatched eggs, forming a colony of individuals which are all the same age. From this cohort, 16-17 juvenile worms were transferred to 10 agarose plates per strain, forming populations of 160 worms in the WT, DST1-Δ, and dHz-Δ strains, and 161 in the UNG1-Δ strain.

The day of transfer was designated as day 0 of the experiment. Worms were retransferred to fresh plates daily in order to prevent confusion between the original worms from day 0 and their offspring, until reproduction had ceased, following which checks were performed daily for deceased worms. All dead worms were removed from the plates once daily. ≥12 timelapse images of each plate taken at 1-second intervals were obtained on days 2, 3, 8, 9, 14, and 15 of the experiment, and analyzed to obtain motility data using FIJI (Image J) software (Amrit et al., 2014; Mack et al., 2018; Schindelin et al., 2012; Weaver et al., 2017; J.-S. Yang et al., 2011).

2.5 Results and Discussion

2.5.1 Transcription Error Rates

2.5.1.1 First Hypothesis- Genomic Uracil

If the first hypothesis, namely that high G-to-A error rates are caused by the pairing of genomic uracil with adenine during transcription, were to be correct, certain transcription error rate patterns would be expected from the different *C. elegans* strains tested in this study.

The expectation would be that the UNG1-Δ strain would have high G-to-A error rates compared to the WT control due to high amounts of genomic uracil, and that the DST1-Δ strain would also have high G-to-A error rates compared to the control due to reduced transcriptional proofreading and fidelity. Finally, that the dHz-Δ strain, having a combination of both of these traits, should have had a significant increase in the G-to-A error rate compared to either of the two parent strains, UNG1-Δ and DST1-Δ, as well as compared to the control.

This was not the case. In fact, while the dHz-Δ strain G-to-A error rates were much higher than were found in the WT or the UNG1-Δ strain, they were significantly lower than those present in the DST1-Δ strain. The DST-Δ G-to-A error rate increased 15 times compared to the WT control, while the dHz-Δ G-to-A error rate was only increased 11 times compared to the WT strain (Figure 2.2).

These results are not in line with the hypothesis that genomic uracil was paired with adenine by RNA Pol II during transcription.

2.5.1.2 Second Hypothesis- abasic Sites

This hypothesis posits that abasic sites, not the presence of genomic uracil specifically, are responsible for the transcription error patterns observed in these nematode strains.

In this case, the expectation would be that the UNG1-Δ condition would prevent excision of genomic uracil, preventing the formation of abasic sites in the genome. If RNA Pol II were truly matching adenines with abasic sites formed by the removal of genomic uracil, possibly due to a phenomenon similar to the A-Rule in DNA replication, this would cause a reduction in the number of observed G-to-A errors where the UNG1 knockout has occurred due to a reduction in abasic site numbers.

This hypothesis is upheld by the G-to-A transcription levels observed in this study (Figure 2.2). The number of G-to-A errors in the dHz-Δ condition are intermediate to either parent strain, though still higher than those found in the control. It is also interesting to note that G-to-A errors in the UNG1-Δ strain were found to be 0.75 times that of the WT condition, which would be expected if this hypothesis were correct.

While the UNG1-Δ knockout produced other effects on organismal health, as evidenced below in the discussion regarding motility and longevity, it seems apparent that in some cases it

may reduce overall transcription error rates slightly compared to the WT and significantly when other factors are in play as is the case in the dHz-Δ condition.

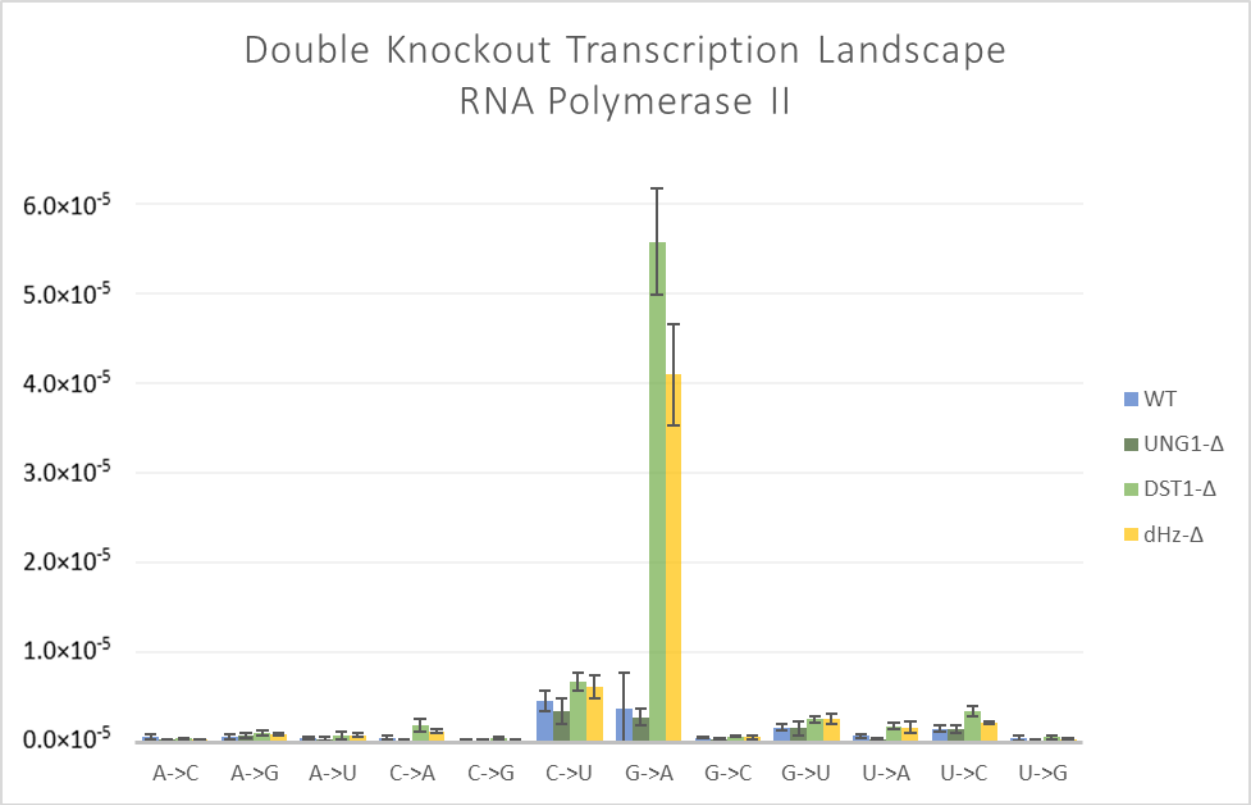

Figure 2.2 Strain Error Rate Comparison in RNA Polymerase II Transcriptional Landscape

Transcriptional landscape depicting comparative mRNA error types in transcripts produced by the action of RNA polymerase II in dHz-Δ, DST1-Δ, UNG1-Δ, and WT (control) *C. elegans* strains. Error bars are standard deviation.

2.5.2 Motility and Longevity Assay:

While transcription errors may be transient and produce no permanent effects from an evolutionary standpoint, they can still produce lasting effects on an individual's health and longevity.

Differences in motility are often taken as a representative of overall health in comparison of *C. elegans* populations.

It must be noted that high-motility strains are likely to produce a large number individuals which crawl off of the agar plates they are on and die from dehydration. This death is unrelated to the experimental conditions they were initially placed under, leading to the requirement to treat them as censors. Ordinarily, censoring is done as a way to alleviate the effects of this type of experimental confound, however when they occur at high levels they will still impact the resulting survival data. Due to this issue, highly motile strains may have notable early-term depressions in survival curves compared to those with lower motility. This is partially due to the individuals which were most active, and thus most "healthy" leaving the population via the edge of the plate. This will therefore skew the longevity of these strains to be lower than would have otherwise been seen. In populations where health/motility is highly variable, lower-than-actual health may be presented in the results, since it will be the least healthy/motile worms which remain on the plate to be analyzed, while the most healthy/motile worms have been lost as censors.

In this experiment, the strains were determined to have statistically significant differences in motility only between the DST1-Δ and WT strains on day 3 of the experiment, however the pattern displayed was intriguing nonetheless.

2.5.2.1 Motility, Longevity, and Death Rates

On day 3 of the experiment when all worm strains exhibited the highest motility levels, as well as the only timepoint at which significant differences in motility were noted between the worm strains, the DST1-Δ and dHz-Δ strains exhibited the lowest motility levels (Figure 2.3). These two strains had previously been determined to have very high G-to-A error rates (Figure

2.2), indicating that significant increases in G-to-A errors may have a detrimental effect on motility levels.

Due to high censor population percentages (Figure 2.6), it is more helpful to look at the relative death rates for each nematode strain (Figure 2.5) than it is to look at the longevity curves (Figure 2.4), since the relative death rate is not as impacted by censors. In this figure, it can be seen that the DST1-Δ strain has the highest relative death rate, while the WT strain has the lowest for the majority of the survival assay.

2.5.2.2 Statistical Differences in Longevity

Statistical differences in longevity ($P \leq 0.05$) overall in the survival assay were found between the WT and DST1-Δ (P-value = 0.007), and the WT and UNG1-Δ (P-value = 0.004) strains only (Table 2.1). There was no statistical difference between WT and dHz-Δ observed (P-value = 0.0718).

Intriguingly, at the early stages of the study, there was a significant difference between the WT and UNG1-Δ strains (P-value = 0.0096), as well as between the dHz-Δ and UNG1-Δ strains (P-value = 0.014), but this lost statistical significance three-fourths of the way through the experiment (Table 2.2).

In contrast, the WT and DST1-Δ (P-value = 0.0006), dHz-Δ and DST1-Δ (P-value = 0.0008), and UNG1-Δ and DST1-Δ (P-value = 0.0146) strains which lacked significance at the onset of the experiment, gained it by the end (Table 2.2).

This may indicate that throughout the lives of these *C. elegans* strains, the mutations present in the dHz-Δ, DST1-Δ, and UNG1-Δ strains have variable effects on the health of each strain. In early and late life stages, health levels fluctuate, leading to the appearance and disappearance of statistical differences between the strains seen here (Table 2.2), however

overall these mutations were not significant enough to cause differences between the majority of the strains in the entire experiment.

In the dHz-Δ strain, it is possible that variances in individual worm health may be present due to interactions between the two knockouts present in this strain. This would allow for the censor activity seen in dHz-Δ worms (Figure 2.6), which suggest a high level of worm movement, to be combined with the information present in the motility results (Figure 2.3) which suggest relatively low worm movement in comparison with the WT strain. If variances in phenotype as evidenced by motility were present in this strain, then a large proportion of the most motile individuals could have left the plate and been censored, while the individuals remaining on the plate would be those which were more negatively affected by the mutations and therefore less motile, explaining the contrast between the censor and motility data shown here.

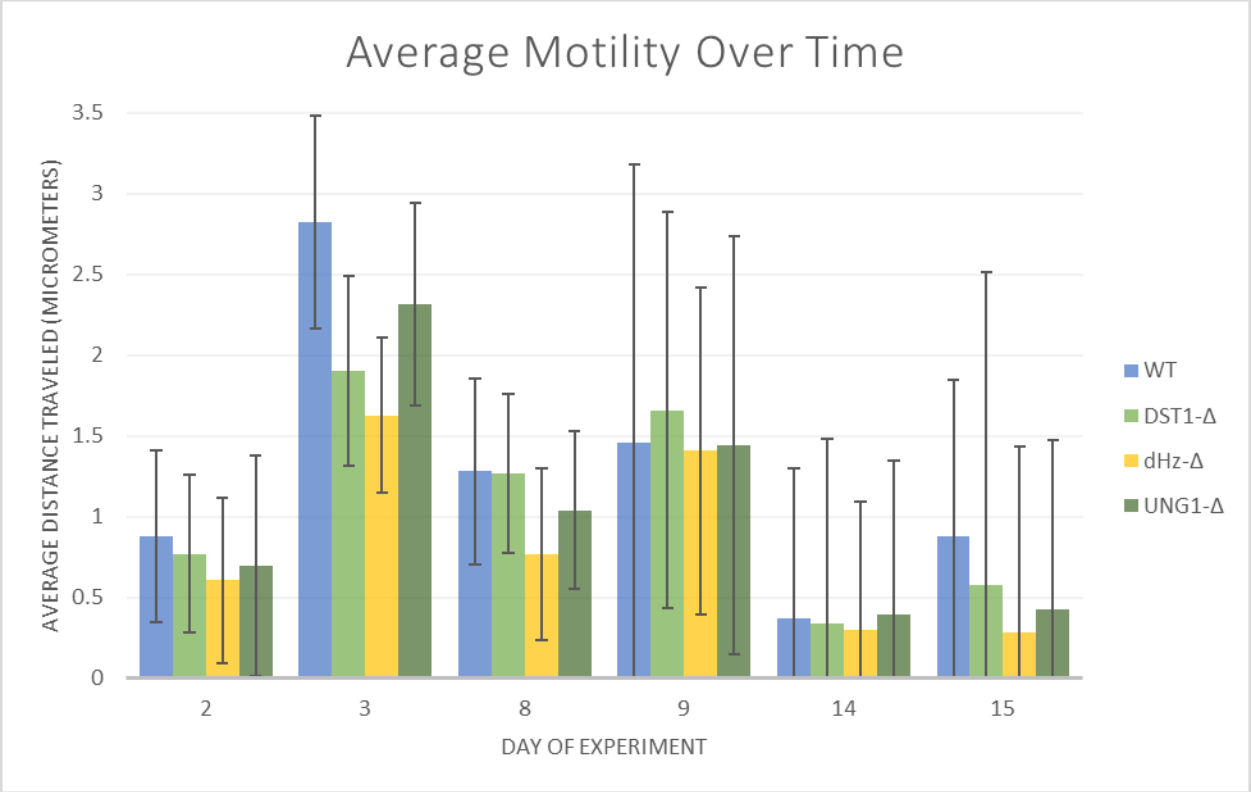

Figure 2.3 *C. elegans* Strain Motility Comparison Over Time

Figure depicts average distance traveled (μm) by each *C. elegans* WT (control), DST1-Δ, dHz-Δ, and UNG1-Δ strain. Error bars are standard deviation.

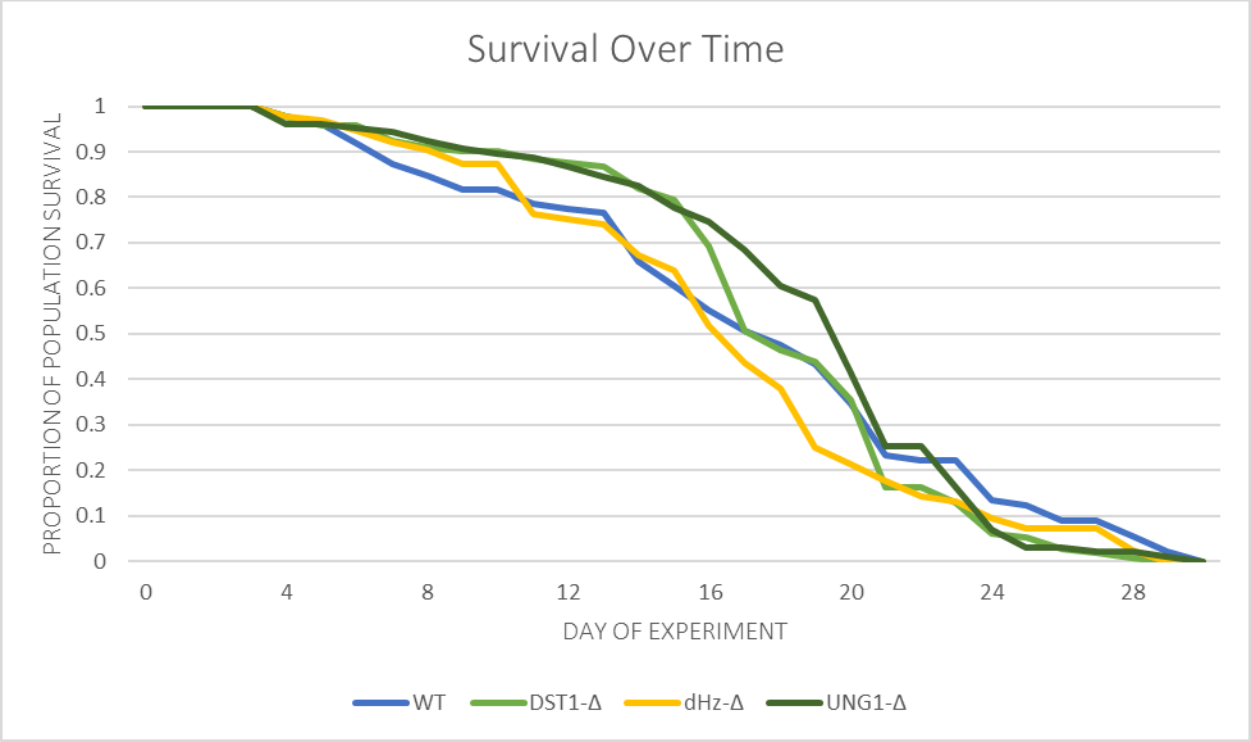

Figure 2.4 *C. elegans* Strain Population Survival Over Time

Figure depicts proportion of population survival for *C. elegans* WT (control), dHz-Δ, DST1-Δ, and UNG1-Δ strains over time

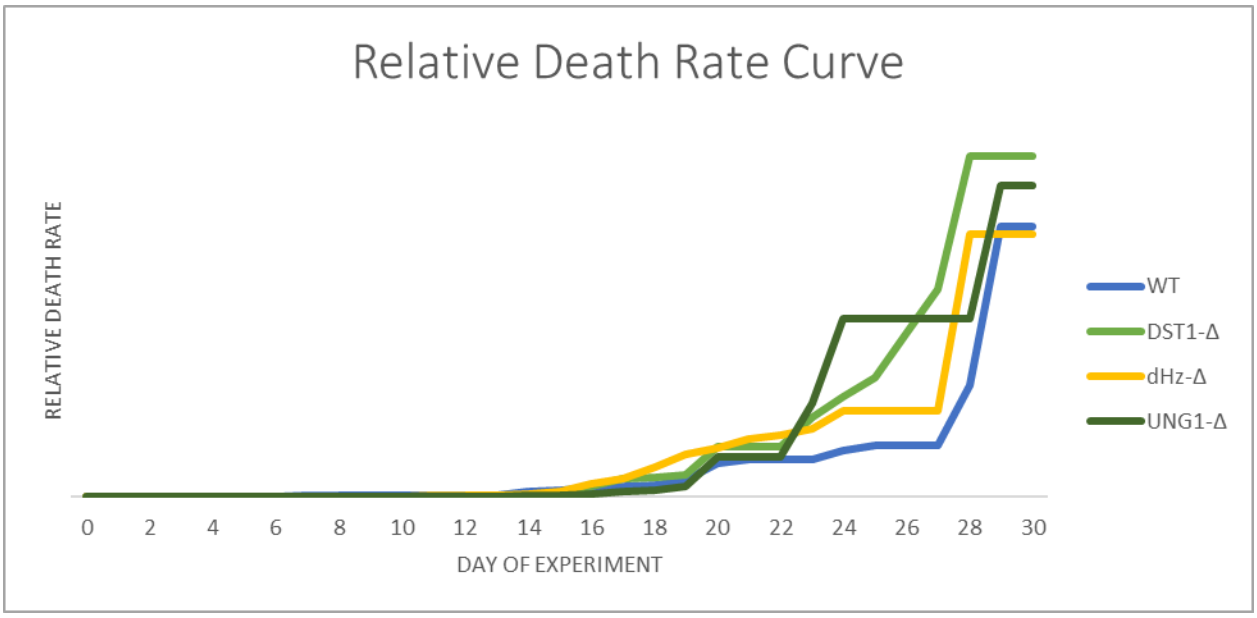

Figure 2.5 *C. elegans* Strain Relative Death Rates Over Time

Figure depicts the relative death rates for *C. elegans* WT (control), dHz-Δ, DST1-Δ, and UNG1-Δ strains over time

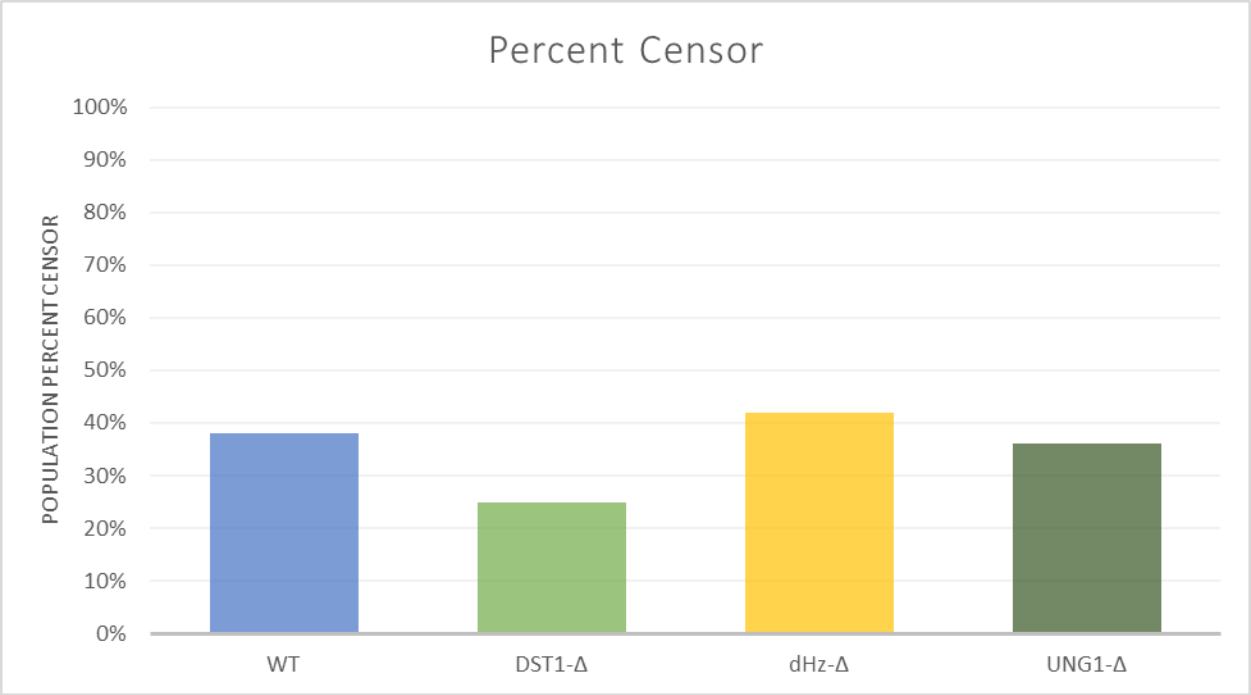

Figure 2.6 *C. elegans* Strain Population Percent Censored Individuals

Figure depicts the percentage of censored individuals for each strain population in the motility and longevity assay. *C. elegans* strains WT (control), DST1-Δ, UNG1-Δ, and dHz-Δ.

Table 2.1 Survival Time F-Test *C. elegans* Strain Comparison

Condition	Ratio of variances	P-value	Bonferroni P-value
WT vs. dHz-Δ	1.35	0.0718	0.2154
WT vs. DST1-Δ	1.76	0.0007*	0.002*
WT vs. UNG1-Δ	1.8	0.0004*	0.0012*
dHz-Δ vs. WT	0.74	0.0718	0.2154
dHz-Δ vs. DST1-Δ	1.3	0.1114	0.3341
dHz-Δ vs. UNG1-Δ	1.33	0.0827	0.2482
DST1-Δ vs. WT	0.57	0.0007*	0.002*
DST1-Δ vs. dHz-Δ	0.77	0.1114	0.3341
DST1-Δ vs. UNG1-Δ	1.02	0.8825	1.0
UNG1-Δ vs. WT	0.55	0.0004*	0.0012*
UNG1-Δ vs. dHz-Δ	0.75	0.0827	0.2482
UNG1-Δ vs. DST1-Δ	0.98	0.8825	1.0

Survival Time F-Test for motility of *C. elegans* WT (control), DST1-Δ, UNG1-Δ, and dHz-Δ strains. (J.-S. Yang et al., 2011).
* Denotes significance levels ≤0.05

Table 2.2 Fisher's Exact Test *C. elegans* Strain Comparison

Condition	P-value at 25%	P-value at 50%	P-value at 75%	P-value at 90%
WT vs. dHz-Δ	0.7524	0.5487	0.8227	0.9109
WT vs. DST1-Δ	0.1436	0.1933	0.0024*	0.0006*
WT vs. UNG1-Δ	0.0096*	0.1151	1	0.3142
dHz-Δ vs. DST1-Δ	0.1851	0.5595	0.0069*	0.0008*
dHz-Δ vs. UNG1-Δ	0.014*	0.0155*	0.8233	0.3708
DST1-Δ vs. UNG1-Δ	0.0689	0.0015*	0.0025*	0.0146*

Fisher's Exact Test for motility of *C. elegans* WT (control), DST1-Δ, UNG1-Δ, and dHz-Δ strains. (J.-S. Yang et al., 2011).
* Denotes significance levels ≤0.05

2.6 Conclusions

Transcription errors have historically been considered transient, and therefore not as significant a risk to health and longevity as things such as DNA mutations, however recent breakthroughs in RNA technology have allowed further research into the effects of these seemingly insignificant errors. One of the most common types of errors, guanosine-to-adenine (G-to-A) errors, has long been thought to be caused by the pairing of genomic uracil caused by cytosine deamination with adenine during DNA replication, and thus might be assumed to follow the same patterns during transcription. The findings of the experiments presented in this paper indicate that this assumption may be incorrect—it suggests that this phenomenon is instead due specifically to adenine being inserted opposite from abasic sites. abasic sites are formed as part of the base excision and repair process in response to genomic uracil. While these abasic sites will be formed in greater numbers when greater amounts of genomic uracil are present in DNA, our evidence suggests that genomic uracil itself is not being directly paired with adenine during transcription, and therefore is not the direct cause of G-to-A errors. It is currently unknown what may be preventing the preferential pairing of adenine with genomic uracil during transcription,

since adenine is normally paired with uracil by RNA Pol II, however it is important to note that genomic uracil is formed by the deamination of cytosine, leading to the possibility that there are structural differences between uracil and genomic uracil. This could reduce the stability in a GU-A pairing in comparison to the bond strength normally seen in a U-A pairing.

Halting the production of abasic sites through Uracil DNA Glycosylase knockout helps to "rescue" the condition of error prone individuals who lack TFIIS proofreading capabilities, reducing the overall levels of errors present in the dHz-Δ strain compared to the DST1-Δ parent strain. While the effects of this rescue seem to be non-uniformly distributed throughout the dHz-Δ strain, causing differences in individual motility as indicated by the disparity between censor numbers and motility assay findings, it seems to decrease the death rate to one closer to that of the WT control, despite the increased levels of transcription errors which are more comparable to the DST1-Δ parental strain. Reduced transcriptional proofreading capabilities in the presence of genomic uracil, such as is found in the DST1-Δ strain, causes both significantly reduced motility and late-term longevity. These findings suggest that transcription errors can have a significant effect on health and longevity, as well as reveal a hitherto unknown mechanism behind one of the most common of these errors.

Future research which may further understanding of this phenomenon could include a double knockdown of NTH1 and UNG1, to investigate effects of a total loss of UDG activity. Induction of cytosine deamination in the DST1-Δ, UNG1-Δ, and dHz-Δ condition to observe how these strains function under high deamination conditions, such as those which may be expected under environmental stress. And finally, exposing a short DNA sequence containing a genomic uracil in a known location to RNA Pol II in the presence or absence of a UDG, in order to clearly determine the preferences of genomic uracil pairing.

CHAPTER III

MORTALITY, TRANSCRIPTIONAL FIDELITY, AND GENE EXPRESSION IN *C. ELEGANS* AND *S. CEREVISIAE* EXPOSED TO THE GLYPHOSATE BASED HERBICIDE ROUNDUP

3.1 Background

For many years, glyphosate-based herbicides (GBHs) have been the center of a debate concerning their potential ability, or lack thereof, to cause cancer and other diseases.

While the Environmental Protection Agency (EPA) as well as multiple research groups have released reports concluding that glyphosate does not cause DNA mutations (De Roos et al., 2003; EPA, 2018; Tarazona et al., 2017), other research groups are unsure whether or not it may cause cancer (Andreotti et al., 2018; Benbrook, 2019; Zhang et al., 2019). Many other research groups have reached the consensus that glyphosate does increase the risk of developing certain types of cancer, as well as many other health issues, in animal models. Despite this, there is still limited evidence to support this hypothesis in humans.

The main disease correlated with long-term GBH use in humans is an increased chance of developing non-Hodgkin's lymphoma, however disorders in animal models exposed to GBHs include anemia, benign and non-benign tumors, gastrointestinal disorders, and birth defects (Eriksson et al., 2008; George et al., 2010; IARC, 2017; Samsel & Seneff, 2013; Schinasi & Leon, 2014; Suárez-Larios et al., 2017; Wang et al., 2019).

Monsanto and Bayer, Monsanto's purchaser, settled tens of thousands of lawsuits concerning these side effects in 2020 with a ten-billion-dollar settlement, indicating the importance of characterizing the consequences of GBH use. Multiple countries have banned the use of GBHs in certain capacities, including Saudi Arabia, Australia, and parts of Europe. Despite this legal and regulatory action, the actual effects of GBH exposure in humans, and the mechanisms which could be behind the effects seen in animal models, are still under debate.

3.2 Glyphosate and Glyphosate-Based Herbicides

Glyphosate, otherwise known as N-phosphonomethyl glycine, is derived from glycine, an amino acid. Glyphosate was first synthesized in 1950 by Dr. Henri Martin, but the discovery went unpublished. The company Dr. Martin worked for was sold, and the rights to glyphosate were acquired by Monsanto and developed into the GBH Roundup used today in 1970. Following development of Roundup Ready crops, use of Roundup and other GBHs increased rapidly in the agricultural community, and it has become ubiquitous in the US and other countries for crop and weed control (Dill et al., 2010). It was described as the "virtually ideal" herbicide in part due to its purported safety (Duke & Powles, 2008), and has been touted as "safe enough to drink" by ecologist Dr. Patrick Moore in 2015, though he declined to demonstrate when offered a glass of the product.

Glyphosate works by inhibiting the shikimate pathway, a metabolic pathway in plants, fungi, bacteria, and a few other domains, but not found in animal species. This pathway is necessary for the biosynthesis of vitamin B9, and the amino acids tryptophan, phenylalanine, and tyrosine. Function of this pathway is necessary for continued survival in organisms possessing it. Glyphosate binds tightly to phosphoenolpyruvate, preventing dephosphorylation and thus formation of chorismic acid, an amino acid precursor (Dill et al., 2010).

Although glyphosate is the active ingredient in these herbicides, another point of interest is the possibility that other ingredients in the formulation might be carcinogenic or otherwise toxic to animal models or humans, or might be interacting with glyphosate to enhance its carcinogenic or toxic potential when used (Defarge et al., 2018). Since most of the ingredients making up commercially available GBHs are proprietary and therefore unlisted, it is unknown what makes up anywhere from 2% to 50% of each different brand and formulation (Heilig, 2012). This may be at least part of what is causing the debate concerning the actual carcinogenic effects of glyphosate, since if some studies are using pure glyphosate, and others are using off-the-shelf products containing glyphosate, they may have different results. Due to these issues, and the fact that pure glyphosate is rarely if ever used outside of a research laboratory, this study uses one of the most popular off-the-shelf weed killers, Roundup® by Bayer rather than pure glyphosate.

3.3 Glyphosate-Based Herbicides and pH

GBHs such as Roundup are somewhat acidic, meaning that treatment with these herbicides may have other effects on organismal health due to an altered cellular environment, rather than any inherent toxicity.

DNA and RNA react differently in acidic and basic conditions. DNA is known to be stable in a pH range of 5-9.5, however even a drop in pH from 7.4-6.5 can perceptibly affect DNA damage and repair, and an acidic pH can induce nucleotide protonation (Mallajosyula & Pati, 2007; Massonneau et al., 2018). RNA is stabilized by an acidic environment, with RNA structures strongest at a pH range of 4-7.5. Above this pH, RNA structures become increasingly susceptible to hydrolysis and alterations in transcriptional regulation (Bernhardt & Tate, 2012; Hall et al., 2008). Due to these different factors, there will be different levels of DNA and RNA

errors that occur as the cellular pH varies, and it cannot be reliably predicted what the ultimate outcome of pH variation will be in regard to transcriptional fidelity. Furthermore, most or all species may encounter environments with varying pHs naturally in the wild, which has led to the development of coping mechanisms for the resulting cellular changes. Using the model organisms used in this publication as an example, *C. elegans* is capable of surviving in a pH range of approximately 3 to 12, while *S. cerevisiae* can survive in a pH range of approximately 2.5 to 8.5 (Cong et al., 2020; Khanna et al., 1997; Matthews & Webb, 1991; Orij et al., 2011). How the damage to the genome and transcriptome varies, and what type of damage occurs, will determine the overall impact on cellular and organismal health.

3.4 Mechanism of Action

While GBHs have been implicated in cancerous cell development in animal models, as well as displaying detrimental effects to single- and multi-cellular eukaryotic health and longevity in these models the mechanism of action for these effects is currently under debate.

Despite some findings that glyphosate and glyphosate-based herbicides are safe and do no increase DNA mutation rates (EPA, 2018; Tincher et al., 2017), other research has shown that via oxidative stress and inflammatory pathway damages, DNA mutations can occur as a result of exposure to even low levels of these weed killers (George et al., 2010; Kwiatkowska et al., 2017; Suárez-Larios et al., 2017; Woźniak et al., 2020). These findings may not fully explain the broad range of diseases linked with GBH use in animal models. Inflammatory and oxidative stress pathways may be triggered by a number of reasons, and low levels of DNA damage alone cannot explain the many diseases glyphosate-based weed killers have been linked to.

One possible explanation may be an increase in transcription error rates. Buildup of partially functional, nonfunctional, or aberrantly functional proteins and RNAs in cells causes a

burden to proofreading and regulatory machinery, and lead to breakdown of normal cellular function. This has been linked to cell death or the formation of various diseases, including precancerous and cancerous cells (Baysal et al., 2017; Brégeon & Doetsch, 2011; Chan et al., 2020; DeOcesano-Pereira et al., 2018; Kung et al., 2018; Vermulst et al., 2015; H. D. Yang & Nam, 2020). Since these adverse effects are broad and transcription errors are difficult to quantify, they may be implicated in many otherwise difficult-to-ascertain mechanisms of action, as is the case when investigating how GBHs might be able to cause disease in animal models.

3.5 Oxidative Stress and Inflammation Damage:

Inflammation, and the oxidative stress which results from it, has been linked with numerous diseases, including cancerous cell formation, due to the DNA and RNA damage it causes. Roundup has been shown to cause inflammation and oxidative stress at even low levels of exposure. This makes oxidative stress and other inflammatory by-products a viable candidate for the root cause behind at least some of the health issues attributed to Roundup use (Degtyareva et al., 2013; Kay et al., 2019; Li et al., 2006; Pandey et al., 2019; Peillex & Pelletier, 2020). Reactive oxygen species (ROS) produced during oxidative stress are strongly linked with damage to cytosine and guanine bases through oxidation and deamination, while acids produced by inflammatory cells have been shown to damage cytosine bases via halogenation (Degtyareva et al., 2013; Kay et al., 2019). Therefore, it is expected that cytosine and guanine transcription errors may be observed under experimental condition, if the hypothesis of oxidative stress under glyphosate exposure conditions is correct (Figure 3.1).

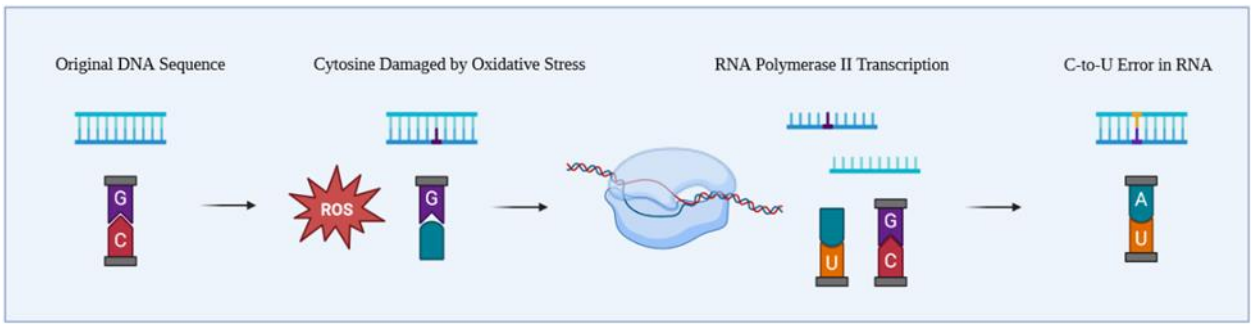

Figure 3.1 C-to-U Transcription Errors from Oxidative Stress

Illustration of how C-to-U transcription errors may be caused by oxidative stress. A cytosine is damaged, forming an adenine analogue, which pairs with uracil during transcription, forming a C-to-U error in the RNA.

3.6 Materials and Methods

3.6.1 Transcription Error Rate Rolling Circle

WT *C. elegans* worms obtained from the University of Minnesota Caenorhabditis Genetics Center were reared in a 20 ºC incubator on agar plates with an Escherichia coli lawn, in accordance with the protocols set out in the online nematode protocol repository WormBook (Stiernagle, 2006), until a sufficient quantity of adult worms were observed. They were then washed from the plates using M9 liquid media containing 5%, 1%, 0.1% and 0% (control) glyphosate. These different experimental concentrations were produced by mixing M9 media with commercially available Roundup concentrate containing 18% glyphosate. The ordinary use instructions for this Roundup product would create a solution containing 0.8 – 0.84% glyphosate.

The nematodes were exposed to the four different experimental concentrations at room temperature for 60 minutes with gentle agitation. Following this, the worms were pelleted using gentle centrifugation before being resuspended in deionized water. This was repeated two more times in order to remove residual Roundup and other contaminants, and centrifuged to produce

100µL worm pellets. Replicates were purified and amplified in accordance with the protocol set out in (Fritsch et al., 2018), and described in detail above in section 2.4.1 of this paper.

WT *S. cerevisiae* yeast were reared in liquid YPD media in a shaker-incubator at 30 °C until a sufficient opacity was observed, indicating a sufficient quantity of cells present in the media. They were then vortexed to isolate the yeast pellet, which was resuspended in YPD liquid media containing 5%, 1%, 0.1% and 0% (control) glyphosate. These different experimental concentrations were produced by mixing YPD media with commercially available Roundup concentrate containing 18% glyphosate. As above, the ordinary use instructions for this Roundup product would create a solution containing approximately 0.8% glyphosate.

The yeast cells were exposed to these different experimental concentrations at 30 °C for 60 minutes with gentle agitation. Following this, the cells were pelleted using centrifugation before being resuspended in deionized water. This was repeated two more times in order to remove Roundup and other contaminants, and the cells were finally centrifuged to produce clean 100µL cell pellets. Replicates were purified and amplified in accordance with the Fritsch et al. protocol, as described in above in section 2.4.1 of this paper.

Sequencing of the resulting nematode and yeast replicates was performed at the University of New Hampshire Hubbard Center for Genome Studies. Data pipeline analysis was performed by Dr. J-F Gout as recommended by (Fritsch et al., 2018; Gout et al., 2017).

3.6.2 Nematode Short-Term Roundup Exposure

C. elegans WT worms raised on agarose plates with an E. coli lawn according to the protocols set out in the Wormbook (Stiernagle, 2006) were washed from their plates using M9 buffer mixed with commercially available Roundup concentrate and containing either 0.05% glyphosate, 0.1% glyphosate, 1% glyphosate, 5% glyphosate, or a control of 0% glyphosate.

They were placed in 15mL tubes and gently agitated for 1 hour before being centrifuged and washed with plain M9 buffer twice. They were then placed on plates lacking an E. coli lawn, and numbers of live vs. dead individuals in the same discrete area were determined manually based on the presence or absence of movement.

3.6.3 Nematode Long-Term Roundup Exposure

On the first day of the experiment (day 0), 8 control (0% glyphosate) agarose plates containing E. coli lawns were seeded with a total of 65 *C. elegans* WT worms, 7 Roundup plates of 0.1% glyphosate with a total of 55 worms, 9 Roundup plates of 1% glyphosate with a total of 75 worms, and 9 Roundup plates of 5% glyphosate with a total of 75 worms. Following transfer, each worm was checked to make sure it was motile, indicating survival following movement to the experimental plate. The day of transfer was designated as day 0. On the subsequent three days of the experiment, the number of living and deceased individuals was counted, and all deceased worms were removed from the plates. Relative motility levels and the presence, absence, and relative levels of reproduction were also visually noted.

3.6.4 Yeast Short-Term Roundup Exposure

Ten 15mL tubes containing 10mL YPD liquid media were seeded with 1mL WT *S. cerevisiae* and cultured at 28 C° with intermittent vortexing until a sufficient yeast pellet volume was achieved. 1mL of this culture was then added to 15mL tubes containing YPD liquid media and Roundup equaling 5% glyphosate, 1% glyphosate, 0.1% glyphosate, and 0% glyphosate, for a total of 10 replicates per experimental condition. Each tube contained a total volume of 10mL following addition of the yeast culture. Immediate OD600 measurements were taken on a

calibrated Thermo Scientific Genesys 20 Spectrophotometer (Thermo Scientific), with further measurements being taken at 60 minute intervals to form a total of 6 measurement points.

3.6.5 Determination of Roundup pH

The pH conditions *S. cerevisiae* and *C. elegans* were exposed to during the Roundup experiments above was determined by producing a batch of YPD liquid media, a batch of M9 buffer, and a batch of agar plates containing 0% (control), 0.1%, 1%, or 5% glyphosate. These growth mediums were then tested using pH strips to determine the pH range of each glyphosate percentage point.

The pH of the 0% and 0.1% glyphosate growth media, whether YPD, agar plates, or M9 buffer was approximately pH 6.5, while that of the 1% glyphosate growth media was approximately pH 6, and that of the 5% glyphosate growth media was approximately pH 5.5.

3.6.6 Nematode pH Exposure

C. elegans WT worms raised on agarose plates with an E. coli lawn according to the protocols set out in the Wormbook (Stiernagle, 2006) were washed from their plates using M9 buffer formulated using hydrochloric acid or sodium hydroxide to a pH of 3, 7, or 10. These pHs were chosen as they form the extreme acidic and basic survivable conditions, as well as the midpoint, for nematodes. The worms were exposed to these environmental conditions in 15mL tubes and gently agitated for 1 hour before being gently centrifuged to pellet the worms. The supernatant containing the pH-adjusted media was removed, and the worms were resuspended in deionized water. This was repeated two more times in order to remove remaining pH-adjusted media and other contaminants, in order to produce clean 100µL worm pellets. Replicates were purified and amplified in accordance with the Fritsch et al. protocol described in detail above in

section 2.4.1. Sequencing was performed at the University of New Hampshire Hubbard Center for Genome Studies. Data pipeline analysis was performed by Dr. J-F Gout as recommended by (Fritsch et al., 2018; Gout et al., 2017).

3.6.7 Yeast pH Exposure

WT *S. cerevisiae* yeast were reared in liquid YPD media in a shaker-incubator at 30 °C until a sufficient opacity was observed, indicating a sufficient quantity of cells present in the media. They were then vortexed to isolate the yeast pellet, which was resuspended in YPD liquid media formulated using hydrochloric acid or sodium hydroxide to a pH of 2.5, 5.5, or 8.5. These pHs were chosen as they form the extreme acidic and basic survivable conditions, as well as the midpoint, for yeast cells. The yeast cells were exposed to these environmental conditions in 15mL tubes with gentle agitation for 1 hour before being gently centrifuged to pellet the cells. The supernatant containing the pH-adjusted media was removed, and the cells were resuspended in deionized water. This was repeated two more times in order to remove remaining pH-adjusted media and other contaminants, in order to produce clean 100µL cell pellets. Replicates were purified and amplified in accordance with the Fritsch et al. protocol described above in 2.4.1. Sequencing was performed at the University of New Hampshire Hubbard Center for Genome Studies. Data pipeline analysis was performed by Dr. J-F Gout as recommended by (Fritsch et al., 2018; Gout et al., 2017).

3.7 Results

3.7.1 Nematode Roundup Short-Term Exposure Results

Significant differences in the numbers of dead individual *C. elegans* nematodes were noted during short-term exposure to Roundup between the control (0%), 1% glyphosate, and 5%

glyphosate exposure points. Significant differences in the number of live worms observed were only noted at the 5% glyphosate exposure point (Figure 3.2). LD50 was attained at approximately 1% glyphosate. These findings are somewhat surprising, given that nematodes lack the Shikimic Pathway, and thus should theoretically be immune to Roundup exposure.

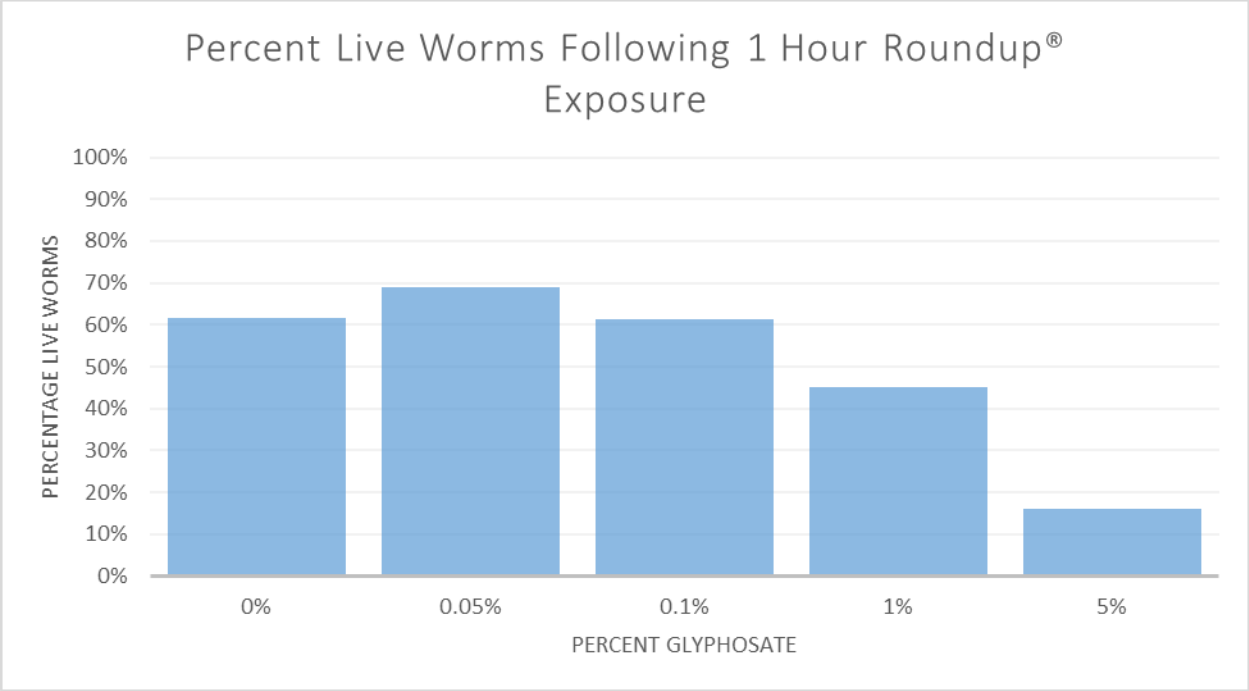

Figure 3.2 Roundup Short-Term *C. elegans* Percent Live Worms

Depicts the percent of live *C. elegans* individuals observed following 1 hour of exposure to Roundup at 4 different glyphosate percentages, and a control lacking Roundup. LD50 attained at approximately 1% glyphosate.

3.7.2 Nematode Roundup Long-Term Exposure Results

Throughout the four-day long-term exposure to Roundup experiment, significant differences were noted at all three glyphosate levels as well as the control (Figure 3.3).

On the initial transfer to the plates (day 0), all worms were observed to move normally. On day 1, 24 hours after being transferred to the plates, the worms present on 5% glyphosate

plates exhibited practically no movement whatsoever. A small number of tracks were evident on several of the plates, indicating that at least some movement had occurred before ceasing. No censors occurred on any of the 5% glyphosate plates throughout the experiment, making it likely that movement ceased completely very soon after transfer. No reproduction was observed on any of the 5% glyphosate replicates.

Slight movement was observed on day 1 in the 1% glyphosate plates, with more tracks being present compared to the 5% plates. Due to increased movement levels, censored individuals occurred, with the majority of incidences occurring on day 1. By day 2, practically all movement had ceased, and no reproduction was observed in all but one of the replicates.

Normal movement was maintained in the 0.1% plates throughout the experiment. Despite evidence towards censor activity (tracks to the edge of the plate, and a disappearance of adult worms) some limited reproductive capabilities were maintained, maintaining the population to a roughly steady level despite the observation of multiple dead worms over the course of the experiment.

Over the course of the experiment, the control (0% glyphosate) plates showed a massive population boom, and no dead worms were observed on any of the three days following transfer. Motility was normal, and while no measurements were taken during the experiment, adult worms on control plates were noticeably larger than those on any of the three glyphosate percentage point plates, leading to the conclusion that in addition to motility and reproduction, growth and development of the nematodes had also been adversely affected by Roundup exposure despite the absence of a Shikimic Pathway in nematodes (Figure 3.3).

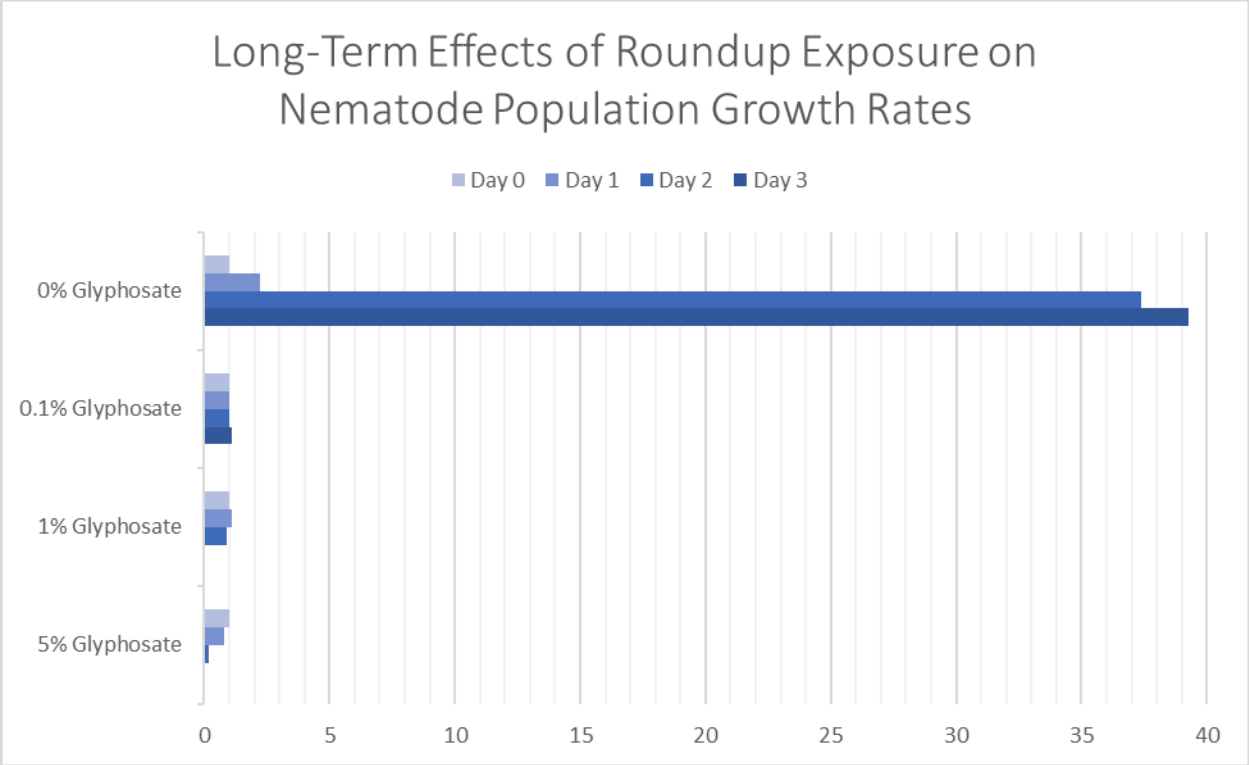

Figure 3.3 Roundup Long-term *C. elegans* Population Effects

Depicts effects of Roundup exposure on *C. elegans* individuals over four days at three different glyphosate percentages (5%, 1%, 0.1%) and a control lacking Roundup (0%). Live worms, dead worms, and censored worms were included in population survival and growth rates.

3.7.3 Yeast Roundup Short-Term Exposure Results

Long-term exposure experiments performed with yeast cultures did not result in reportable data due to a total absence of reproduction in 5% glyphosate replicates, therefore only short-term exposure results are presented here.

At 0% glyphosate (control) levels, population growth proceeded steadily upwards following a slight dip noted at the 60-minute mark, and followed what would be expected for the early stages of S-curve growth typical of yeast growth curves after transfer to fresh media. At just 0.1% glyphosate, growth proceeded very slowly, and did not exhibit the expected growth pattern. In the 1% and 5% exposure points, population growth was negative throughout, and after

300 minutes the 1% glyphosate group presented with statistically stagnant population, while the 5% group had a significant drop in population from the initial transfer. This suggests that while even small amounts of Roundup at the 0.1% glyphosate experimental condition either a). kills a portion of the yeast cells but does not restrict reproduction, allowing the population to grow slightly, or b). does not kill many cells exposed to it, but reduces reproduction significantly. At higher (1% or 5% glyphosate) exposure points, the effect is more pronounced, leading to a steady decline in the population over even a short time period.

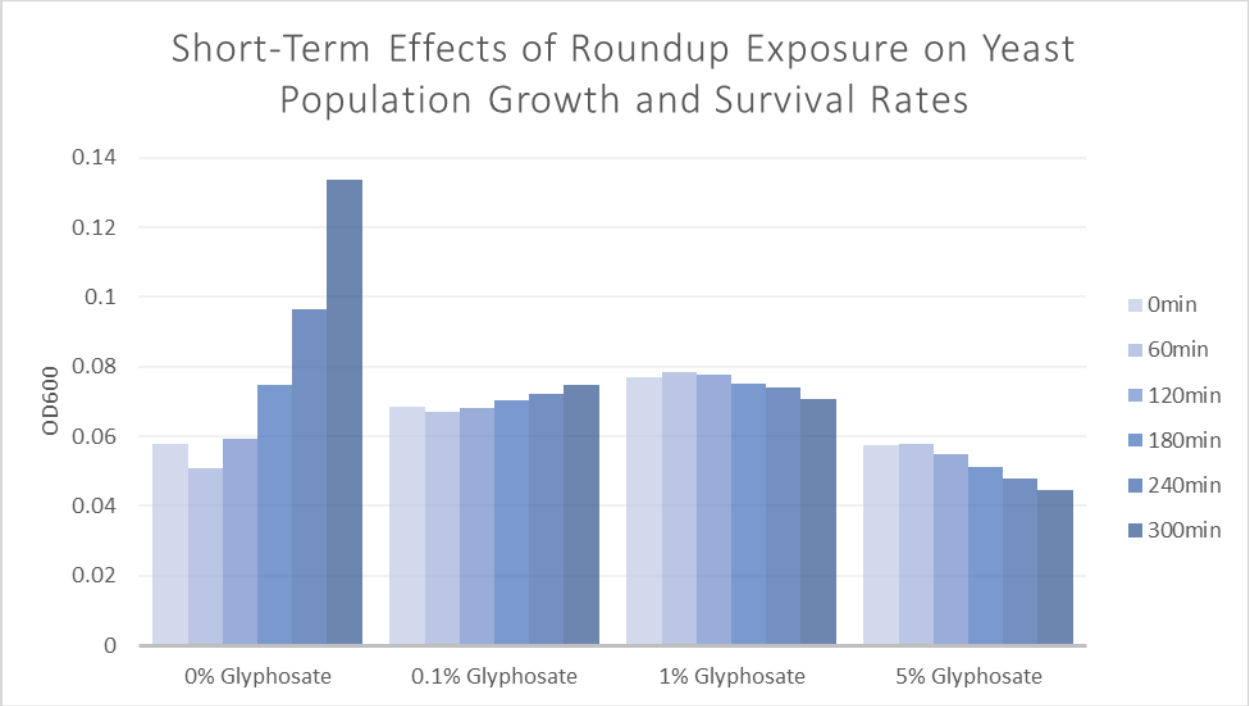

Figure 3.4 Roundup Short-Term *S. cerevisiae* Population Effects

Depicts relative effects of Roundup exposure on *S. cerevisiae* population growth and survival rates estimated via OD600 readings. Three different glyphosate percentages (5%, 1%, 0.1%) and a control lacking Roundup (0%). OD600 measurements taken over 6 timepoints at 60-minute intervals.

3.7.4 Transcription Error Rate Results

3.7.4.1 Roundup Transcription Errors

3.7.4.1.1 *S. cerevisiae* Roundup Transcription Errors

S. cerevisiae RNA Pol II transcriptional landscapes exhibited a strong increase in C-to-U and G-to-A errors in the Roundup exposure samples when compared to the control. Furthermore, these transcription errors increased as the glyphosate exposure percentage increased, although the increase in transcription errors was not proportional to the increase in glyphosate (Figure 3.5).

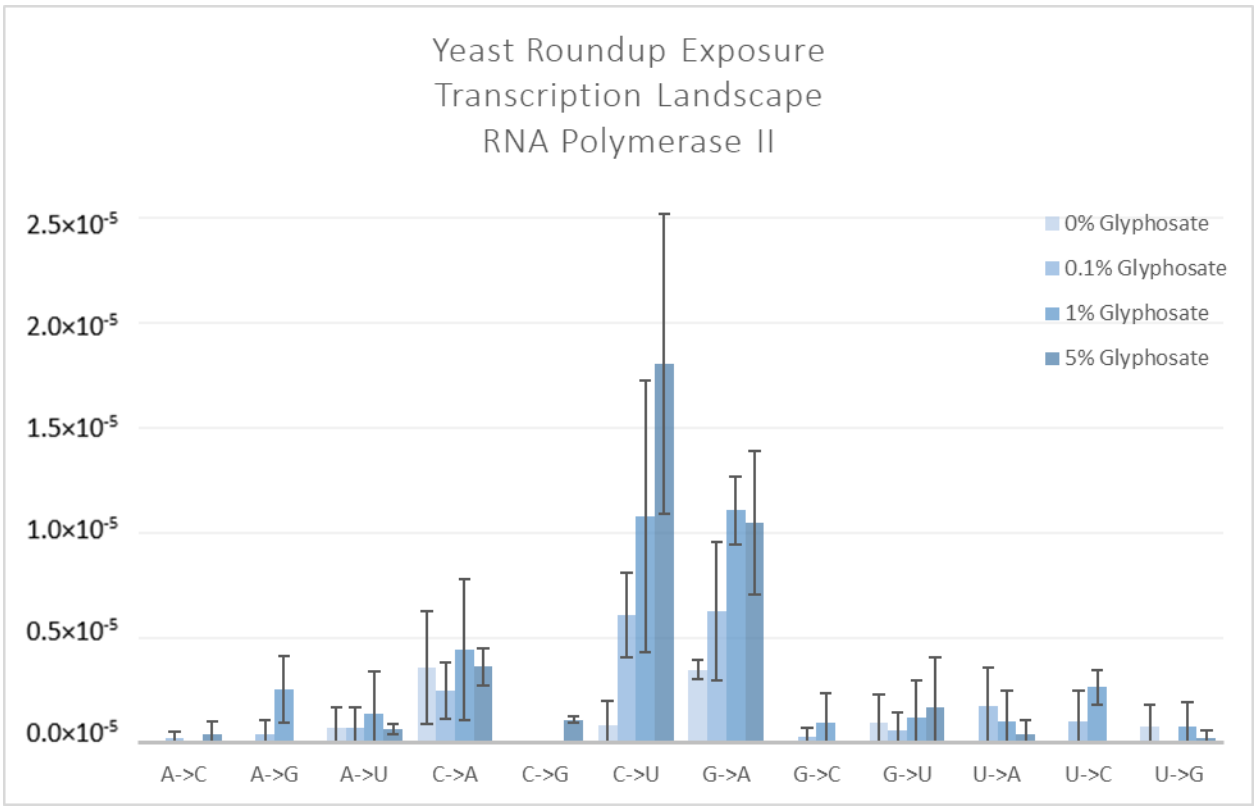

Figure 3.5 Roundup *S. cerevisiae* RNA Polymerase II Transcription Landscape

Transcription landscape depicting mRNA transcription errors produced by RNA polymerase II following *S. cerevisiae* treatment with three different glyphosate percentages (5%, 1%, 0.1%) and a control lacking Roundup (0%). Error bars: Standard deviation.

3.7.4.1.2 *C. elegans* Roundup Transcription Errors

In contrast to the clear trends displayed in the *S. cerevisiae* RNA Pol II transcription error landscape, those found in *C. elegans* did not follow a consistent pattern. This may be due to the fact that while yeast cells possess a Shikimic Pathway which may be inhibited by glyphosate exposure, nematodes do not possess this pathway. While the C-to-U error rates displayed an increase in the Roundup glyphosate points when compared to the control, this trend did not smoothly follow as glyphosate exposure increased (Figure 3.6).

G-to-A errors were not increased in any of the glyphosate exposure percentages, however at the 5% glyphosate point G-to-U errors were seen to be increased (Figure 3.6).

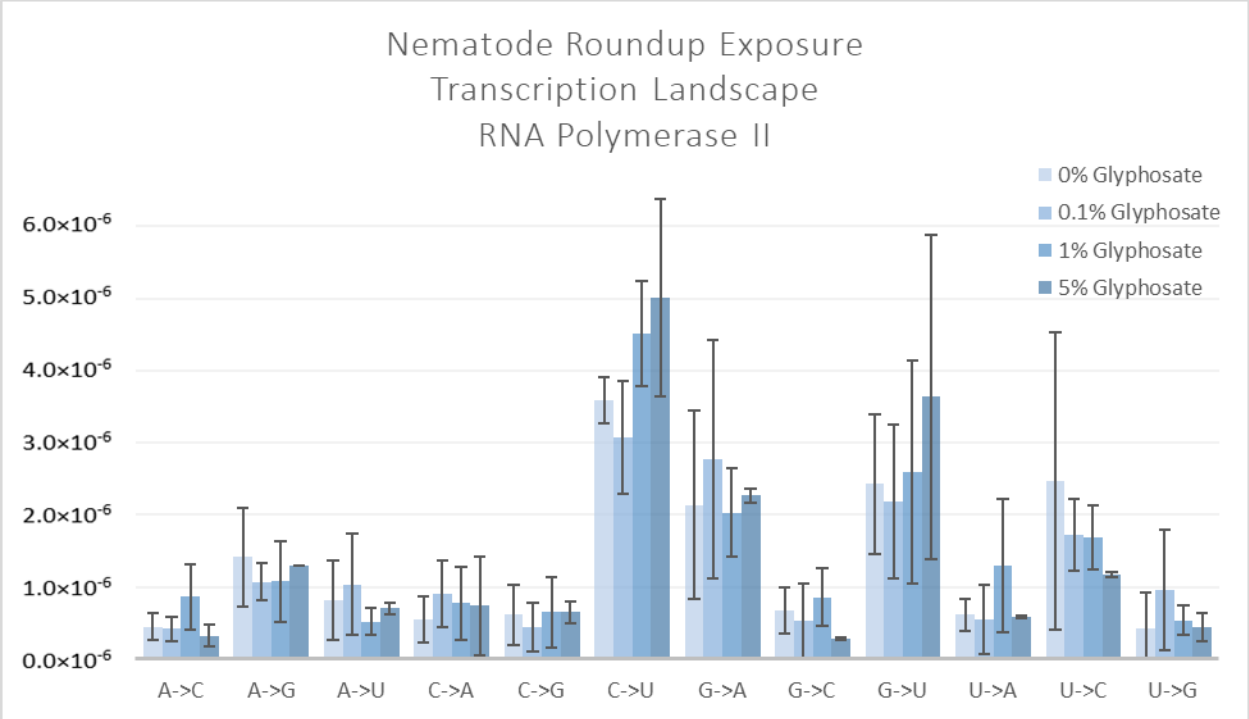

Figure 3.6 Roundup *C. elegans* RNA Polymerase II Transcription Landscape

Transcription landscape depicting mRNA transcription errors produced by RNA polymerase II following *C. elegans* treatment with three different glyphosate percentages (5%, 1%, 0.1%) and a control lacking Roundup (0%). Error bars: Standard deviation.

3.7.4.1.3 Comparison of Roundup Results

These differences in transcription error patterns may be attributed to the presence of a Shikimic Pathway in yeast cells, but the absence of this pathway in nematodes. While the interruption of this pathway in yeast should not be expected to directly affect mRNA errors, the stress impact on these cells should be higher in *S. cerevisiae* than in *C. elegans* individuals.

These findings indicate that exposure to Roundup does not directly affect transcription error rates, but rather interrupts the normal function of cellular biological processes. Given the differences in genetic composition and thus cellular processes present between yeast and nematodes, the effects of this disruption may manifest differently between the two species.

Despite this, there is still a clear trend indicating that exposure to Roundup does increase overall transcription error rates, particularly at higher exposure points. The error with the most significant results, as well as the one which corresponded over both yeast and nematode experiments was the C-to-U transition error and to a lesser extent the G-to-U error. In combination with the high levels of G-to-A errors found in the yeast transcription error landscape, these findings correspond with the hypothesis that oxidative stress-caused DNA and RNA damage of cytosines may be responsible for at least a portion of transcription errors displayed here.

3.7.4.2 pH Transcription Errors

3.7.4.2.1 *S. cerevisiae* pH Transcription Errors

In yeast, high levels of G-to-A and U-to-C RNA Pol II transcription errors were found under both acidic and basic conditions, but not in the midpoint (neutral) pH environment. C-to-A errors were found to be elevated at the neutral pH in comparison to the acidic and basic conditions, while C-to-U errors were elevated at the acidic pH in comparison to the neutral and

basic conditions (Figure 3.7). The general trend was for transcription error rates to be highest under acidic conditions, with acidic transcription errors forming approximately 42%, neutral errors 28%, and basic errors 30% of the total errors present

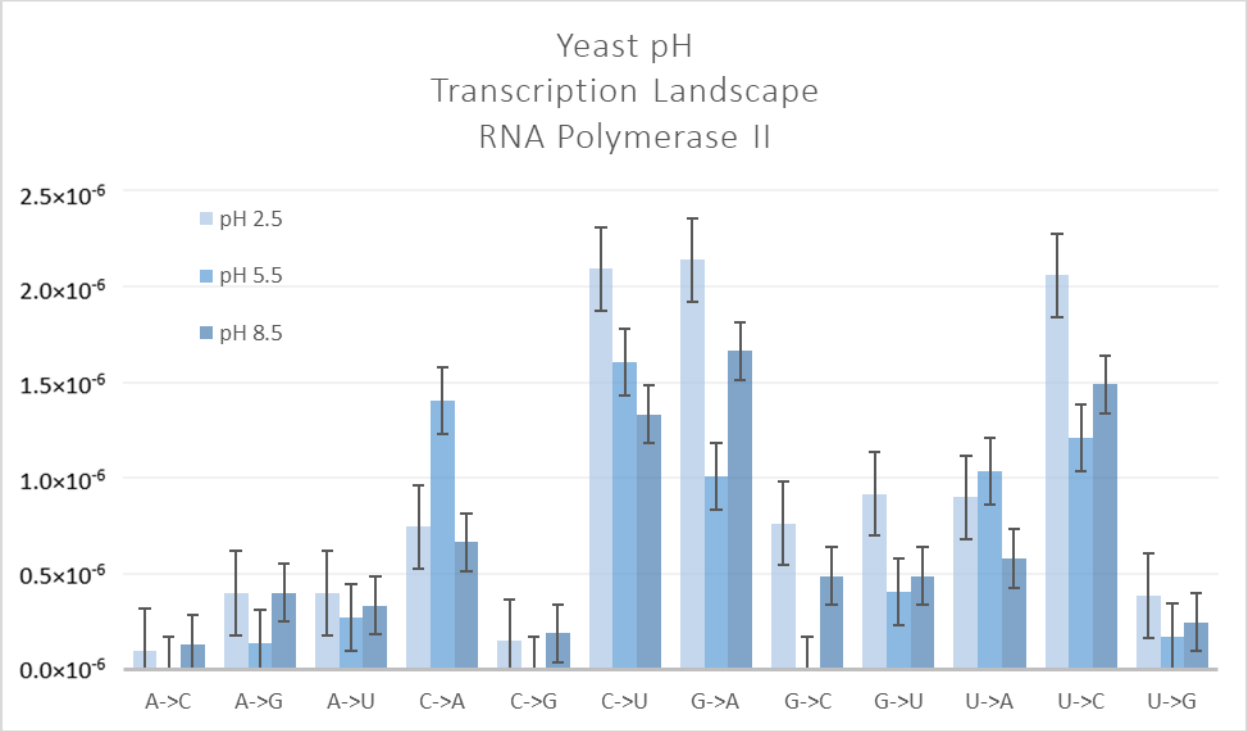

Figure 3.7 pH *S. cerevisiae* RNA Polymerase II Transcription Landscape

Transcription landscape depicting mRNA transcription errors produced by RNA polymerase II in *S. cerevisiae* at pH 2.5, 5.5, and 8.5. Error bars: Standard Error.

3.7.4.2.2 *C. elegans* pH Transcription Errors

In nematodes, basic environmental conditions produced the greatest amounts of RNA Pol II transcription errors. For the basic condition, C-to-G and G-to-A transcription errors displayed the greatest increase in comparison to the acidic and midpoint (neutral) conditions. Under acidic conditions, only G-to-U errors displayed a significant increase in comparison to the neutral and basic conditions. There were no cases where neutral conditions produced significantly high

numbers of transcription errors in comparison to the acidic or basic conditions (Figure 3.8). The overall proportions of each pH error were approximately similar, with acidic condition transcription errors forming roughly 31%, neutral errors forming 32%, and basic errors forming 37% of the total errors present.

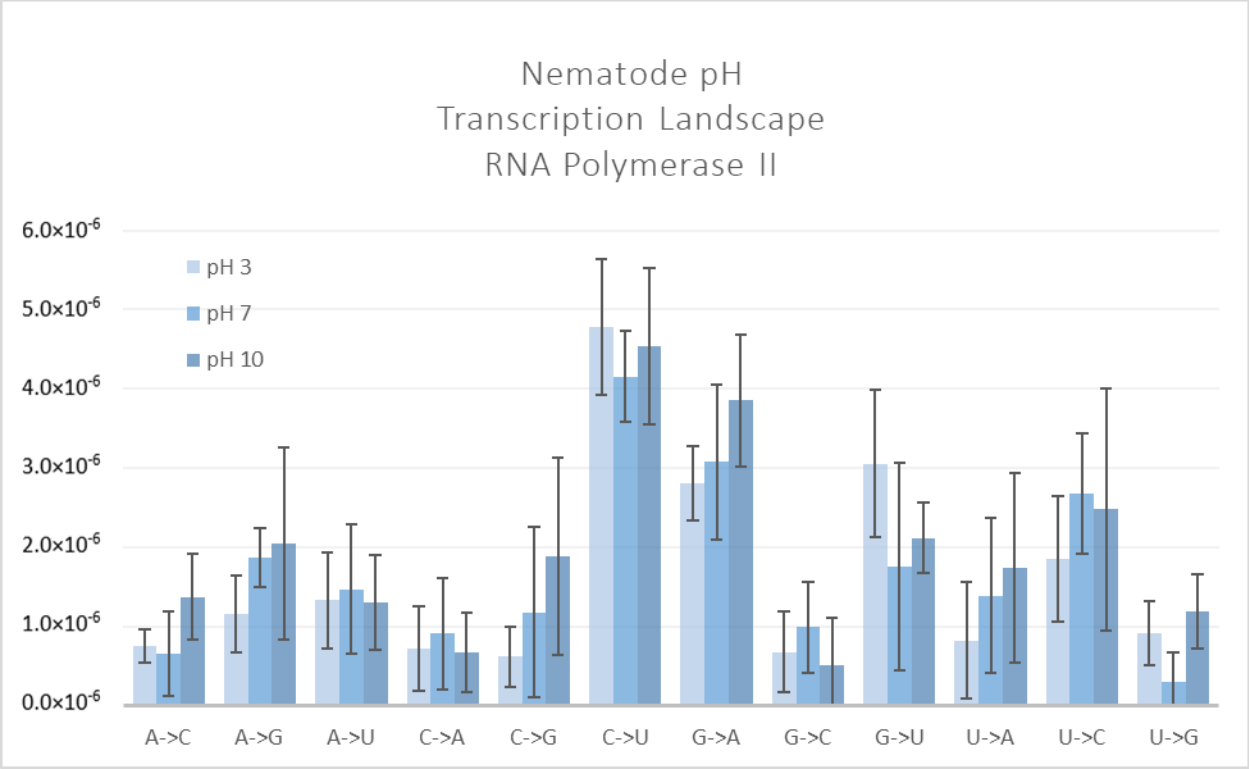

Figure 3.8 pH *C. elegans* RNA Polymerase II Transcription Landscape

Transcription landscape depicting mRNA transcription errors produced by RNA polymerase II in *C. elegans* at pH 3, 7, and 10. Error bars: Standard deviation.

3.7.4.3 Roundup pH Growth Media Results

0% glyphosate growth mediums YPD, M9 buffer, and agarose plates, were all found to have a pH of approximately 6.5-6.8. There was no discernable change in the 0.1% glyphosate condition, however at the 1% condition the YPD and agarose plate growth mediums dropped to a

pH of approximately 6, while the M9 buffer remained around a pH of 6.5. The 5% glyphosate condition decreased the pH of the YPD and agarose plates to a pH of approximately 5.5, while the M9 buffer lowered to a pH around 6.

3.7.5 Combining pH Results and Roundup Results

Given that DNA and RNA damage can arise due to changes in environmental pH, and the fact that Roundup is itself slightly acidic, one possible explanation for the transcriptional error rates found in *C. elegans* and *S. cerevisiae* is simply that these increases in mRNA errors were caused by the reduction in pH. Due to the fact that the Roundup growth media used in these experiments did not exhibit a pH of less than 5.5, it is unlikely that RNA damage was occurring due to a reduction in mRNA stability, however it is still possible that DNA damage arose as a result of the acidic nature of Roundup and the DNA depurination which could result.

Given that the pHs tested during these experiments were much more acidic than the pHs found under Roundup exposure conditions, it would be expected that were an acidic pH a major driver of transcription errors, a much higher transcription error rate would be found in the extremely acidic pH assay replicates than in the Roundup exposure assay replicates. This was not the case.

The increases in mRNA error levels present in nematodes and yeast exposed to Roundup were higher than those found in those exposed to an extreme acidic pH. In *C. elegans*, the rate of G-to-U errors in the pH 3 condition were 0.8 times that found in the 5% glyphosate exposure point, while in *S. cerevisiae* the rate of G-to-U errors at the pH 2.5 condition were 0.5 times that found at the 5% glyphosate exposure point. Given that the pH of the Roundup-containing growth media did not decrease below a pH of 5.5, it is likely that fewer transcription errors were occurring specifically as a result of environmental pH than were seen at the pH 3 and pH 2.5

conditions present in the pH assay. This leads to the conclusion that pH is not the primary driver in the transcription error rates and patterns observed following yeast and nematode exposure to Roundup.

3.7.6 Gene Expression and Ontology Results

The control (0%) vs. 5% glyphosate exposure experimental conditions showed the greatest differences in expression. While the overall gene expression patterns were not too different in nematodes (Figure 3.7), there was a clear difference in yeast heat plot gene expression (Figure 3.8).

When observing significantly differentially expressed genes, an obvious trend can be seen regarding the phenotypic terms over-represented in *S. cerevisiae* and *C. elegans* replicates (Figure 3.9, Figure 3.10). In yeast, terms include those concerned with cellular fitness, response to oxidative stress, and reproduction. In nematodes, most of the terms involve reproduction in the form of embryonic development and fitness, though terms involving protein expression appear as well. From this, it can be seen that the most differentially expressed terms differ between the two species, but still primarily involve health and reproduction.

When observing the overall gene ontology results for each species, the overall picture can be seen even more clearly (Figure 3.11, Figure 3.12). While these graphs cannot be compared between species, due to the fact that the results are relative to the experimental data and not on a fixed scale, they provide a more comprehensive depiction for the effect that Roundup exposure has on an organism's health and longevity. Terms which appear make it clear that significant differences in binding capabilities, RNA and protein production, nuclear regulation, and oxidative stress responses were present between the control (0%) and 5% glyphosate exposure conditions. These findings thus provide further evidence to support the hypothesis that not only

does glyphosate exposure significantly impact many cellular functions, disrupting homeostasis and therefore increasing risks of disease, but that inflammation and oxidative stress may be one of the underlying causes of this reaction.

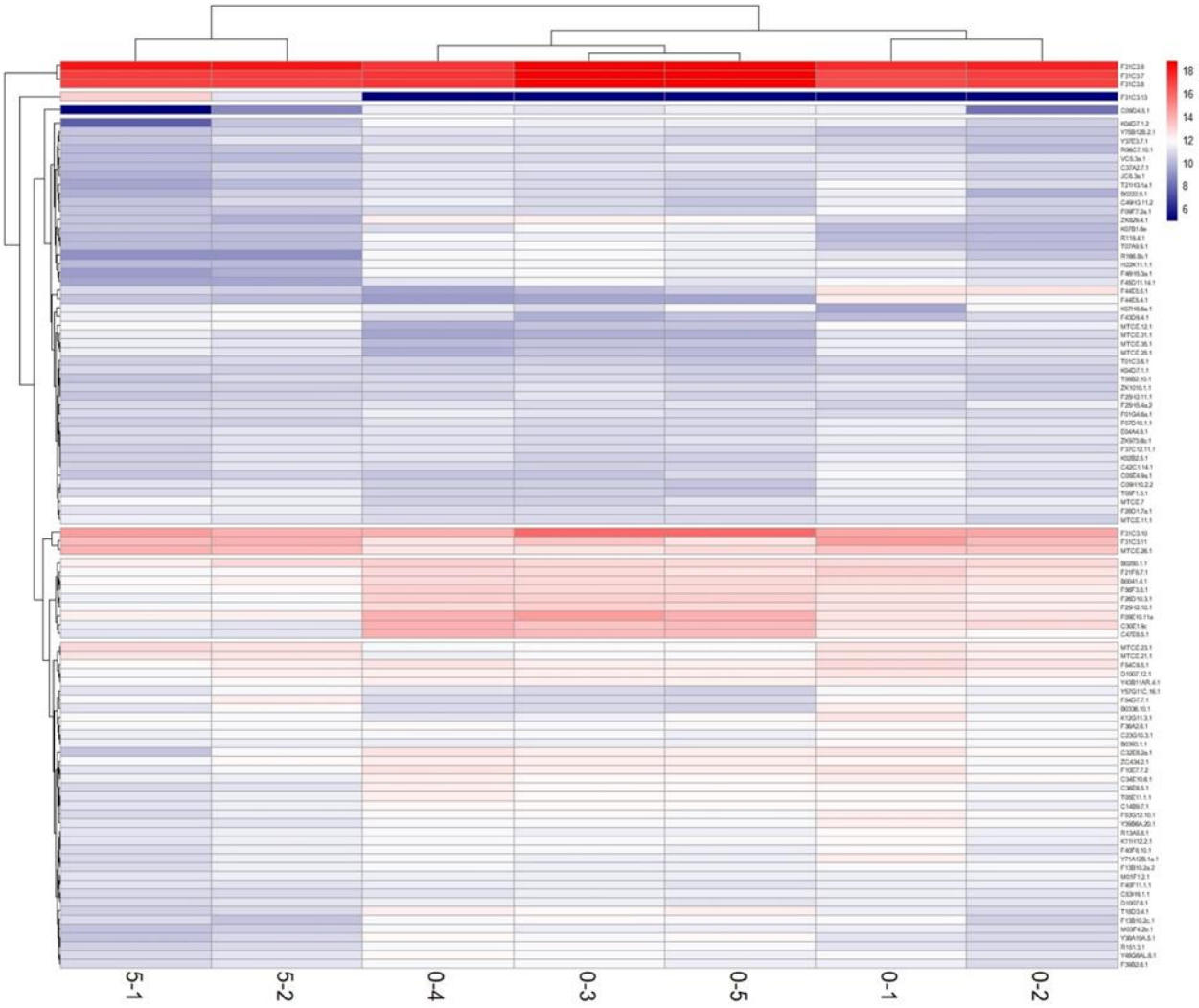

Figure 3.9 Roundup *C. elegans* Differential Expression Heat Plot

Heat plot of gene expression levels between 4 experimental replicates of *C. elegans* control (0%), and 2 experimental replicates exposed to 5% glyphosate. Horizontal labels indicate sample type and replicate, with the first number representing glyphosate percentage, and the number following the dash indicating replicates. (RStudio Team, 2020).

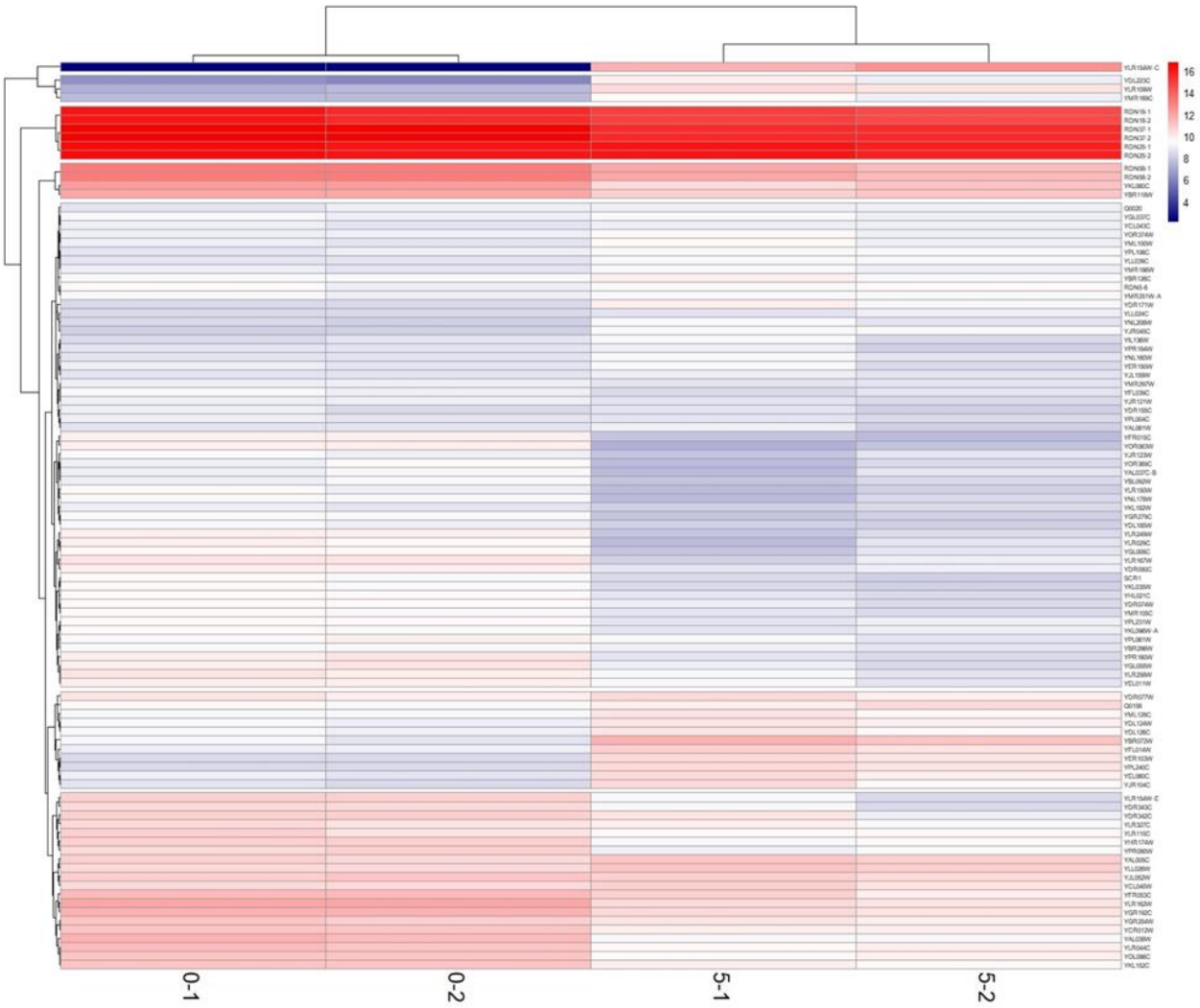

Figure 3.10 Roundup *S. cerevisiae* Differential Expression Heat Plot

Heat plot of gene expression levels between 2 experimental replicates of *S. cerevisiae* control (0%), and 2 experimental replicates exposed to 5% glyphosate. Horizontal labels indicate sample type and replicate, with the first number representing glyphosate percentage, and the number following the dash indicating replicates. (RStudio Team, 2020).

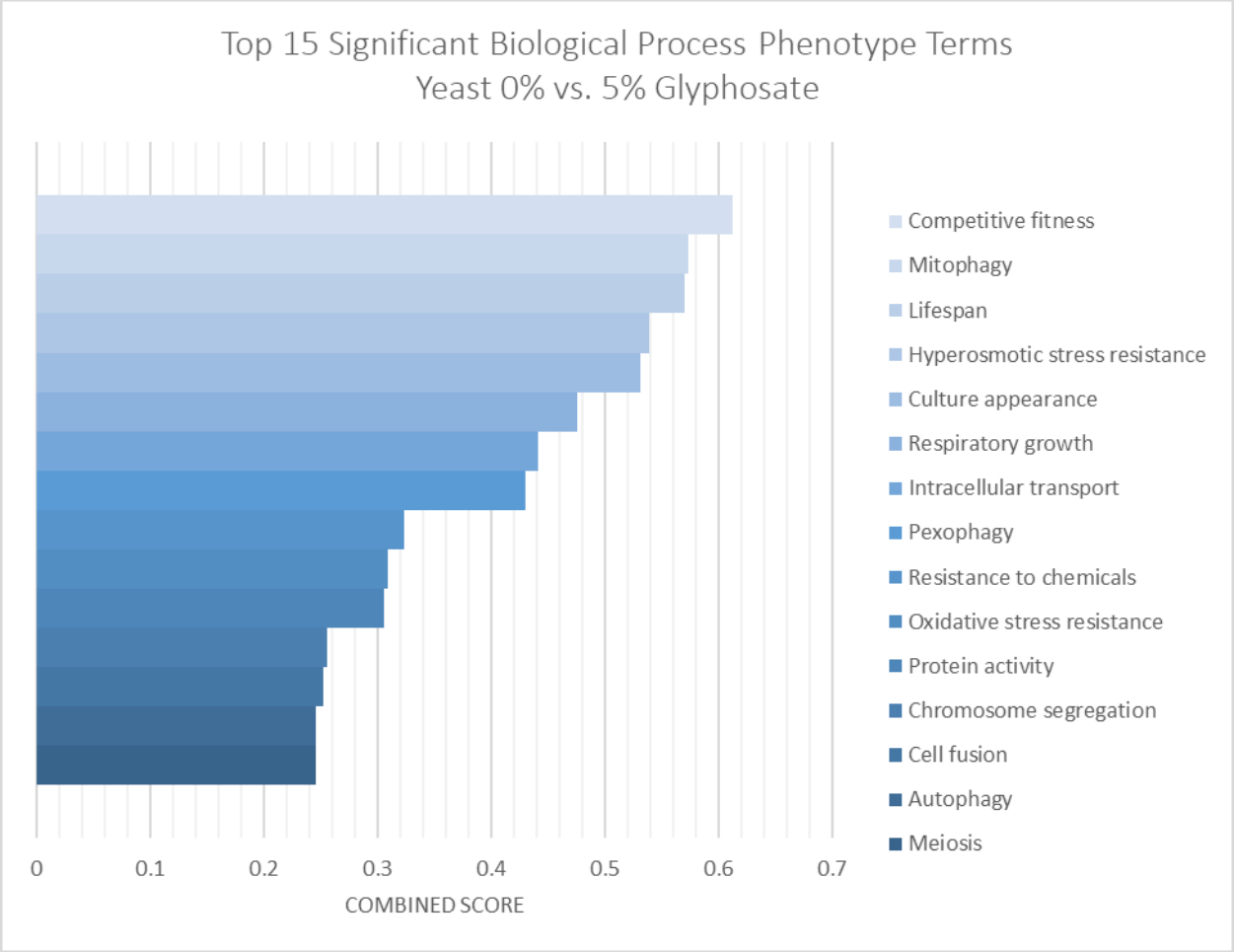

Figure 3.11 Roundup *S. cerevisiae* Top 15 Significantly Enriched BP Phenotype Terms

YeastEnrichr Enrichment Analysis plot depicting the top 15 biological process phenotype terms significantly enriched in *S. cerevisiae* in the control (0%) vs. 5% glyphosate experimental condition. Combined score: log p-value * z-score. (Chen et al., 2013; Kuleshov et al., 2016).

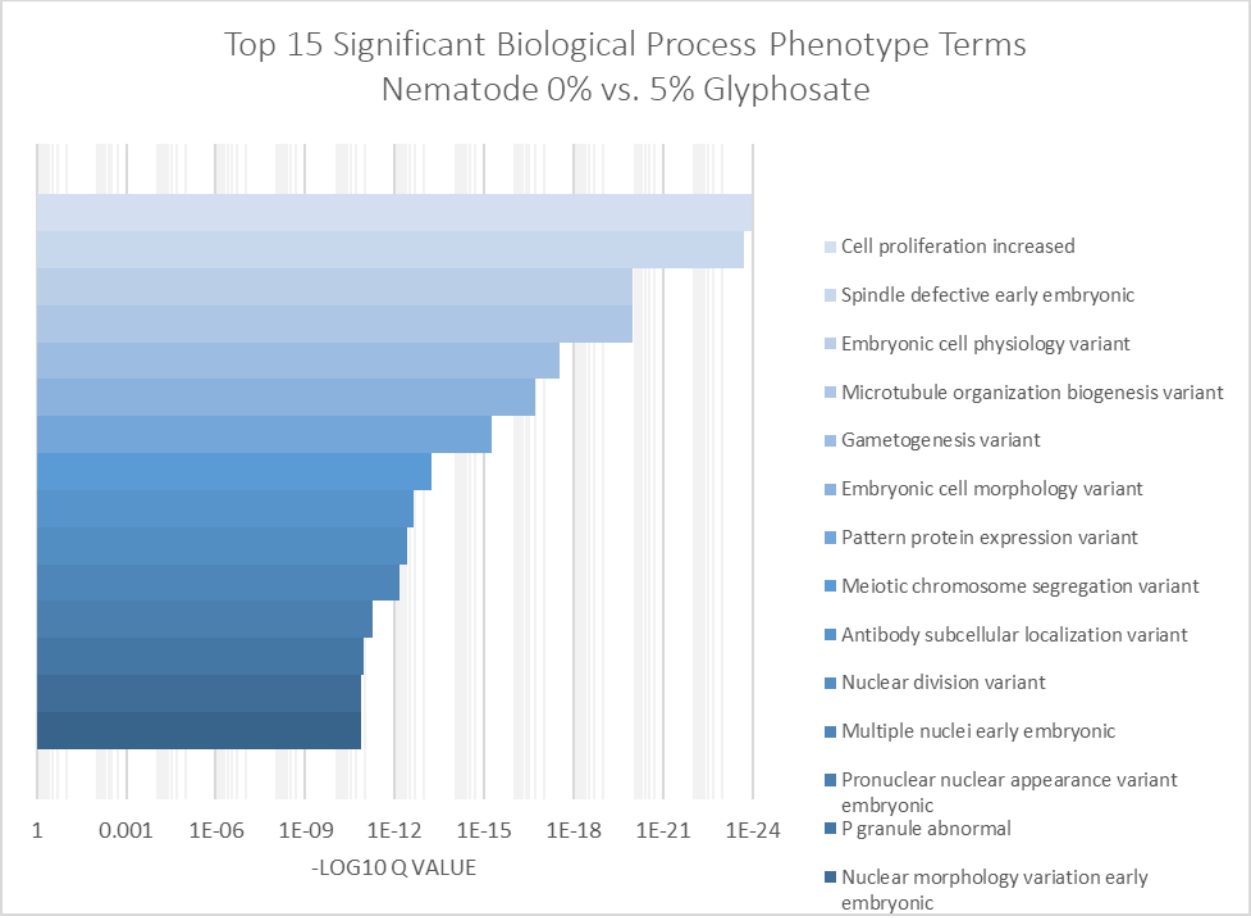

Figure 3.12 Roundup *C. elegans* Top 15 Significantly Enriched BP Phenotype Terms

WormBase Enrichment Analysis plot depicting the top 15 biological process phenotype terms significantly enriched in *C. elegans* in the control (0%) vs. 5% glyphosate experimental condition. (Angeles-Albores et al., 2016).

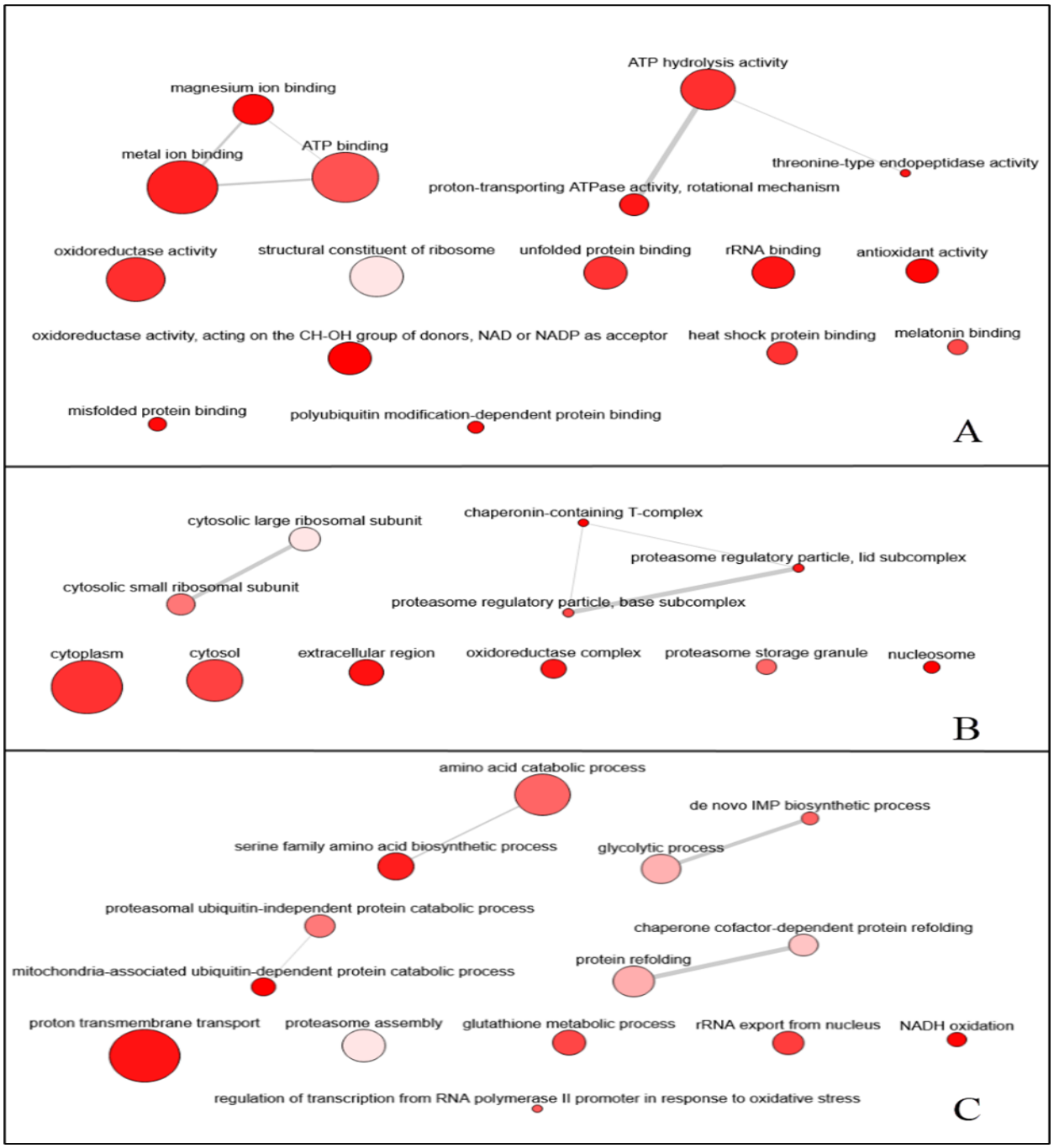

Figure 3.13 Roundup *S. cerevisiae* ReviGo Plot

ReviGo plot showing Molecular Functions (A), Cellular Components (B), and Biological Processes (C), significantly represented under the experimental conditions of *S. cerevisiae* control (0%) vs. 5% glyphosate exposure. Bubble color corresponds to the relative p-value associated with each provided GO term. Bubble size corresponds to the relative associated LogSize value for each GO term. (Supek et al., 2011; Supek & Škunca, 2017).

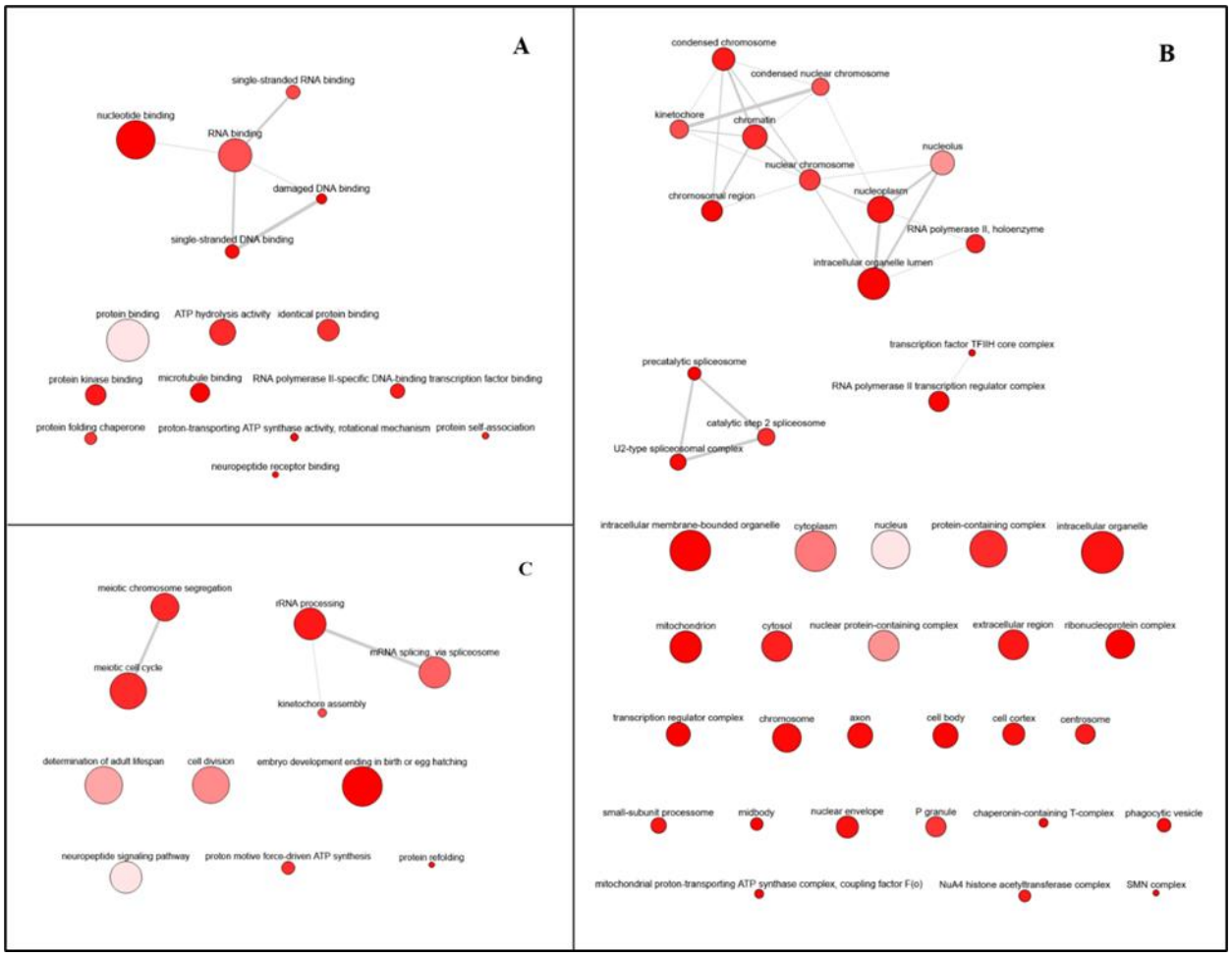

Figure 3.14 Roundup *C. elegans* ReviGo Plot

ReviGo plot showing Molecular Functions (A), Cellular Components (B), and Biological Processes (C), significantly represented under the experimental conditions of *C. elegans* control (0%) vs. 5% glyphosate exposure. Bubble color corresponds to the relative p-value associated with each provided GO term. Bubble size corresponds to the relative associated LogSize value for each GO term. (Supek et al., 2011; Supek & Škunca, 2017).

3.8 Conclusions

Glyphosate, and glyphosate-based herbicides (GBHs), were widely considered to be safe for human use from their invention in 1970 by Monsanto, until the mid-2010s. Various disputes have been waged in the scientific and legal communities regarding this question. Numerous studies have concluded that GBHs exposure does cause disease in animal models, and that there

is a strong correlation between long-term GBH exposure and development of non-Hodgkin's Lymphoma in humans. A further debate is currently in progress regarding the mechanism(s) behind the ability of GBHs to bring about these diseases.

One possible avenue for discussion is the inflammation and related oxidative stress which has previously been shown to be linked with GBH use. Inflammation and oxidative stress have been shown to cause DNA and RNA damage, and can disrupt cellular function in ways which could increase the risks of developing at least some of the diseases linked with GBH exposure in animal model organisms lacking the Shikimic Pathway.

In this project, it was shown not only that exposure to even small amounts of GBH Roundup significantly impact the health, longevity, and reproductive rates of both *S. cerevisiae* and *C. elegans*. It reduced lifespan, reduced or eliminated reproductive capabilities, increased transcription error rates, and altered gene expression levels in both species, though not in precisely the same ways. These differences could possibly be attributed to the presence of the Shikimic Pathway in yeast cells, and the absence of this pathway in nematodes. While GBHs are slightly acidic, it was determined that the effects of this acidic environment were not sufficient to cause the patterns seen.

The transcription error rates and gene ontology results indicated inflammatory and oxidative stress involvement. More research will be necessary to fully understand the mechanism of action and consequences of GBH exposure on transcription fidelity and organismal health in general.

CHAPTER IV

INCIDENCE OF OFF-TARGET H-ADAR EDITING IN *S. CEREVISIAE*

4.1 Introduction

Adenosine Deaminases that Act on RNA (ADAR) are a group of evolutionarily conserved post-transcriptional editing enzymes that bind to double-stranded RNA and convert adenosine (A) to inosine (I). When these edited RNA transcripts are translated by ribosomes, I is recognized as guanine (G), causing an A-to-G transition mutation. This editing has been shown to be integral in neural development and function, with mutations in ADAR genes having been linked with multiple neurological disorders, while overexpression of ADAR genes has been shown to increase the risks of developing cancer (Bass, 2002; Chalk et al., 2019; Keegan et al., 2004; Tan et al., 2017). In humans, only a small number of sites have been proven to display functional mRNA editing, and it is currently unknown what the scope and impact may be of any off-target, nonfunctional editing by h-ADAR proteins.

4.2 ADAR and RNA Editing

Since its discovery in 1987, research into ADAR has determined that the action of this enzyme is vital for, among other things, neurological development and proteome plasticity (Albertin et al., 2022; Grice & Degnan, 2015; Liscovitch-Brauer et al., 2017; Yablonovitch et al., 2017). ADAR works by catalyzing the hydrolytic deamination of A to form I. I is a nucleoside commonly found in tRNAs, but which can be found in mRNAs. The tissue distribution of I in mRNAs varies greatly between species (Tan et al., 2017). Specific conditions are required for

ADAR binding and successful catalytic activity. The main activation requirement is the presence of the sequence 5´-UAG-3´ in double-stranded mRNA, with the central A base being converted to form the sequence 5´-UIG-3´ (Nishikura, 2010; Thomas & Beal, 2017). While these edited sites are relatively rare throughout the entirety of the transcriptome, ADAR has been shown to target specific locations or tissues with high frequency, in particular neurological tissue (Aruscavage & Bass, 2000; Eifler et al., 2013; Macbeth & Bass, 2007).

It is likely however, that ADAR-induced editing is occurring at a low but constant rate throughout the transcriptome wherever 5´-UAG-3´ adenosines are present in double-stranded mRNA. While other factors may be involved with ADAR attraction to certain editing sites, other regions may be erroneously edited if they meet enough of the criteria to bind with ADAR. This lower-level editing may also be an important factor driving transcript variation and disease.

In order to determine the amount of non-evolutionarily adapted "off-target" editing caused by the presence of ADAR, *S. cerevisiae* expressing human ADAR (h-ADAR) was chosen. *S. cerevisiae* lacks any ADAR genes, allowing definite identification of edits occurring as a result of h-ADAR expression. Rolling Circle sequencing was used due to the capabilities of this technique to provide identification of edits occurring at extremely low frequencies in the transcriptome, in order to determine the true A-to-I editing rate (Fritsch et al., 2018).

4.3 Materials and Methods

4.3.1 YEpTOP2PGAL1 Plasmid Amplification

A small amount of the YEpTOP2PGAL1 plasmid, which carries the hADAR gene linked to the GAL galactose promoter, an ampicillin resistance gene for antibiotic resistance selection in E. coli, and the ura3 gene for uracil drop-out selection in *S. cerevisiae* was obtained.

It was necessary to amplify the amount of plasmid using E. coli cell transformation, culture, and plasmid extraction from E. coli cultured cells in order to produce a sufficient quantity of the YEpTOP2PGAL1 plasmid for yeast transformation. This was performed by mixing pre-competent E. coli with the YEpTOP2PGAL1 plasmid, and plating on selective ampicillin plates. Following colony formation, successfully transformed cells were reared in liquid media containing ampicillin until a sufficient cellular density was achieved for plasmid extraction (Elbing & Brent, 2019; Mix & Go! Competent Cells-Zymo 10B, n.d.; Tuttle et al., 2021). Plasmid extraction was achieved using the protocol set out in (Addgene: Handling Plasmids from Addgene - Purifying Plasmid DNA, n.d.).

4.3.2 *S. cerevisiae* Transformation

The chosen yeast strain was BCY123, which is negative for the URA3 gene required for uracil synthesis, allowing for selection based on growth media which lacks uracil (-uracil). If yeast cells are successfully transformed with the YEpTOP2PGAL1 plasmid, colonies will be observed to form on -uracil plates. Competence in the BCY123 strain was induced using prior to transformation using the protocol (Yeast Transformation Protocols, n.d.). *S. cerevisiae* cells were reared at 30 °C with mild agitation for the entirety of this experiment.

4.3.3 *S. cerevisiae* Growth Conditions for Induction of h-ADAR Expression

Given that the h-ADAR gene in the YEpTOP2PGAL1 plasmid is expressed under the control of a GAL promoter, h-ADAR will only be expressed while galactose is being used by the cell. Given these conditions, there are three stages of growth conditions which must be gone through in order to stimulate h-ADAR expression (Macbeth & Bass, 2007).

Firstly, the *S. cerevisiae* cells transfected with the YEpTOP2PGAL1 plasmid must be grown in synthetic -uracil drop-out media containing dextrose as the sole carbohydrate source for 24 hours. Next, the cells were pelleted and the supernatant containing dextrose was removed, before resuspending the cells in -uracil drop-out media containing both glycerol and lactic acid for 24 hours. This was done in order to ensure total usage of any traces of dextrose before proceeding to the final stage of h-ADAR expression. Finally, the cells were pelleted, the supernatant containing glycerol and lactic acid was removed, and the yeast pellet was resuspended in -uracil drop-out media containing galactose as the sole carbohydrate source. Following 24 hours growth in this final culture, the cells were pelleted, washed to remove contaminants, and used for Rolling Circle sequencing according to the protocol (Fritsch et al., 2018). Control samples were prepared in the same way for the first step of the protocol, however instead of being transferred to flasks containing -uracil drop out media containing glycerol and lactic acid and then to galactose, the resulting yeast cell pellets were transferred to fresh flasks containing -uracil drop-out media with dextrose as the sole carbohydrate source in order to prevent risks of h-ADAR expression in the control.

4.4 Results and Discussion

The transcriptional landscape for RNA Pol II, which transcribes mRNAs, displayed an increase in A-to-G errors of ~60 times in the h-ADAR condition when compared to the control (Figure 4.1). These findings suggest that there is a huge increase in the incidence of A-to-I editing under h-ADAR gene expression conditions, given that A is edited to I, and I is recognized as G during sequencing.

Additionally, it was observed that not all types of RNA molecules were affected by the expression of h-ADAR genes. Ribosomal RNAs (rRNAs) produced by RNA Polymerase I (RNA

Pol I) and Transfer RNAs (tRNAs) produced by RNA Polymerase III (RNA Pol III), did not display a similar increase in A-to-I or A-to-G error rates (Figure 4.2, Figure 4.3). This indicates that h-ADAR editing, even when off-target, does not affect tRNAs or rRNAs.

Interestingly, both the RNA Pol I and the RNA Pol III transcription landscapes display significant increases in the C-to-U error rates and lesser increases in the G-to-C and G-to-U error rates in the h-ADAR expression experimental condition compared to the control, a pattern which does not extend to the RNA Pol II transcription landscape (Figure 4.1, Figure 4.2, Figure 4.3). As mentioned above in chapter III, C-to-U errors in particular and C- and G- errors in general may result due to inflammation, oxidative stress, or other damage to C and G DNA bases. One possibility is that this pattern may have arisen due to differences in RNA lifespans. While most mRNAs have a half-life of just a few minutes, rRNAs and tRNAs can function for up to several days in the cell. The yeast cells may have gone through stressful and thus damaging cellular conditions due to the stress of altering the available carbohydrate source and thus being forced to switch metabolic pathways. In this case, the tRNAs and rRNAs produced under these conditions would still be present in the cells used for the Rolling Circle sequencing protocol 24 hours later, but most or all of the mRNAs produced would have already been replaced and thus not show the same transcription error patterns.

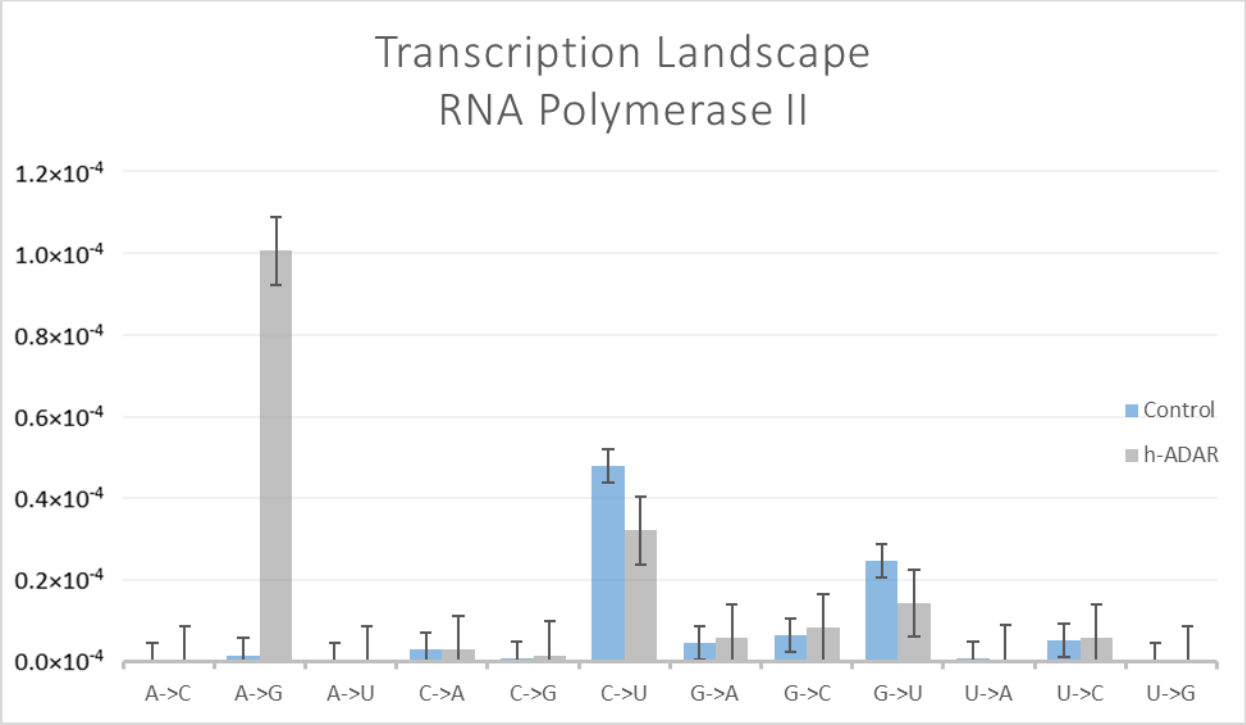

Figure 4.1 h-ADAR Expression Transcription Landscape for RNA Polymerase II

Transcription landscape depicting mRNA transcription errors produced by RNA polymerase II in *S. cerevisiae* expressing the h-ADAR gene vs. control yeast not expressing this gene. Error bars: Standard Error.

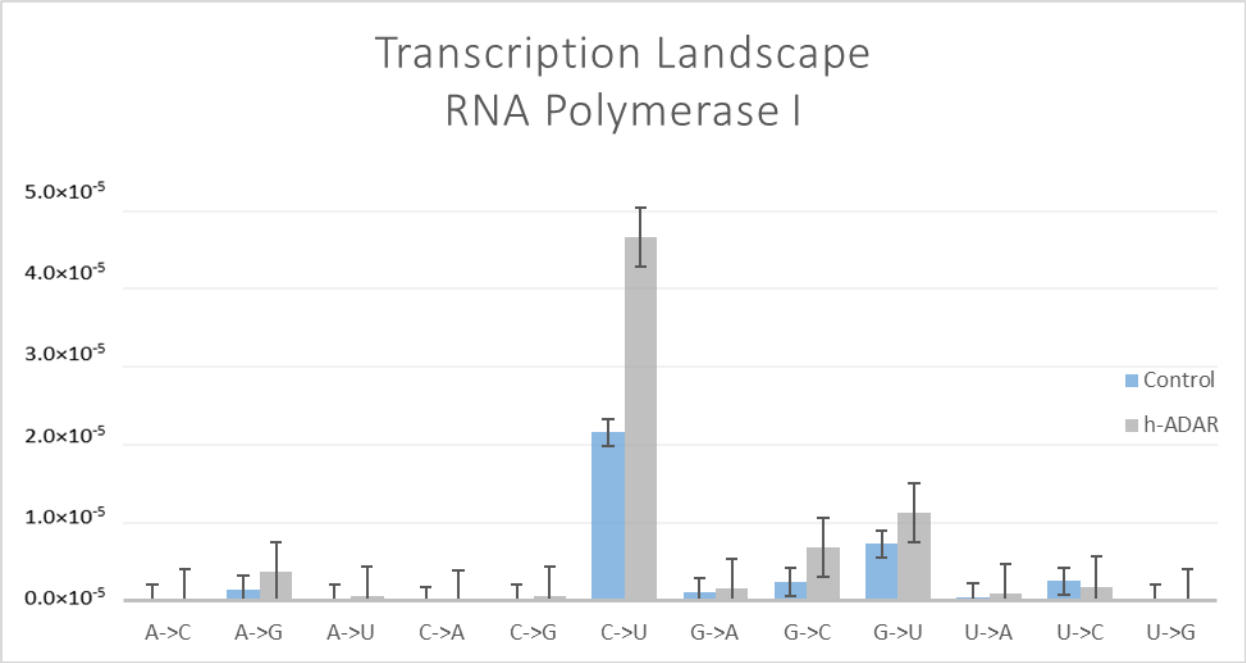

Figure 4.2 h-ADAR Expression Transcription Landscape for RNA Polymerase I

Transcription landscape depicting mRNA transcription errors produced by RNA polymerase I in *S. cerevisiae* expressing the h-ADAR gene vs. control yeast not expressing this gene. Error bars: Standard Error.

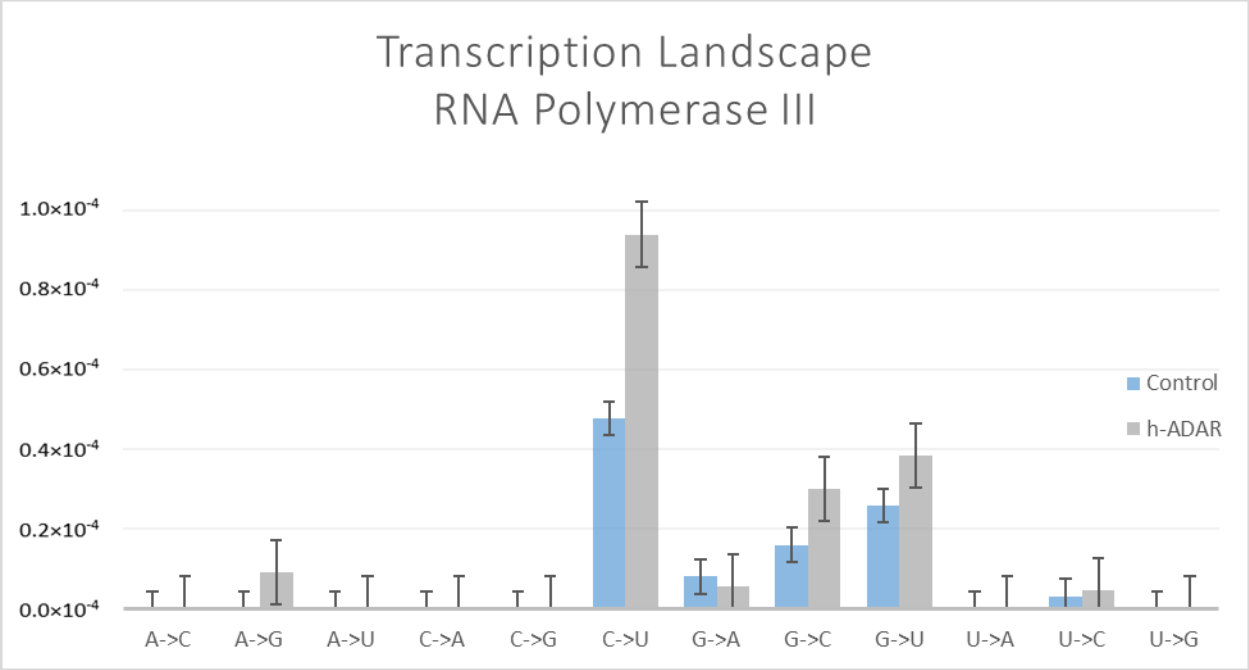

Figure 4.3 h-ADAR Expression Transcription Landscape for RNA Polymerase III

Transcription landscape depicting mRNA transcription errors produced by RNA polymerase III in *S. cerevisiae* expressing the h-ADAR gene vs. control yeast not expressing this gene. Error bars: Standard Error.

4.5 Conclusions

While frequently-occurring editing events produced by RNA editing genes such as h-ADAR may cause readily apparent links to cellular function or disease, low-level off-target editing may be involved in just as significant but difficult to see effects. It is therefore necessary to quantify the frequency of these off-target editing events in order to be able to investigate their impact on health and disease development.

It was determined that even in a species which has no ADAR genes, and thus can have had no evolutionary conservation of ADAR editing sites such as *S. cerevisiae*, a huge number of A-to-I edits were occurring in the mRNA transcriptome upon expression of h-ADAR. This suggests that a far greater number of A-to-I, and thus A-to-G mRNA errors are constantly

occurring in the genomes of species which naturally possess ADAR genes than was previously suspected. suspected. Additional research from collaborators at the University of Southern California has shown that cephalopod species with naturally high levels of RNA editing also have frequently occurring editing mistakes.

If this were the case, ADAR gene editing may be placing a burden on cellular proofreading and repair machinery, reducing the energy efficiency of cells and possibly even causing cytotoxic mRNAs to appear. While organisms which naturally possess ADAR genes may have tolerance for these "background" A-to-I off-target edits, an increase in off-target ADAR editing may exceed the threshold for cellular proofreading and repair machinery to be able to both cope with off-target ADAR edits, as well as complete all other necessary transcriptome and proteome regulatory functions, leading to a reduction in cellular health and increased potential for development of cancer.

It is therefore important to understand how off-target ADAR editing in cells, tissues, and organs may target mRNA sequences linked with human health and disease states.

REFERENCES

Addgene: Handling Plasmids from Addgene—Purifying Plasmid DNA. (n.d.). Retrieved September 14, 2021, from https://www.addgene.org/protocols/purify-plasmid-dna/

Albertin, C. B., Medina-Ruiz, S., Mitros, T., Schmidbaur, H., Sanchez, G., Wang, Z. Y., Grimwood, J., Rosenthal, J. J. C., Ragsdale, C. W., Simakov, O., & Rokhsar, D. S. (2022). Genome and transcriptome mechanisms driving cephalopod evolution. Nature Communications, 13(1), Article 1. https://doi.org/10.1038/s41467-022-29748-w

Amrit, F. R. G., Ratnappan, R., Keith, S. A., & Ghazi, A. (2014). The C. elegans lifespan assay toolkit. Methods, 68(3), 465–475. https://doi.org/10.1016/j.ymeth.2014.04.002

Anagnostou, M. E., Chung, C., McGann, E., Verheijen, B. M., Kou, Y., Chen, L., & Vermulst, M. (2021). Transcription errors in aging and disease. Translational Medicine of Aging, 5, 31–38. https://doi.org/10.1016/j.tma.2021.05.002

Andreotti, G., Koutros, S., Hofmann, J. N., Sandler, D. P., Lubin, J. H., Lynch, C. F., Lerro, C. C., De Roos, A. J., Parks, C. G., Alavanja, M. C., Silverman, D. T., & Beane Freeman, L. E. (2018). Glyphosate Use and Cancer Incidence in the Agricultural Health Study. Journal of the National Cancer Institute, 110(5), 509–516. https://doi.org/10.1093/jnci/djx233

Angeles-Albores, D., N Lee, R. Y., Chan, J., & Sternberg, P. W. (2016). Tissue enrichment analysis for C. elegans genomics. BMC Bioinformatics, 17(1), 366. https://doi.org/10.1186/s12859-016-1229-9

Aruscavage, P. J., & Bass, B. L. (2000). A phylogenetic analysis reveals an unusual sequence conservation within introns involved in RNA editing. RNA (New York, N.Y.), 6(2), 257–269. https://doi.org/10.1017/s1355838200991921

Auerbach, P., Bennett, R. A. O., Bailey, E. A., Krokan, H. E., & Demple, B. (2005). Mutagenic specificity of endogenously generated abasic sites in Saccharomyces cerevisiae chromosomal DNA. Proceedings of the National Academy of Sciences of the United States of America, 102(49), 17711–17716. https://doi.org/10.1073/pnas.0504643102

Bass, B. L. (2002). RNA editing by adenosine deaminases that act on RNA. Annual Review of Biochemistry, 71, 817–846. https://doi.org/10.1146/annurev.biochem.71.110601.135501

Baudrimont, A., Voegeli, S., Viloria, E. C., Stritt, F., Lenon, M., Wada, T., Jaquet, V., & Becskei, A. (2017). Multiplexed gene control reveals rapid mRNA turnover. Science Advances, 3(7), e1700006. https://doi.org/10.1126/sciadv.1700006

Baysal, B. E., Sharma, S., Hashemikhabir, S., & Janga, S. C. (2017). RNA Editing in Pathogenesis of Cancer. Cancer Research, 77(14), 3733–3739. https://doi.org/10.1158/0008-5472.CAN-17-0520

Benbrook, C. M. (2019). How did the US EPA and IARC reach diametrically opposed conclusions on the genotoxicity of glyphosate-based herbicides? Environmental Sciences Europe, 31(1), 2. https://doi.org/10.1186/s12302-018-0184-7

Bernhardt, H. S., & Tate, W. P. (2012). Primordial soup or vinaigrette: Did the RNA world evolve at acidic pH? Biology Direct, 7, 4. https://doi.org/10.1186/1745-6150-7-4

Brégeon, D., & Doetsch, P. W. (2011). Transcriptional mutagenesis: Causes and involvement in tumor development. Nature Reviews. Cancer, 11(3), 218–227. https://doi.org/10.1038/nrc3006

Brenner, S., Jacob, F., & Meselson, M. (1961). An Unstable Intermediate Carrying Information from Genes to Ribosomes for Protein Synthesis. Nature, 190(4776), Article 4776. https://doi.org/10.1038/190576a0

Caenorhabditis Genetics Center (CGC). (n.d.). Retrieved December 12, 2022, from https://cgc.umn.edu/

Chalk, A. M., Taylor, S., Heraud-Farlow, J. E., & Walkley, C. R. (2019). The majority of A-to-I RNA editing is not required for mammalian homeostasis. Genome Biology, 20(1), 268. https://doi.org/10.1186/s13059-019-1873-2

Chan, T. W., Fu, T., Bahn, J. H., Jun, H.-I., Lee, J.-H., Quinones-Valdez, G., Cheng, C., & Xiao, X. (2020). RNA editing in cancer impacts mRNA abundance in immune response pathways. Genome Biology, 21(1), 268. https://doi.org/10.1186/s13059-020-02171-4

Chen, E. Y., Tan, C. M., Kou, Y., Duan, Q., Wang, Z., Meirelles, G. V., Clark, N. R., & Ma'ayan, A. (2013). Enrichr: Interactive and collaborative HTML5 gene list enrichment analysis tool. BMC Bioinformatics, 14, 128. https://doi.org/10.1186/1471-2105-14-128

Cong, Y., Yang, H., Zhang, P., Xie, Y., Cao, X., & Zhang, L. (2020). Transcriptome Analysis of the Nematode Caenorhabditis elegans in Acidic Stress Environments. Frontiers in Physiology, 11, 1107. https://doi.org/10.3389/fphys.2020.01107

Cooper, G. M. (2000). Translation of mRNA. The Cell: A Molecular Approach. 2nd Edition. https://www.ncbi.nlm.nih.gov/books/NBK9849/

Crick, F. H. (1958). On protein synthesis. Symposia of the Society for Experimental Biology, 12, 138–163.

De Roos, A. J., Zahm, S., Cantor, K., Weisenburger, D., Holmes, F., Burmeister, L., & Blair, A. (2003). Integrative assessment of multiple pesticides as risk factors for non-Hodgkin's lymphoma among men. Occupational and Environmental Medicine, 60(9), e11. https://doi.org/10.1136/oem.60.9.e11

Defarge, N., Spiroux de Vendômois, J., & Séralini, G. E. (2018). Toxicity of formulants and heavy metals in glyphosate-based herbicides and other pesticides. Toxicology Reports, 5, 156–163. https://doi.org/10.1016/j.toxrep.2017.12.025

Degtyareva, N. P., Heyburn, L., Sterling, J., Resnick, M. A., Gordenin, D. A., & Doetsch, P. W. (2013). Oxidative stress-induced mutagenesis in single-strand DNA occurs primarily at cytosines and is DNA polymerase zeta-dependent only for adenines and guanines. Nucleic Acids Research, 41(19), 8995–9005. https://doi.org/10.1093/nar/gkt671

DeOcesano-Pereira, C., Velloso, F. J., Carreira, A. C. O., Ribeiro, C. S. P., Winnischofer, S. M. B., Sogayar, M. C., & Trombetta-Lima, M. (2018). Post-Transcriptional Control of RNA Expression in Cancer. Gene Expression and Regulation in Mammalian Cells - Transcription From General Aspects. https://doi.org/10.5772/intechopen.71861

Dill, G. M., Sammons, R. D., Feng, P. C. C., Kohn, F., Kretzmer, K., Mehrsheikh, A., Bleeke, M., Honegger, J. L., Farmer, D., Wright, D., & Haupfear, E. A. (2010). Glyphosate: Discovery, Development, Applications, and Properties. In V. K. Nandula (Ed.), Glyphosate Resistance in Crops and Weeds (pp. 1–33). John Wiley & Sons, Inc. https://doi.org/10.1002/9780470634394.ch1

Duke, S. O., & Powles, S. B. (2008). Glyphosate: A once-in-a-century herbicide. https://web.archive.org/web/20190702211642/https://naldc.nal.usda.gov/download/17918/PDF

Eifler, T., Pokharel, S., & Beal, P. A. (2013). RNA-Seq Analysis Identifies A Novel Set of Editing Substrates for Human ADAR2 Present in Saccharomyces cerevisiae. Biochemistry, 52(45), 10.1021/bi4006539. https://doi.org/10.1021/bi4006539

Elbing, K., & Brent, R. (2019). Growth of E. coli in liquid medium. Current Protocols in Molecular Biology, 125(1), e81. https://doi.org/10.1002/cpmb.81

Elsakrmy, N., Zhang-Akiyama, Q.-M., & Ramotar, D. (2020). The Base Excision Repair Pathway in the Nematode Caenorhabditis elegans. Frontiers in Cell and Developmental Biology, 8, 598860. https://doi.org/10.3389/fcell.2020.598860

EPA. (2018). Revised Glyphosate Issue Paper: Evaluation of Carcinogenic Potential. https://www.regulations.gov/document/EPA-HQ-OPP-2009-0361-0073

Eriksson, M., Hardell, L., Carlberg, M., & Åkerman, M. (2008). Pesticide exposure as risk factor for non-Hodgkin lymphoma including histopathological subgroup analysis. International Journal of Cancer, 123(7), 1657–1663. https://doi.org/10.1002/ijc.23589

Fadda, E., & Pomès, R. (2011). On the molecular basis of uracil recognition in DNA: Comparative study of T-A versus U-A structure, dynamics and open base pair kinetics. Nucleic Acids Research, 39(2), 767–780. https://doi.org/10.1093/nar/gkq812

Fritsch, C., Gout, J.-F. P., & Vermulst, M. (2018). Genome-wide Surveillance of Transcription Errors in Eukaryotic Organisms. Journal of Visualized Experiments : JoVE, 139. https://doi.org/10.3791/57731

George, J., Prasad, S., Mahmood, Z., & Shukla, Y. (2010). Studies on glyphosate-induced carcinogenicity in mouse skin: A proteomic approach. Journal of Proteomics, 73, 951–964. https://doi.org/10.1016/j.jprot.2009.12.008

Gout, J.-F., Li, W., Fritsch, C., Li, A., Haroon, S., Singh, L., Hua, D., Fazelinia, H., Smith, Z., Seeholzer, S., Thomas, K., Lynch, M., & Vermulst, M. (2017). The landscape of transcription errors in eukaryotic cells. Science Advances, 3(10), e1701484. https://doi.org/10.1126/sciadv.1701484

Gout, J.-F., Thomas, W. K., Smith, Z., Okamoto, K., & Lynch, M. (2013). Large-scale detection of in vivo transcription errors. Proceedings of the National Academy of Sciences, 110(46), 18584–18589. https://doi.org/10.1073/pnas.1309843110

Grice, L. F., & Degnan, B. M. (2015). The origin of the ADAR gene family and animal RNA editing. BMC Evolutionary Biology, 15(1), 4. https://doi.org/10.1186/s12862-015-0279-3

Hagen, L., Peña-Diaz, J., Kavli, B., Otterlei, M., Slupphaug, G., & Krokan, H. E. (2006). Genomic uracil and human disease. Experimental Cell Research, 312(14), 2666–2672. https://doi.org/10.1016/j.yexcr.2006.06.015

Hall, R. A., Vullo, D., Innocenti, A., Scozzafava, A., Supuran, C. T., Klappa, P., & Mühlschlegel, F. A. (2008). External pH influences the transcriptional profile of the carbonic anhydrase, CAH-4b in Caenorhabditis elegans. Molecular and Biochemical Parasitology, 161(2), 140–149. https://doi.org/10.1016/j.molbiopara.2008.06.013

Heilig, G. (2012). Killing weeds in the garden with glyphosate. MSU Extension. https://www.canr.msu.edu/news/killing_weeds_in_the_garden_with_glyphosate

Hong, M., Tao, S., Zhang, L., Diao, L.-T., Huang, X., Huang, S., Xie, S.-J., Xiao, Z.-D., & Zhang, H. (2020). RNA sequencing: New technologies and applications in cancer research. Journal of Hematology & Oncology, 13(1), Article 1. https://doi.org/10.1186/s13045-020-01005-x

IARC. (2017). Some Organophosphate Insecticides and Herbicides. International Agency for Research on Cancer. http://www.ncbi.nlm.nih.gov/books/NBK436774/

Kapur, M., & Ackerman, S. L. (2018). mRNA Translation Gone Awry: Translation Fidelity and Neurological Disease. Trends in Genetics : TIG, 34(3), 218–231. https://doi.org/10.1016/j.tig.2017.12.007

Kay, J., Thadhani, E., Samson, L., & Engelward, B. (2019). Inflammation-Induced DNA Damage, Mutations and Cancer. DNA Repair, 83, 102673. https://doi.org/10.1016/j.dnarep.2019.102673

Keegan, L. P., Leroy, A., Sproul, D., & O'Connell, M. A. (2004). Adenosine deaminases acting on RNA (ADARs): RNA-editing enzymes. Genome Biology, 5(2), 209.

Khanna, N., Cressman III, C. P., Tatara, C. P., & Williams, P. L. (1997). Tolerance of the Nematode Caenorhabditis elegans to pH, Salinity, and Hardness in Aquatic Media. Archives of Environmental Contamination and Toxicology, 32(1), 110–114. https://doi.org/10.1007/s002449900162

Krokan, H. E., Drabløs, F., & Slupphaug, G. (2002). Uracil in DNA – occurrence, consequences and repair. Oncogene, 21(58), Article 58. https://doi.org/10.1038/sj.onc.1205996

Krokan, H. E., Otterlei, M., Nilsen, H., Kavli, B., Skorpen, F., Andersen, S., Skjelbred, C., Akbari, M., Aas, P. A., & Slupphaug, G. (2001). Properties and functions of human uracil-DNA glycosylase from the UNG gene. Progress in Nucleic Acid Research and Molecular Biology, 68, 365–386. https://doi.org/10.1016/s0079-6603(01)68112-1

Kuleshov, M. V., Jones, M. R., Rouillard, A. D., Fernandez, N. F., Duan, Q., Wang, Z., Koplev, S., Jenkins, S. L., Jagodnik, K. M., Lachmann, A., McDermott, M. G., Monteiro, C. D., Gundersen, G. W., & Ma'ayan, A. (2016). Enrichr: A comprehensive gene set enrichment analysis web server 2016 update. Nucleic Acids Research, 44(W1), W90-97. https://doi.org/10.1093/nar/gkw377

Kung, C.-P., Maggi, L. B., & Weber, J. D. (2018). The Role of RNA Editing in Cancer Development and Metabolic Disorders. Frontiers in Endocrinology, 9. https://doi.org/10.3389/fendo.2018.00762

Kusumoto-Matsuo, R., Kanda, T., & Kukimoto, I. (2011). Rolling circle replication of human papillomavirus type 16 DNA in epithelial cell extracts. Genes to Cells, 16(1), 23–33. https://doi.org/10.1111/j.1365-2443.2010.01458.x

Kwiatkowska, M., Reszka, E., Woźniak, K., Jabłońska, E., Michałowicz, J., & Bukowska, B. (2017). DNA damage and methylation induced by glyphosate in human peripheral blood mononuclear cells (in vitro study). Food and Chemical Toxicology, 105, 93–98. https://doi.org/10.1016/j.fct.2017.03.051

Laverty, D. J., Averill, A. M., Doublié, S., & Greenberg, M. M. (2017). The A-Rule and Deletion Formation During Abasic and Oxidized Abasic Site Bypass by DNA Polymerase θ. ACS Chemical Biology, 12(6), 1584–1592. https://doi.org/10.1021/acschembio.7b00211

Li, Z., Wu, J., & DeLeo, C. J. (2006). RNA damage and surveillance under oxidative stress. IUBMB Life, 58(10), 581–588. https://doi.org/10.1080/15216540600946456

Liscovitch-Brauer, N., Alon, S., Porath, H. T., Elstein, B., Unger, R., Ziv, T., Admon, A., Levanon, E. Y., Rosenthal, J. J. C., & Eisenberg, E. (2017). Trade-off between transcriptome plasticity and genome evolution in cephalopods. Cell, 169(2), 191-202.e11. https://doi.org/10.1016/j.cell.2017.03.025

Liu, X., Zou, X., Li, H., Zou, Z., Yang, J., Wang, C., Wu, S., & Zhang, H. (2018). Bypass of an Abasic Site via the A-Rule by DNA Polymerase of Pseudomonas aeruginosa Phage PaP1. Chemical Research in Toxicology, 31(1), 58–65. https://doi.org/10.1021/acs.chemrestox.7b00287

Macbeth, M. R., & Bass, B. L. (2007). Large-scale overexpression and purification of ADARs from Saccharomyces cerevisiae for biophysical and biochemical studies. Methods in Enzymology, 424, 319–331. https://doi.org/10.1016/S0076-6879(07)24015-7

Mack, H. I. D., Heimbucher, T., & Murphy, C. T. (2018). The nematode Caenorhabditis elegans as a model for aging research. Drug Discovery Today: Disease Models, 27, 3–13. https://doi.org/10.1016/j.ddmod.2018.11.001

Mallajosyula, S. S., & Pati, S. K. (2007). Effect of Protonation on the Electronic Properties of DNA Base Pairs: Applications for Molecular Electronics. The Journal of Physical Chemistry B, 111(40), 11614–11618. https://doi.org/10.1021/jp076063m

Massonneau, J., Ouellet, C., Lucien, F., Dubois, C. M., Tyler, J., & Boissonneault, G. (2018). Suboptimal extracellular pH values alter DNA damage response to induced double-strand breaks. FEBS Open Bio, 8(3), 416–425. https://doi.org/10.1002/2211-5463.12384

Matthews, T. M., & Webb, C. (1991). Culture Systems. In M. F. Tuite & S. G. Oliver (Eds.), Saccharomyces (pp. 249–282). Springer US. https://doi.org/10.1007/978-1-4899-2641-8_8

Mix & Go! Competent Cells-Zymo 10B. (n.d.). ZYMO RESEARCH. Retrieved September 24, 2021, from https://www.zymoresearch.com/products/mix-and-go-competent-cells-zymo-10b

Nishikura, K. (2010). Functions and Regulation of RNA Editing by ADAR Deaminases. Annual Review of Biochemistry, 79, 321–349. https://doi.org/10.1146/annurev-biochem-060208-105251

Olinski, R., Slupphaug, G., Foksinski, M., & Krokan, H. E. (2021). Genomic Uracil and Aberrant Profile of Demethylation Intermediates in Epigenetics and Hematologic Malignancies. https://www.mdpi.com/1422-0067/22/8/4212

Orij, R., Brul, S., & Smits, G. J. (2011). Intracellular pH is a tightly controlled signal in yeast. Biochimica et Biophysica Acta (BBA) - General Subjects, 1810(10), 933–944. https://doi.org/10.1016/j.bbagen.2011.03.011

Owiti, N., Lopez, C., Singh, S., Stephenson, A., & Kim, N. (2017). Def1 and Dst1 play distinct roles in repair of AP lesions in highly transcribed genomic regions. DNA Repair, 55, 31–39. https://doi.org/10.1016/j.dnarep.2017.05.003

Pandey, A., Dhabade, P., & Kumarasamy, A. (2019). Inflammatory Effects of Subacute Exposure of Roundup in Rat Liver and Adipose Tissue. Dose-Response, 17(2), 1559325819843380. https://doi.org/10.1177/1559325819843380

Peillex, C., & Pelletier, M. (2020). The impact and toxicity of glyphosate and glyphosate-based herbicides on health and immunity. Journal of Immunotoxicology, 17(1), 163–174. https://doi.org/10.1080/1547691X.2020.1804492

Porta-de-la-Riva, M., Fontrodona, L., Villanueva, A., & Cerón, J. (2012). Basic Caenorhabditis elegans Methods: Synchronization and Observation. Journal of Visualized Experiments : JoVE, 64, 4019. https://doi.org/10.3791/4019

Rao, D. N., Dryden, D. T. F., & Bheemanaik, S. (2014). Type III restriction-modification enzymes: A historical perspective. Nucleic Acids Research, 42(1), 45–55. https://doi.org/10.1093/nar/gkt616

RStudio Team. (2020). RStudio: Integrated Development for R. http://www.rstudio.com/

Samsel, A., & Seneff, S. (2013). Glyphosate's Suppression of Cytochrome P450 Enzymes and Amino Acid Biosynthesis by the Gut Microbiome: Pathways to Modern Diseases. Entropy, 15(4), Article 4. https://doi.org/10.3390/e15041416

Schinasi, L., & Leon, M. E. (2014). Non-Hodgkin Lymphoma and Occupational Exposure to Agricultural Pesticide Chemical Groups and Active Ingredients: A Systematic Review and Meta-Analysis. International Journal of Environmental Research and Public Health, 11(4), 4449–4527. https://doi.org/10.3390/ijerph110404449

Schindelin, J., Arganda-Carreras, I., Frise, E., Kaynig, V., Longair, M., Pietzsch, T., Preibisch, S., Rueden, C., Saalfeld, S., Schmid, B., Tinevez, J.-Y., White, D. J., Hartenstein, V., Eliceiri, K., Tomancak, P., & Cardona, A. (2012). Fiji. Nature Methods. https://www.nature.com/articles/nmeth.2019#citeas

Sire, J., Quérat, G., Esnault, C., & Priet, S. (2008). Uracil within DNA: An actor of antiviral immunity. Retrovirology, 5(1), Article 1. https://doi.org/10.1186/1742-4690-5-45

Stiernagle, T. (2006). Maintenance of C. elegans. WormBook. https://doi.org/10.1895/wormbook.1.101.1

Strauss, B. S. (1991). The 'A rule' of mutagen specificity: A consequence of DNA polymerase bypass of non-instructional lesions? BioEssays, 13(2), 79–84. https://doi.org/10.1002/bies.950130206

Suárez-Larios, K., Salazar-Martínez, A.-M., & Montero-Montoya, R. (2017). Screening of Pesticides with the Potential of Inducing DSB and Successive Recombinational Repair. Journal of Toxicology, 2017. https://doi.org/10.1155/2017/3574840

Supek, F., Bošnjak, M., Škunca, N., & Šmuc, T. (2011). REVIGO Summarizes and Visualizes Long Lists of Gene Ontology Terms. PLoS ONE, 6(7), e21800. https://doi.org/10.1371/journal.pone.0021800

Supek, F., & Škunca, N. (2017). Visualizing GO Annotations. In C. Dessimoz & N. Škunca (Eds.), The Gene Ontology Handbook (pp. 207–220). Springer. https://doi.org/10.1007/978-1-4939-3743-1_15

Tan, M. H., Li, Q., Shanmugam, R., Piskol, R., Kohler, J., Young, A. N., Liu, K. I., Zhang, R., Ramaswami, G., Ariyoshi, K., Gupte, A., Keegan, L. P., George, C. X., Ramu, A., Huang, N., Pollina, E. A., Leeman, D. S., Rustighi, A., Sharon Goh, Y. P., … Li, J. B. (2017). Dynamic landscape and regulation of RNA editing in mammals. Nature, 550(7675), 249–254. https://doi.org/10.1038/nature24041

Tarazona, J. V., Court-Marques, D., Tiramani, M., Reich, H., Pfeil, R., Istace, F., & Crivellente, F. (2017). Glyphosate toxicity and carcinogenicity: A review of the scientific basis of the European Union assessment and its differences with IARC. Archives of Toxicology, 91(8), 2723–2743. https://doi.org/10.1007/s00204-017-1962-5

Thermo Scientific. (n.d.). Retrieved December 13, 2022, from https://www.fishersci.com/shop/products/genesys-20-visible-spectrophotometer-2/14385445

Thomas, J. M., & Beal, P. A. (2017). How do ADARs bind RNA? New protein-RNA structures illuminate substrate recognition by the RNA editing ADARs. BioEssays : News and Reviews in Molecular, Cellular and Developmental Biology, 39(4), 10.1002/bies.201600187. https://doi.org/10.1002/bies.201600187

Tincher, C., Long, H., Behringer, M., Walker, N., & Lynch, M. (2017). The Glyphosate-Based Herbicide Roundup Does not Elevate Genome-Wide Mutagenesis of Escherichia coli. G3 (Bethesda, Md.), 7(10), 3331–3335. https://doi.org/10.1534/g3.117.300133

Tonkin, L. A., Saccomanno, L., Morse, D. P., Brodigan, T., Krause, M., & Bass, B. L. (2002). RNA editing by ADARs is important for normal behavior in Caenorhabditis elegans. The EMBO Journal, 21(22), 6025–6035. https://doi.org/10.1093/emboj/cdf607

Tsai, S. Q., Nguyen, N. T., Malagon-Lopez, J., Topkar, V. V., Aryee, M. J., & Joung, J. K. (2017). CIRCLE-seq: A highly sensitive in vitro screen for genome-wide CRISPR-Cas9 nuclease off-targets. Nature Methods, 14(6), 607–614. https://doi.org/10.1038/nmeth.4278

Tuttle, A. R., Trahan, N. D., & Son, M. S. (2021). Growth and Maintenance of Escherichia coli Laboratory Strains. Current Protocols, 1(1), e20. https://doi.org/10.1002/cpz1.20

Vermulst, M., Denney, A. S., Lang, M. J., Hung, C.-W., Moore, S., Moseley, M. A., Mosely, A. M., Thompson, J. W., Thompson, W. J., Madden, V., Gauer, J., Wolfe, K. J., Summers, D. W., Schleit, J., Sutphin, G. L., Haroon, S., Holczbauer, A., Caine, J., Jorgenson, J., … Erie, D. A. (2015). Transcription errors induce proteotoxic stress and shorten cellular lifespan. Nature Communications, 6, 8065. https://doi.org/10.1038/ncomms9065

Wang, L., Deng, Q., Hu, H., Liu, M., Gong, Z., Zhang, S., Xu-Monette, Z. Y., Lu, Z., Young, K. H., Ma, X., & Li, Y. (2019). Glyphosate induces benign monoclonal gammopathy and promotes multiple myeloma progression in mice. Journal of Hematology & Oncology, 12. https://doi.org/10.1186/s13045-019-0767-9

Weaver, K. J., May, C. J., & Ellis, B. L. (2017). Using a health-rating system to evaluate the usefulness of Caenorhabditis elegans as a model for anthelmintic study. PLoS ONE, 12(6), e0179376. https://doi.org/10.1371/journal.pone.0179376

Woźniak, E., Reszka, E., Jabłońska, E., Mokra, K., Balcerczyk, A., Huras, B., Zakrzewski, J., & Bukowska, B. (2020). The selected epigenetic effects of aminomethylphosphonic acid, a primary metabolite of glyphosate on human peripheral blood mononuclear cells (in vitro). Toxicology in Vitro, 66, 104878. https://doi.org/10.1016/j.tiv.2020.104878

Yablonovitch, A. L., Deng, P., Jacobson, D., & Li, J. B. (2017). The evolution and adaptation of A-to-I RNA editing. PLoS Genetics, 13(11), e1007064. https://doi.org/10.1371/journal.pgen.1007064

Yang, H. D., & Nam, S. W. (2020). Pathogenic diversity of RNA variants and RNA variation-associated factors in cancer development. Experimental & Molecular Medicine, 52(4), Article 4. https://doi.org/10.1038/s12276-020-0429-6

Yang, J.-S., Nam, H.-J., Seo, M., Han, S. K., Choi, Y., Nam, H. G., Lee, S.-J., & Kim, S. (2011). OASIS: Online Application for the Survival Analysis of Lifespan Assays Performed in Aging Research. PLoS ONE, 6(8), e23525. https://doi.org/10.1371/journal.pone.0023525

Yang, Y., Park, S.-H., Alford-Zappala, M., Lee, H.-W., Li, J., Cunningham, R. P., & Cao, W. (2019). Role of Endonuclease III Enzymes in Uracil Repair. Mutation Research, 813, 20–30. https://doi.org/10.1016/j.mrfmmm.2018.12.001

Yeast Transformation Protocols. (n.d.). Retrieved September 24, 2021, from https://www.sigmaaldrich.com/US/en/technical-documents/protocol/protein-biology/protein-expression/yeast-transformation-protocols

Zhang, L., Rana, I., Shaffer, R. M., Taioli, E., & Sheppard, L. (2019). Exposure to Glyphosate-Based Herbicides and Risk for Non-Hodgkin Lymphoma: A Meta-Analysis and Supporting Evidence. Mutation Research, 781, 186–206. https://doi.org/10.1016/j.mrrev.2019.02.001

APPENDIX A

CHAPTER II SUPPLEMENTARY CONTENT

Table A.1 Fleming-Harrington (Weighted Log-Rank) Test

Condition	X^2	P-value	Bonferroni P-value
WT vs. dHz-Δ	3.010	0.083	0.248
WT vs. DST1-Δ	6.880	0.009*	0.026*
WT vs. UNG1-Δ	3.340	0.068	0.203
dHz-Δ vs. DST1-Δ	0.390	0.533	1.0
dHz-Δ vs. UNG1-Δ	0.070	0.797	1.0
DST1-Δ vs. UNG1-Δ	0.430	0.513	1.0

Fleming-Harrington test comparison between *C. elegans* nematode strain survival statistics. Weighted for late-term study sensitivity. (J.-S. Yang et al., 2011).
* Denotes significance levels ≤0.05.

Table A.2 Chow Test

Condition	F-value	P-value	Bonferroni P-value
WT vs. dHz-Δ	3.75	0.0307*	0.0921
WT vs. DST1-Δ	12.96	0.000033*	0.0001*
WT vs. UNG1-Δ	29.68	0*	0*
dHz-Δ vs. DST1-Δ	4.28	0.0197*	0.0592
dHz-Δ vs. UNG1-Δ	19.87	0.000001*	0.000002*
DST1-Δ vs. UNG1-Δ	8.61	0.0007*	0.002*

Chow test comparison between *C. elegans* nematode strain survival statistics. (J.-S. Yang et al., 2011).
* Denotes significance levels ≤0.05

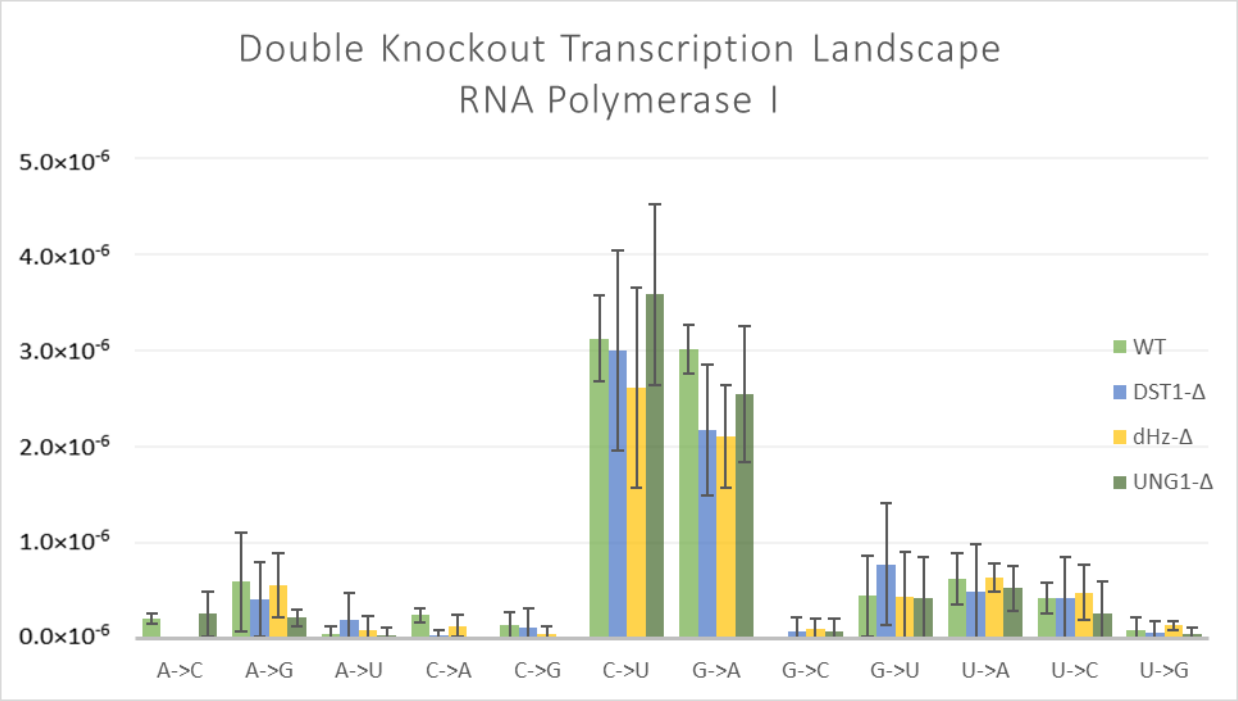

Figure A.1 Strain Error Rate Comparison in RNA Polymerase I Transcriptional Landscape

Transcriptional landscape depicting comparative mRNA error types in transcripts produced by the action of RNA polymerase I in dHz-Δ, DST1-Δ, UNG1-Δ, and WT (control) *C. elegans* strains. Error bars: Standard deviation.

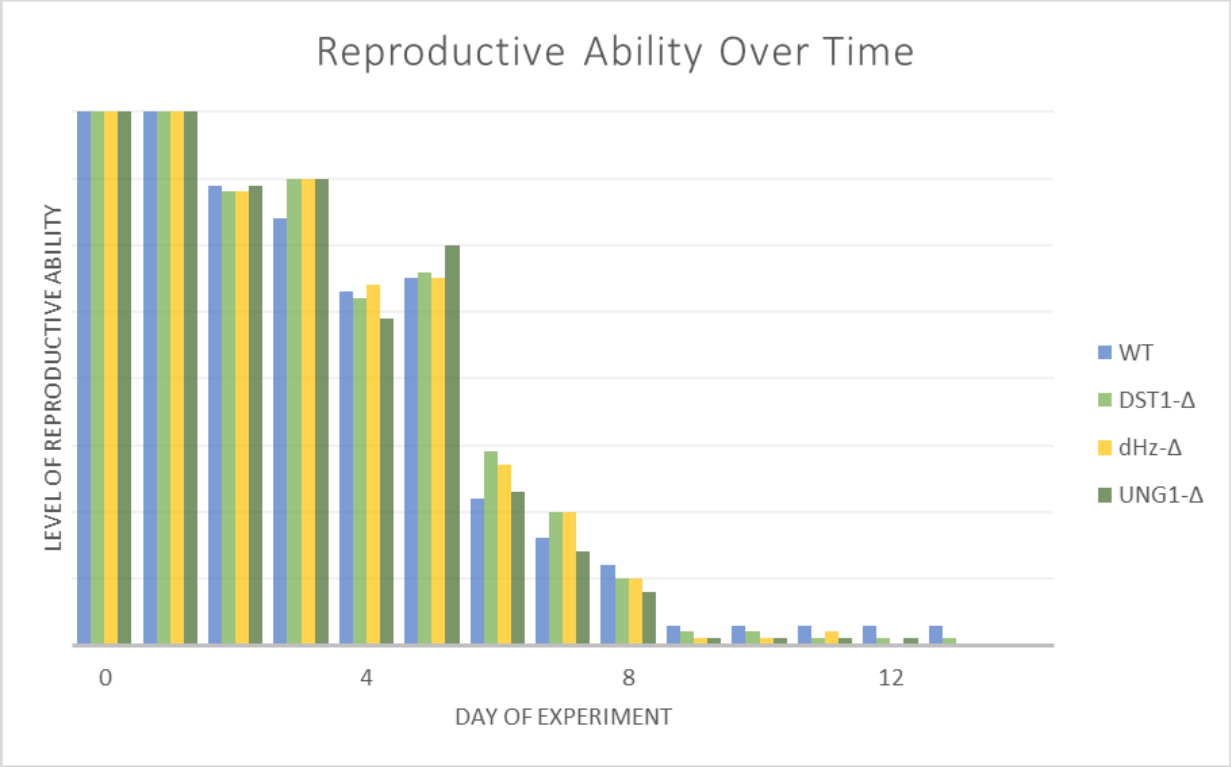

Figure A.2 *C. elegans* Strain Comparative Reproductive Ability Over Time

Depicts the level of reproductive ability of *C. elegans* strains WT, dHz-Δ, DST1-Δ, and UNG1-Δ over time, from not yet begun to reproduce to cessation of reproduction at advanced age.

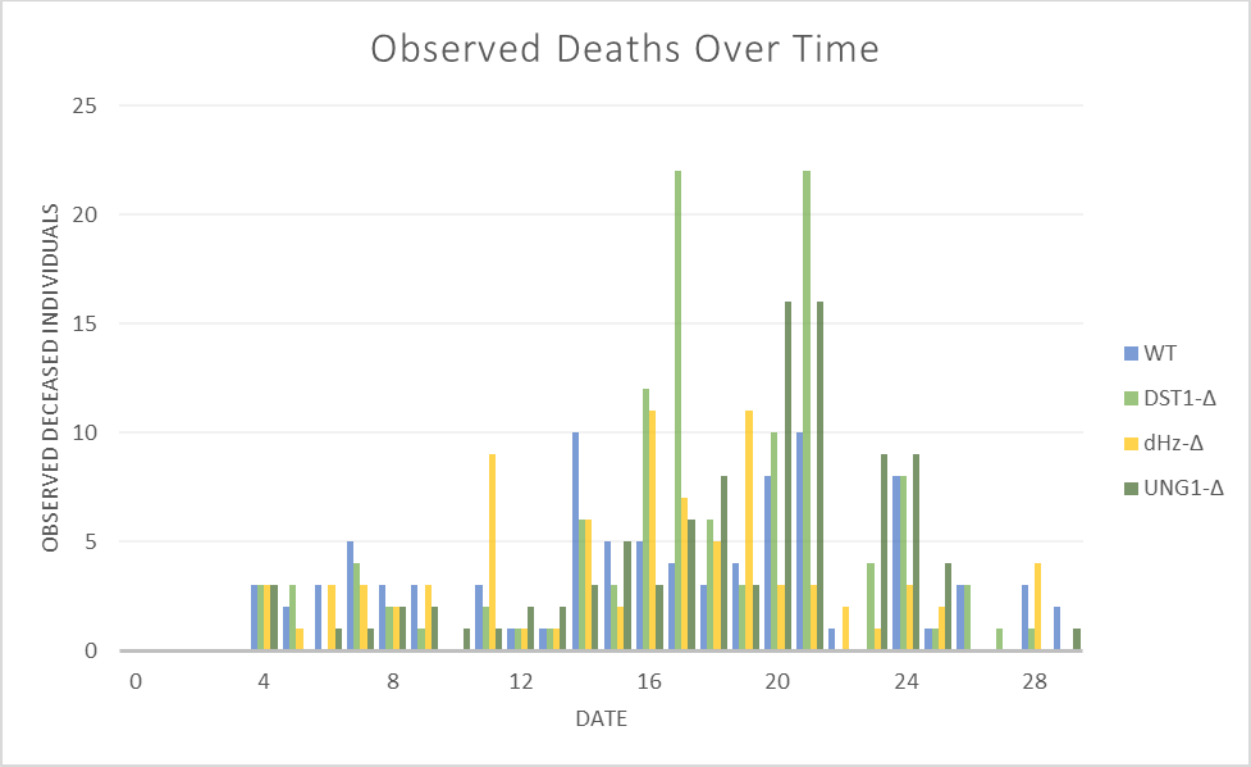

Figure A.3 *C. elegans* Observed Deaths Per Day by Strain

Depicts observed deceased individual worms per day for *C. elegans* strains WT, dHz-Δ, DST1-Δ, and UNG1-Δ.

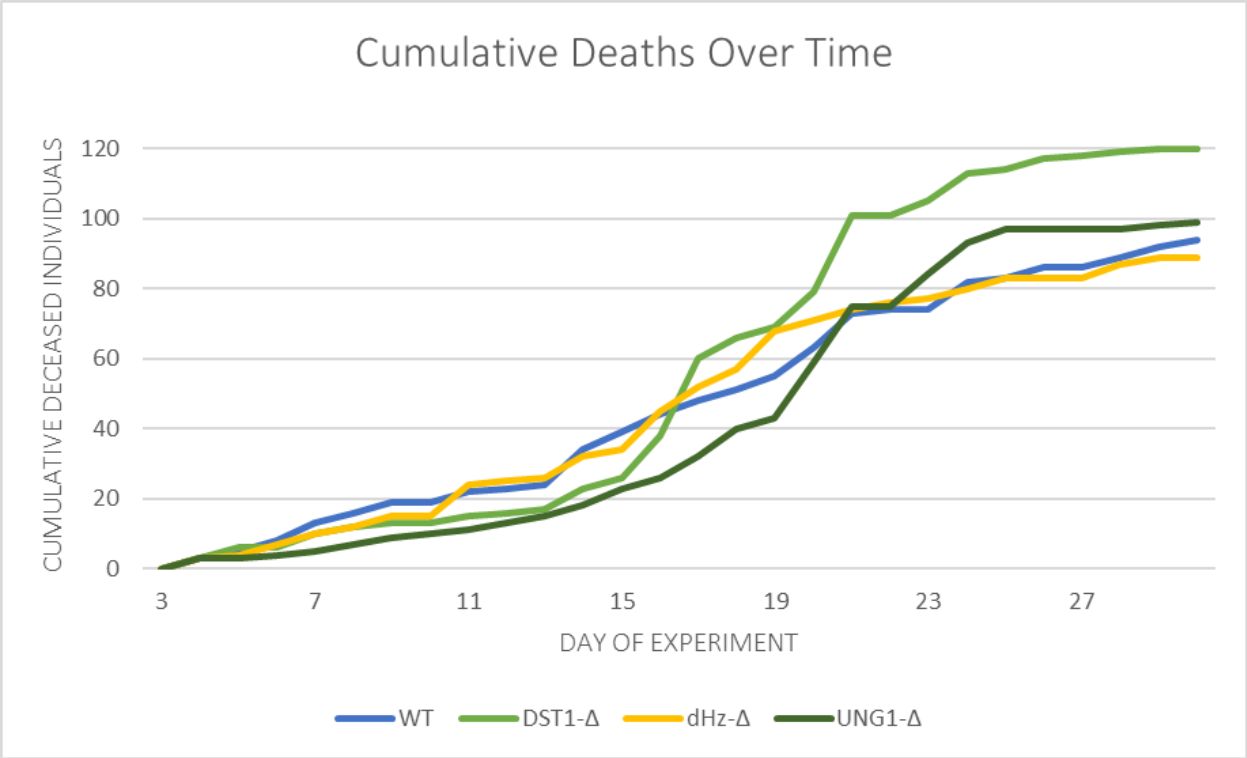

Figure A.4 *C. elegans* Cumulative Deaths Over Time

Depicts cumulative numbers of observed deceased worms for *C. elegans* strains WT, dHz-Δ, DST1-Δ, and UNG1-Δ.

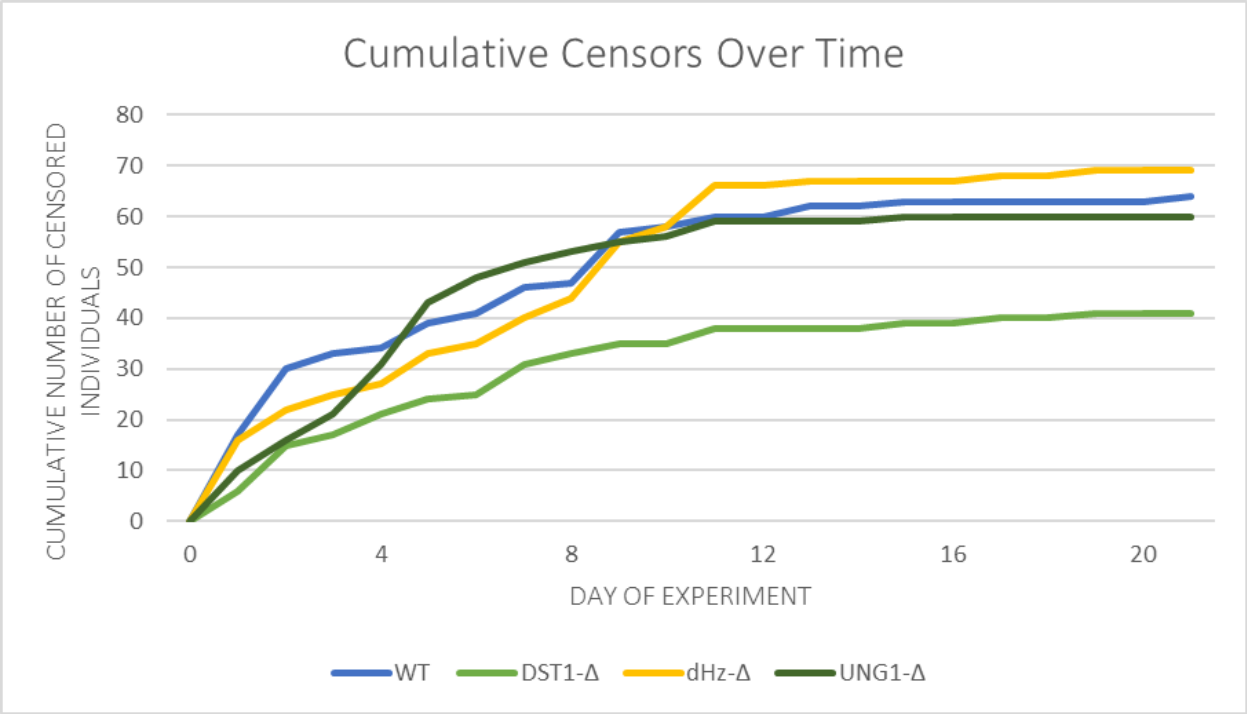

Figure A.5 *C. elegans* Cumulative Censors Over Time

Depicts cumulative censored individuals over time for *C. elegans* strains WT, dHz-Δ, DST1-Δ, and UNG1-Δ.

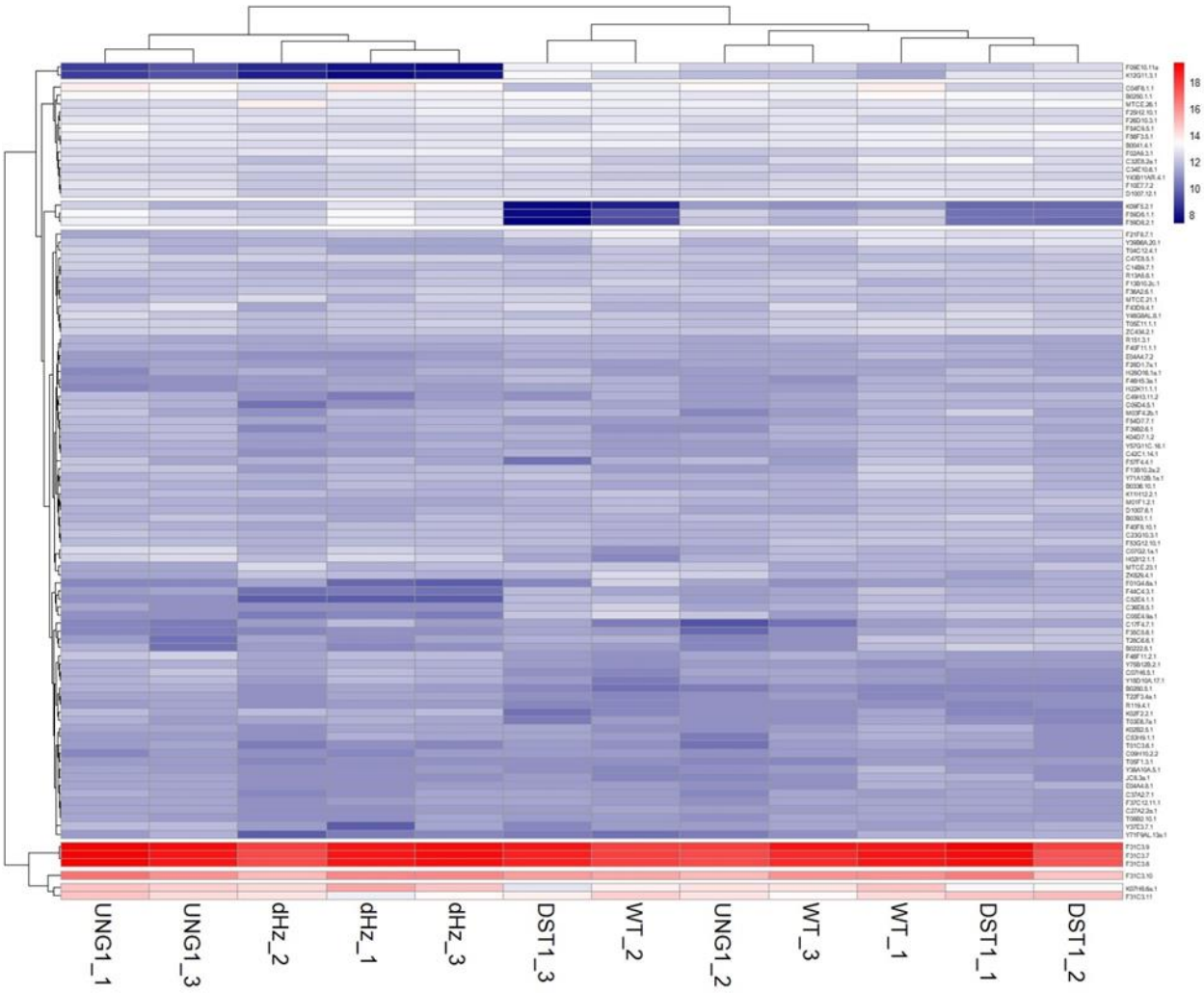

Figure A.6 *C. elegans* Strain Differential Gene Expression Heat Map

Heat map depicting differential gene expression levels for *C. elegans* strains WT, dHz-Δ, DST1-Δ, and UNG1-Δ. Horizontal axis label format: strain_replicate.

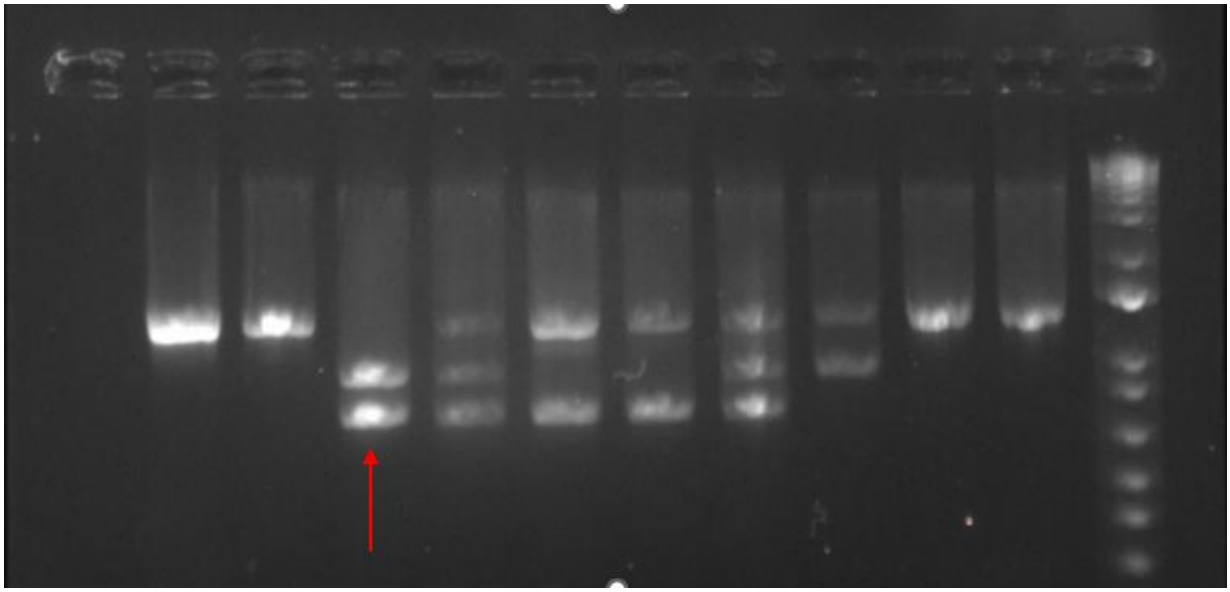

Figure A.7 Homozygous double knockout UNG1-Δ x DST1-Δ Southern Blot Gel

Depicts a Southern Blot gel loaded with DNA extracted from F2 offspring resulting from the crossing of homozygous knockout *C. elegans* strains UNG1-Δ and DST1-Δ. The red arrow indicates the successful homozygous double knockout offspring dHz-Δ.

APPENDIX B

CHAPTER III SUPPLEMENTAL CONTENT

B.1 RNA Polymerase I Transcription Landscapes for *C. elegans* and *S. cerevisiae* for Roundup Exposure Experiment

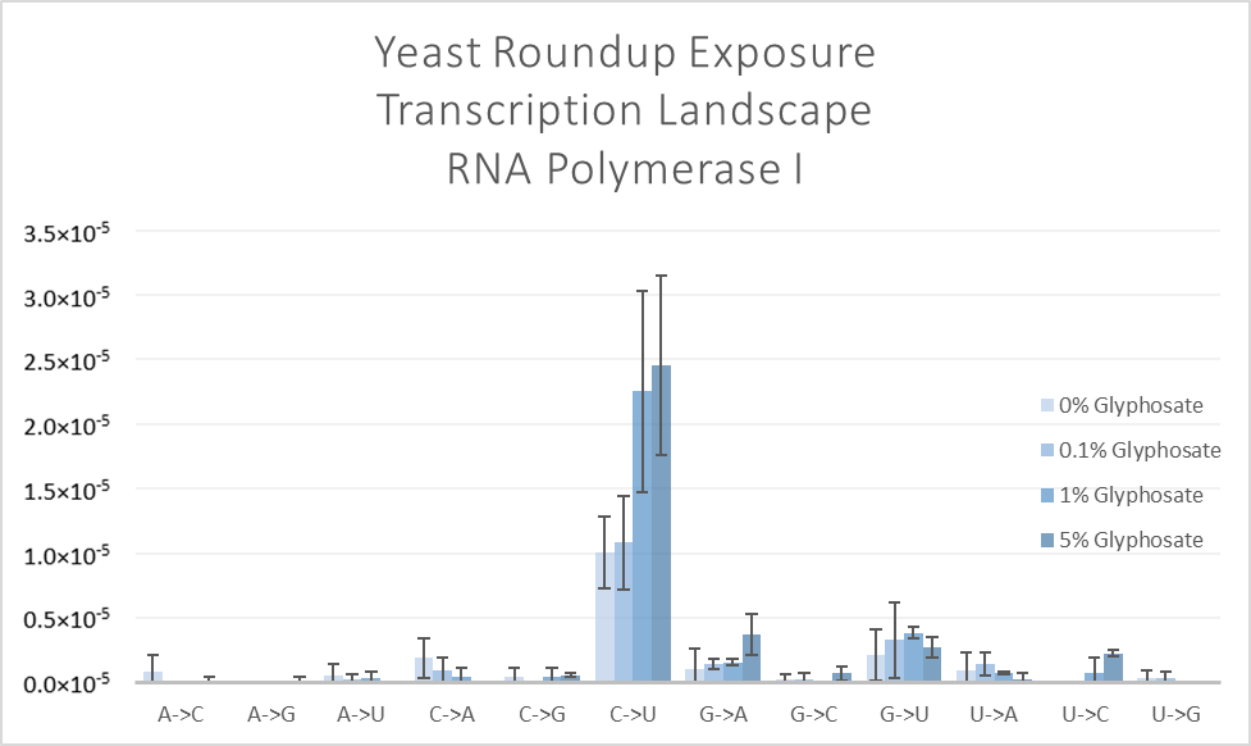

Figure B.1 Roundup Exposure *S. cerevisiae* Error Rate Comparison in RNA Polymerase I Transcriptional Landscape

Transcription landscape depicting mRNA transcription errors produced by RNA polymerase I following *S. cerevisiae* treatment with three different glyphosate percentages (5%, 1%, 0.1%) and a control lacking Roundup (0%). Error bars: Standard deviation.

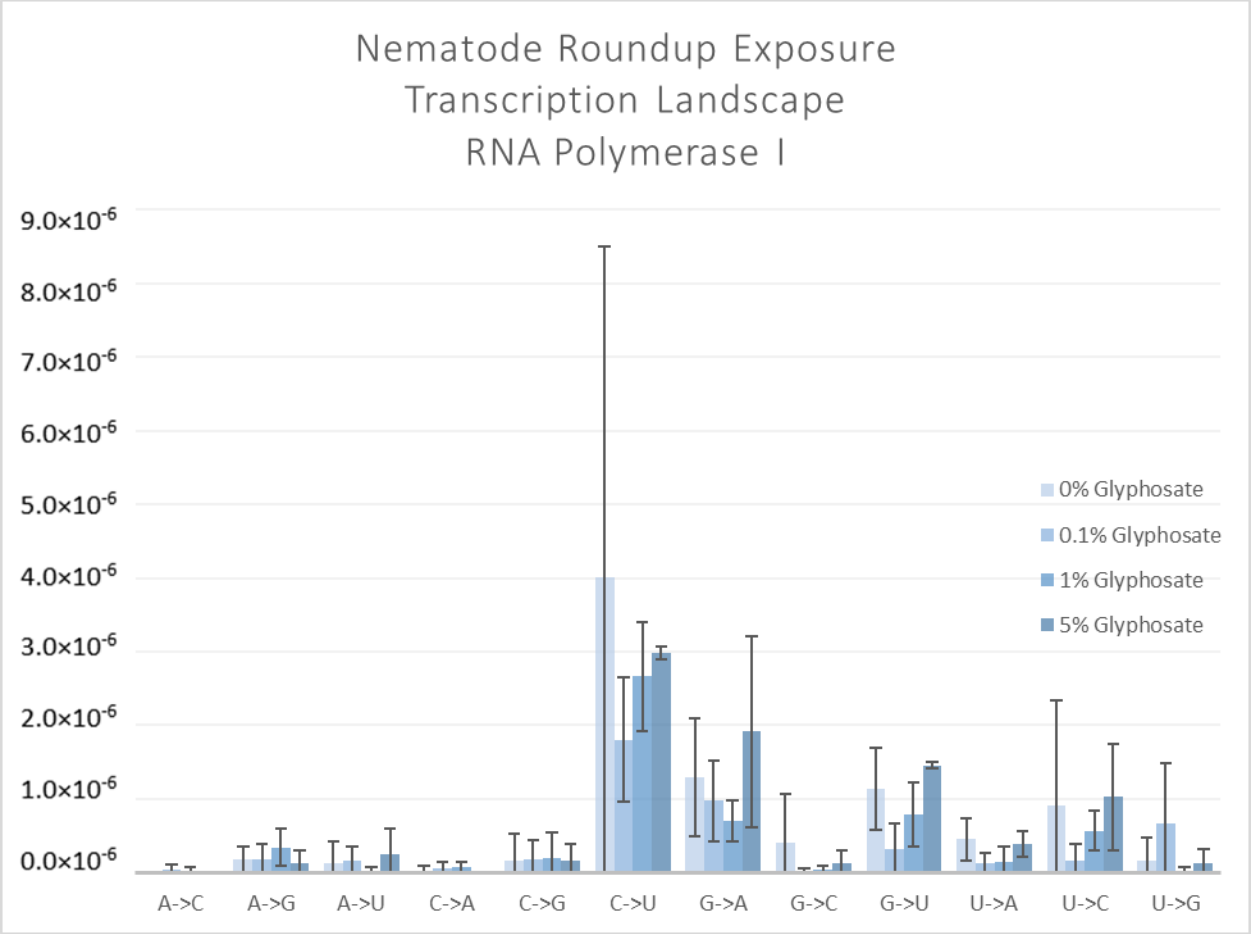

Figure B.2 Roundup Exposure *C. elegans* Error Rate Comparison in RNA Polymerase I Transcriptional Landscape

Transcription landscape depicting mRNA transcription errors produced by RNA polymerase I following *C. elegans* treatment with three different glyphosate percentages (5%, 1%, 0.1%) and a control lacking Roundup (0%). Error bars: Standard deviation.

B.2 Long-Term Roundup Exposure Experiment in *S. cerevisiae*

Figure B.3 *S. cerevisiae* Long-Term 5% Glyphosate Roundup Exposure

Depicts *S. cerevisiae* WT yeast following long-term exposure to 5% glyphosate from Roundup. Reared in liquid YPD media in 15mL tube at 30 °C with gentle agitation.

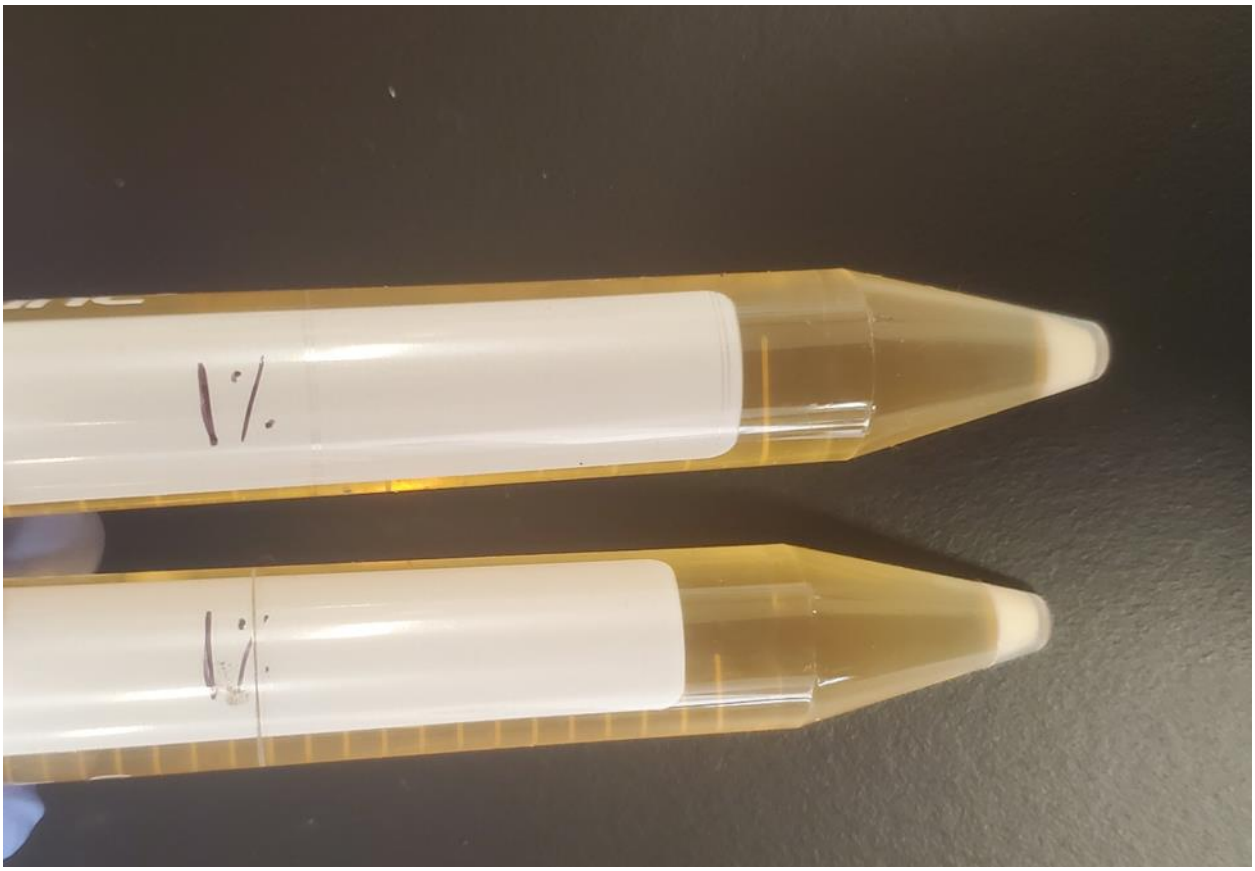

Figure B.4 *S. cerevisiae* Long-Term 1% Glyphosate Roundup Exposure

Depicts *S. cerevisiae* WT yeast following long-term exposure to 1% glyphosate from Roundup. Reared in liquid YPD media in 15mL tube at 30 °C with gentle agitation.

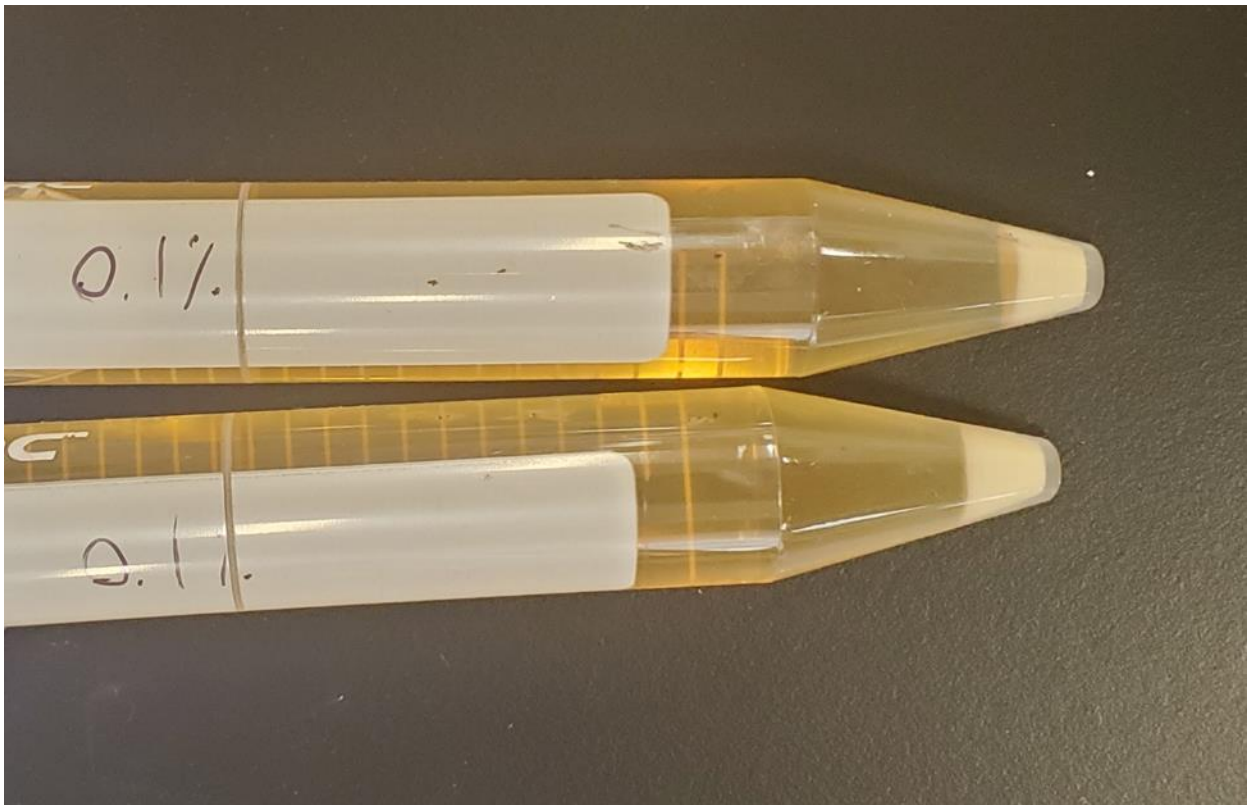

Figure B.5 *S. cerevisiae* Long-Term 0.1% Glyphosate Roundup Exposure

Depicts *S. cerevisiae* WT yeast following long-term exposure to 0.1% glyphosate from Roundup. Reared in liquid YPD media in 15mL tube at 30 °C with gentle agitation.

Figure B.6 *S. cerevisiae* Long-Term 0% (Control) Glyphosate Roundup Exposure

Depicts *S. cerevisiae* WT yeast following long-term exposure to 0% glyphosate (control replicates) from Roundup. Reared in liquid YPD media in 15mL tube at 30 °C with gentle agitation.

B.3 pH Experiment Supplemental Materials

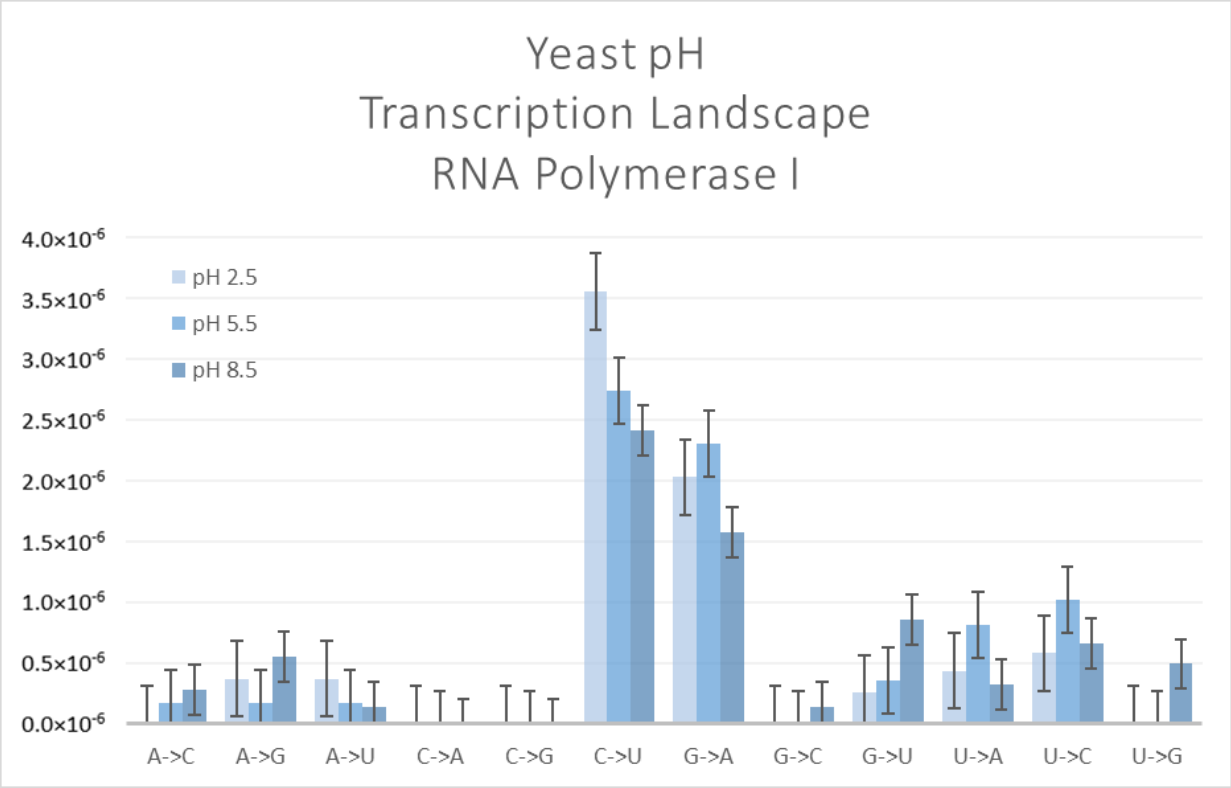

Figure B.7 *S. cerevisiae* pH Error Rate Transcriptional Landscape RNA Polymerase I

Transcription landscape depicting mRNA transcription errors produced by RNA polymerase I following *S. cerevisiae* exposure to three different pH environments (pH 2.5, 5.5, and 8.5). Error bars: Standard Error.

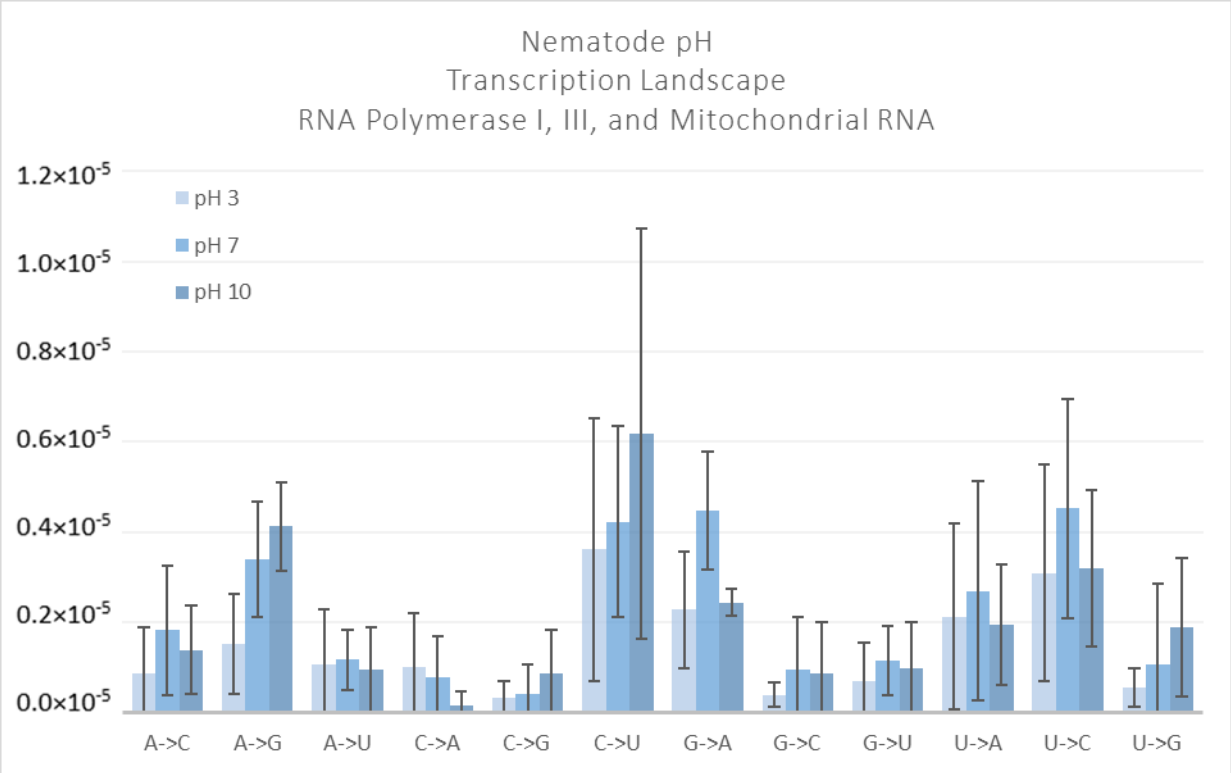

Figure B.8 *C. elegans* pH Error Rate Transcription Landscape for RNA Polymerase I, III, and Mitochondrial RNA

Transcription landscape depicting mRNA transcription errors produced by RNA polymerase I following *C. elegans* exposure to three different pH environments (pH 3, 7, and 10). Error bars: Standard deviation.

APPENDIX C

CHAPTER IV SUPPLEMENTAL CONTENT

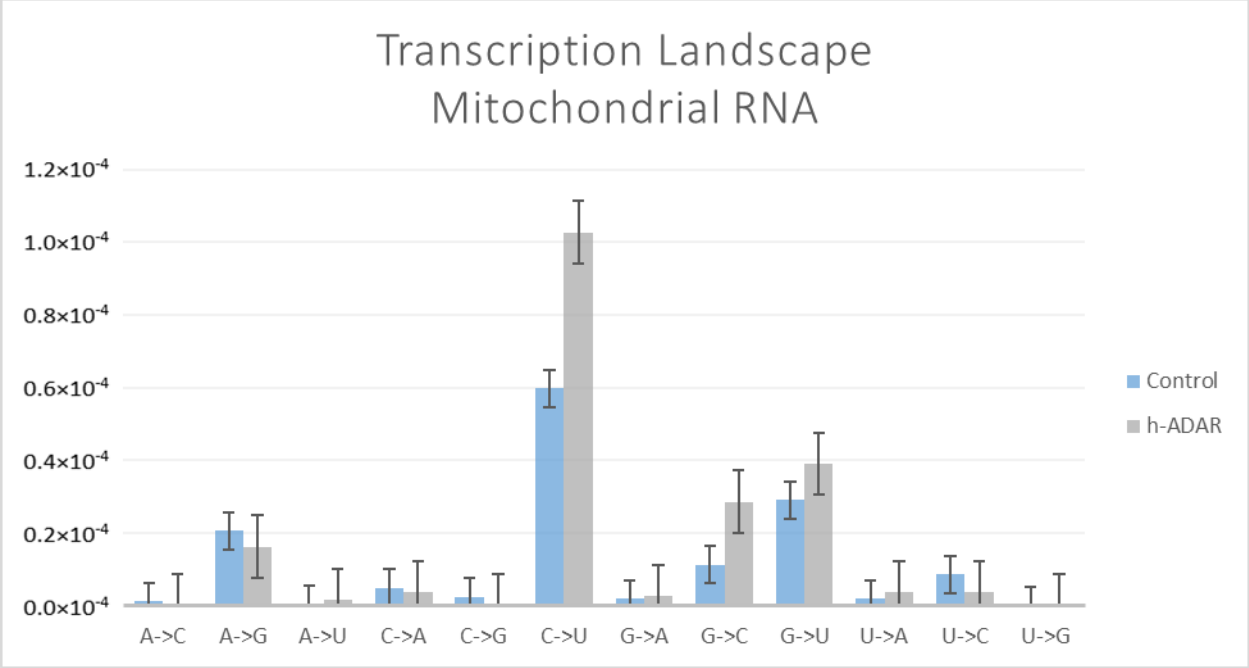

Figure C.1 h-ADAR Expression Transcription Landscape for Mitochondrial RNA

Transcription landscape depicting mitochondrial RNA transcription errors in *S. cerevisiae* expressing the h-ADAR gene vs. control yeast not expressing this gene. Error bars: Standard Error.